ANALYSIS AND PERFORMANCE OF CHOPPER-FED D. C. MOTORS UNDER MOTORING AND REGENERATIVE BRAKING

By

H. SATPATHI

TH
EE/1981/D
sa839
EE
1981
D
SAT
ANA

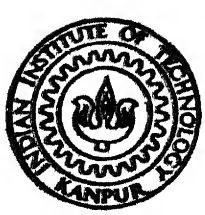

DEPARTMENT OF ELECTRICAL ENGINEERING

INDIAN INSTITUTE OF TECHNOLOGY, KANPUR

JULY, 1981

ANALYSIS AND PERFORMANCE OF CHOPPER-FED D. C. MOTORS UNDER MOTORING AND REGENERATIVE BRAKING

A Thesis Submitted
in Partial Fulfilment of the Requirements
for the Degree of
DOCTOR OF PHILOSOPHY

By
H. SATPATHI

to the
DEPARTMENT OF ELECTRICAL ENGINEERING
INDIAN INSTITUTE OF TECHNOLOGY, KANPUR
JULY, 1981

EE-1981-D-SAT-ANA

I.I.T. KANPUR
CENTRAL LIBRARY
Acc. No. A 70620
MAY 1982

This work is dedicated to Almighty God, the Embodiment of Truth, Love and Supreme Bliss solidified, in loving memory of my parents.

CERTIFICATE

Certified that this work 'Analysis and Performance of Chopper Fed D.C. Motors Under Motoring and Regenerative Braking' by H. Satpathi has been carried out under our supervision and that this work has not been submitted elsewhere for a degree.

Dr. G.K. Dubey
Professor

Dr. L.P. Singh
Professor

Department of Electrical Engineering
Indian Institute of Technology
Kanpur

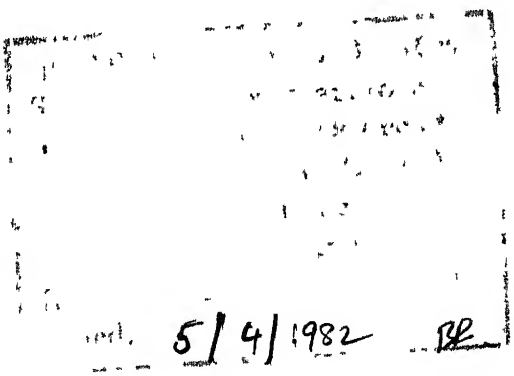

ACKNOWLEDGEMENTS

I express my indebtedness with a deep sense of gratitude to Dr. G.K. Dubey and Dr. L.P. Singh for their guidance and encouragement throughout the course of this investigation. Their sincere interest in the work is gratefully acknowledged.

I wish to acknowledge my gratefulness to Dr. I.R. Smith of Loubrough University, U.K., for his constructive suggestions to investigate the eddy current effect in d.c. machines. I am also grateful to Dr. S.K. Sen of B.E. College, Sibpur, Howrah for his valuable suggestions. I take this opportunity to thank all my fellow research scholars, especially, M/s H.K. Patel, A. Anwar, S.N. Tiwari, Sachchidananda, Y. Venkataramani, A.J. Kellogg, P. Raja Sekharam, R.S. Sanbhag, S. Bhatt and P.C. Mahanta for their suggestions and co-operation. I also thank Mr. N.D. Sharma and all other technical and laboratory staff members for their co-operation.

Thanks are also due to Mr. J.S. Rawat for his skilful typing the manuscript and Mr. T. Tiwari for his careful cyclostyling.

I sincerely appreciate the patience, the sense of responsibility and co-operation of my wife Saraju during the period of my study.

I must appreciate my children Debashish and Subhashis for allowing me to carry out the work undisturbed.

Haripada Satpathi

TABLE OF CONTENTS

LIST OF FIGURES

LIST OF PRINCIPAL SYMBOLS

V	D.C. supply voltage in volts.
E	Armature induced e.m.f. in volts
e	Instantaneous armature induced e.m.f.,volts.
i, i_a	Instantaneous values of current, amps.
I_{a1}, I_{a2}	Maximum and minimum level of armature current, amps.
i_p	Peak value of current ripple, amps.
I_{av}	Average armature current, amps.
L_s	Inductance of source, Henry.
L_a	Armature circuit inductance, [illegible] Henry.
L_f	Field circuit inductance, [illegible] Henry.
$L(I_{av})$	D.C. inductance of combined armature and field circuits of d.c. series machine.
L_c	Inductance of external choke, Henry
L_{eq}	Equivalent armature circuit inductance with eddy current in d.c. series machine, Henry.
$L_{in}(I_{av})$	Incremental inductance as a function of average current, Henry.
R, R_a	Total armature circuit resistance, ohms.
R_{eq}	Total equivalent armature circuit resistance with eddy current, ohms.
$K; K'$	Back e.m.f. coefficient of machine, volts/ rad-sec^{-1}.

$K(I_{av})$ Back e.m.f. coefficient of machine, volts/ rad-sec^{-1} as a function of average armature current.

$K'(I_{av}) = K(I_{av}).I_{av}$.

T Period of chopper.

T_a Armature circuit time constant, secs.

T_a' Armature circuit time const. including source inductance, secs.

δ Mark period ratio of chopper.

δ_c (Commutation interval/period) of chopper.

μ Loss of chopper on time due to source inductance.

C_p Buffer condenser bank

C Commutating capacitor, μF

a $(\frac{T}{T_a} - \frac{T}{T_a'})$

T_e Electromagnetic torque.

T_{br} Electromagnetic braking torque.

k_1, k_2 Frolich's constants.

α $= (\frac{i_p}{I_{av}})$

η_{rg} Efficiency of regeneration.

ϕ Flux in Wb

P_{rg} Regenerative power, watts.

P_{rdy} Dynamic braking loss, watts.

ω	Speed in rad-sec^{-1}
$\gamma_0, \gamma_0', \gamma_1', \Omega_0$	Natural frequencies
t_c	Chopper circuit turn off time in presence of source inductance.
t_{co}	Chopper circuit turn off time in absence of source inductance.
X_c =	$\sqrt{\frac{L_s}{C}}$
X_o =	V/I_{a2}
X =	$\frac{V}{I_{a2}} / \sqrt{\frac{L_c}{C}}$.
V_2	Maximum voltage on the commutating capacitor due to source inductance, volts
V_1	Minimum voltage on commutating capacitor, volts
v_n	Normalised voltage on the capacitor, $\frac{V_2}{V}$, p.u.

SYNOPSIS

H. SATPATHI
Ph.D.
Department of Electrical Engineering
Indian Institute of Technology, Kanpur
April, 1981

ANALYSIS AND PERFORMANCE OF CHOPPER-FED D.C. MOTORS UNDER MOTORING AND REGENERATIVE BRAKING

D.C. choppers provide an efficient and economic way of controlling d.c. separately and series excited motors supplied from constant voltage d.c. bus bars because of their low cost, high efficiency, less space, fast response and their ability to regenerate down to very low speed. Chopper controlled d.c. motors find applications in under ground traction and in battery operated vehicles. They have also been employed in 1500V main line d.c. traction where resistance control was used previously. The other advantages of chopper control in relation to traction application are smooth acceleration, better adhesion due to smooth and stepless control of voltage, and less maintenance. This thesis presents analysis and performance of chopper controlled d.c. separately and series excited motors under motoring and regenerative braking.

1. Performance and Analysis of Chopper fed D.C. Separately excited Motor:

1.1 Motoring Operation:

H.Irie et.al. [1] andK. Nitta et.al. [2] have described

the methods of calculating the motor performance and H. Barton [3] has derived the steady state transfer characteristics of chopper, for d.c. separately excited motor fed by a time ratio controlled (TRC) chopper with square wave output voltage, taking into account the discontinuous conduction. Parimelalagon and Rajagopalan [4] have presented four methods of analysis using various approximations for a non-square output voltage TRC chopper with load current dependent commutation. Alexandrovitz and Zabar [5] have described analogue computer simulation and Damle and Dubey [6] have described a digital computer programme based on point by point solution of differential equations valid for each mode of operation and using final conditions of the previous mode as initial conditions for each mode for a chopper with load dependent commutation. None of the methods of analysis reported so far have taken into account the effect of source inductance, armature reaction and discontinuous conduction in d.c. separately excited motor fed by a chopper with load dependent commutation.

In the present work, methods of analysis have been developed which take into account the effect of source inductance, discontinuous conduction, armature reaction and commutation pulse effect. Steady state transfer characteristics of chopper with load current dependent commutation have also been derived. The approach allows realisation of analytical

methods involving much less computation time compared to exact solution of differential equations. A good correlation has been obtained between predicted and measured curves.

The source inductance has considerable influence on the performance of the motor, and discontinuous conduction does take place in case of chopper with load dependent commutation unless the chopper is operated at high frequency.

1.2 Regenerative Braking:

G. Kimura and M. Shioya [7] have derived a method of analysis of TRC chopper controlled d.c. separately excited motor under regenerative braking assuming ideal square wave output voltage, neglecting chopper commutation pulse and armature reaction of machine. The effect of source inductance on the performance characteristics of machine has not been investigated.

In this part of the thesis, a systematic analysis has been carried out to predict the braking characteristics under regeneration. The analysis has been done both for square wave chopper and non-square wave output chopper with load dependent commutation. Normalised boundaries have been obtained which separate the regions of continuous and discontinuous conduction on the normalised speed torque plane for various values of $\frac{T}{T_a}$ ratio. An approach has been presented for selecting a suitable value of armature circuit filter inductance with a

view to reduce the area of discontinuous conduction to a small region, to optimize the regenerative power, maximise the efficiency of regeneration and to keep the armature current ripple within low tolerable limits. The effects of chopper commutation pulse, armature reaction of machine and the effect of source inductance on the braking characteristics have been investigated. The predicted results agree well with the actual results.

2. Chopper Controlled D.C. Series Motors:

2.1 Motoring operation:

The main problem in the analysis of chopper controlled d.c. series motor arises due to non-linearity of the magnetic circuit of the motor. The analytical methods of analysis of d.c. series motor fed by chopper with square wave output voltage have been described by P.W. Franklin [8] for choppers with current limit control (CLC) and by Dubey and Shepherd [9], for choppers with TRC as well as CLC. B. Mellitt and M.H. Rashid [10] and Damle and Dubey [11] have described computer based numerical methods of analysis for calculation of motor performance when fed by a chopper with load dependent commutation. Dubey [12] has developed an analytical method for this case by extending the method described in Reference [9]. None of these methods account for the effect of eddy currents. T. Fujimaki et.al [13] have developed a dynamic model of the

motor which takes eddy current effect into account. The relevant equations have then been employed to predict transient response. None of the above methods have taken the effect of source inductance into account.

In this part of the thesis, a general method of analysis of a TRC chopper controlled d.c. series motor has been presented. First, a systematic modelling of a series motor has been done. The saturation of magnetic circuit, armature reaction and eddy current effects have been taken into account in this modelling. An empirical formula has been suggested to take into account the variation of field and armature circuit inductances with armature current. The machine back e.m.f. coefficient has been taken as function of average armature current and it takes into account both saturation and armature reaction effect. To estimate the effects of eddy currents on the armature induced e.m.f., two approaches have been used. First, a dynamic field circuit model based on field theory has been identified using transient response. Secondly, an empirical formulation based on extensive experimental results on typical d.c. machines having different designs of magnetic circuits, has been developed to take into account the eddy current effect. The second approach being much simpler to implement in the analysis of chopper fed series motor, has finally been adapted. The effect of chopper commutation pulse

has been taken in to account in the analysis. The influence of source inductance on the machine performance and chopper commutation has been investigated. It has been shown that for reliable prediction of ripple in armature current, incremental inductances should be used and eddy current effect should be taken into account. The predicted results agree well with the experimental results.

2.2 Regenerative Braking Operation:

The regenerative braking of chopper controlled dc series motor is some what complicated because of stability problems. R. Wagner [14] has reported that instability of operation occurs resulting in loss of current control, at high speeds. He has suggested circuits to overcome these problems. Farrer and McLoughlin [15] and Loderer [16] have considered the circuit aspects of regenerative braking.

The thesis describes a steady state analysis method of chopper-fed dc series motor under regenerative braking taking into account the effect of magnetic saturation, chopper commutation interval and the effect of source inductance.

The effects of commutating capacitor, armature circuit inductance and source inductance on the braking speed-torque characteristics, braking power and stability of the drive have been investigated. It has been noted that an oversized commutation capacitor improved the stability and that the

source inductance while improves the stability of braking characteristics it reduces the regenerated power for the same values of speed and duty ratio.

The predicted results corroborate well with experimental results.

The last part of the thesis describes the effect of source inductance on the commutation in various chopper circuits. A discussion has been given in the concluding part of the thesis.

CHAPTER I

INTRODUCTION

D.C. choppers are used for the speed control of d.c. series and separately excited motors supplied from constant voltage d.c. busbars because of high efficiency, economy, less space, simple control circuitry, fast response and their ability to regenerate down to a very low speed. Choppers have been employed in 1500V main line traction where resistance control was used previously and it has been reported in the literature that a net saving of energy of the order of 20-30% has been achieved. The other advantages of chopper control in relation to traction application are smooth acceleration due to stepless control of voltage, better adhesion and less maintenance.

A detailed analysis of chopper controlled d.c. separately and series excited motors under motoring and regenerative braking, taking various parameters and machine nonlinearities into account, has been undertaken in the present investigation.

1.1 STATE OF ART:

In this section a brief review of the existing literature has been presented.

1.1.1 Chopper Control of D.C. Separately Excited Motor

D.C. separately excited motors have good torque-speed characteristics and therefore, they are preferred in variable speed drives fed from constant voltage d.c. bus bars. Chopper control of d.c. separately excited motor provides a wide range of speed control.

H. Irie et al [1] and K. Nitta et al [2] have described analysis of TRC chopper controlled d.c. separately excited motor for square wave output voltage including discontinuous conduction. T.H. Barton [3] has derived the steady state transfer characteristics of a square wave chopper. Parimelalagon and Rajagopalan [4] have presented four methods of analysis using various approximations for a TRC chopper fed d.c. separately excited motor using load current dependent commutation. Alexandrovitz and Zabar [5] have described analogue computer simulation and Damle and Dubey [6] have presented a digital computer based analysis.

1.1.2 Chopper Control of d.c. Separately Excited Motor under Regenerative Braking

Regenerative braking is used to save energy. The chopper is suitable for regenerative braking in d.c. motors. It is connected in parallel with the armature circuit of the motor. By controlling the duty ratio, the regenerated

power is controlled. Usually an additional external inductance is connected in the armature circuit. G. Kimura and M. Shioya [7] have derived a method of analysis of TRC chopper controlled separately excited motor under regenerative braking assuming ideal square wave output voltage neglecting armature reaction and the effect of source inductance.

1.1.3 Chopper Control of Series Motor

D.C. series motors are widely used in railway traction due to their high starting torque characteristics. D.C. choppers are suitable for efficient and smooth control of series motors. P.W. Franklin [8] presented an analytical method of performance calculation of d.c. series motor fed by choppers with current limit control (CLC) and Dubey and Shepherd [9] have developed methods of analysis of the motor when fed by choppers with TRC as well as CLC. B. Mellitt and M.H. Rashid [10] and P.D. Damle and G.K. Dubey [11] have described computer based analysis of TRC chopper fed d.c. series motors with load dependent commutation taking saturation of the magnetic circuit into account. Dubey [12] has extended the analytical method described in reference [9] to the case of chopper with load dependent commutation. T. Fujimaki et al [13] have developed a dynamic model of a series motor taking into account variation of armature and

field inductances with magnetic saturation and eddy current effects. A graphical technique has been used to identify the dynamic field circuit parameters. Then a digital computer simulation has been done under transient conditions.

1.1.4 Regenerative Braking of Chopper Controlled Series Motor

Regenerative braking of chopper controlled d.c. series motor has many problems associated with it. In some cases, regenerative braking is carried out by connecting the field circuit to a separate source, i.e. as a separately excited motor. R. Wagner [14] has reported instability of operation of chopper controlled series motor under regenerative braking resulting in loss of current control at high speeds. He has suggested some circuits to over come these problems. W. Farrer and McLoughlin [15] and P. Loderer[16] have described different circuit aspects of regenerative braking.

1.2 PRESENT INVESTIGATION:

The present work aims at studying performances and developing simple effective analytical methods for reliable prediction of performances of TRC chopper fed d.c. separately and series excited motors under motoring and regenerative braking.

A method of analysis has been developed for a TRC load current commutated chopper controlled d.c. separately excited motor taking discontinuous conduction into account. The effects of source inductance, armature reaction of the machine and the effect of chopper commutation pulse on the motor performance have been highlightened. A number of new modes are present which have not been reported so far. It is shown that the source inductance influences the performance of d.c. separately excited motor by reducing the effective 'on interval' of the chopper. As a result, the torque speed characteristics become more drooping than in the case when there is no source inductance. The effect of source inductance and discontinuous conduction on chopper commutation has been considered. The influence of chopper frequency on motor performance has been investigated. If the chopper operating frequency is not high, it has been found that discontinuous conduction does occur in a wide range of torque-speed plane. It is experimentally established that the use of a suitable buffer condenser bank at the source terminals neutralizes the effect of source inductance. The influence of chopper commutation interval and source inductance on the transfer characteristics have been discussed.

Analysis has also been done for regenerative braking of TRC chopper fed d.c. separately excited motors. First, an analysis is presented using a square wave output voltage. The normalised boundaries of discontinuous conduction have been shown on the normalized torque-speed plane for different $\frac{T}{T_a}$ ratio. An approach has been presented for selecting a suitable value of armature circuit filter inductance with a view to reduce the region of discontimuous conduction, keep the armature current ripple within permissible limits, optimize the regenerative power, and to maximize the efficiency of regeneration. Secondly, the analysis has been extended for nonsquare wave chopper taking chopper commutation interval into account. The effects of armature reaction and source inductance have been included. Use of a buffer condenser at the source terminals neutralizes the effect of source inductance.

The performance equations of chopper controlled d.c. series motors are nonlinear. For the purposes of analysis, a method of modelling of series machine has been developed. The saturation of magnetic circuit, the effect of armature reaction and the influence of eddy currents induced in the field cores due to time varying excitation current supplied by the chopper have been taken into account in the modelling.

An empirical formula has been developed to take into account the variation of field and armature circuit inductances. The machine back e.m.f. coefficient has been taken as a function of average armature current, taking into account both saturation and armature reaction effect. To evaluate the effects of eddy current on the dynamic armature induced e.m.f., two approaches are used. First, a dynamic field circuit model based on field theory has been identified from transient response using a least square error criteria. Secondly, an empirical formulation has been done based on extensive experimental results. The second approach being simpler, has been used in the analysis of chopper fed series motor. The effect of chopper commutation pulse and also the effect of source inductance on the motor performance have been taken into account. It has been found that eddy currents do not influence the machine torque-speed characteristics significantly but they do influence the armature current ripple appreciably. It is shown that for correct prediction of ripple in armature current, incremental inductances are to be used along with eddy current. It has been found that the source inductance adversely affects the performance of chopper controlled motor.

Method of analysis has been presented for TRC chopper controlled series motor under regenerative braking taking into account saturation of magnetic circuit, armature reaction and chopper commutation interval and the influence of source inductance. The effects of chopper commutating capacitor, $\frac{T}{T_a}$ ratio and the influence of source inductance on the braking characteristics of the motor are investigated. It has been found that stability of operation under regenerative braking of chopper fed series motors is quite critical. An oversized commutating capacitor improves the stability of operation. The source inductance while improves the stability of braking characteristics, it reduces the regenerative power for the same values of speed and duty ratio. A suitable value of buffer condenser at the source terminals neutralizes the effect of source inductance.

1.3 DETAILS OF VARIOUS CHAPTERS:

Chapter II describes the analysis and performance of chopper controlled d.c. separately excited motor.

Chapter III presents the regenerative braking aspects of separately excited d.c. motors controlled by a chopper.

Modelling, analysis and performance of chopper fed d.c. series motors are described in Chapter IV.

Chapter V deals with analysis and performance of chopper controlled series motors under regenerative braking.

Chapter VI considers the effect of source inductance on commutation of various choppers.

Chapter VII presents important conclusions of the complete work.

CHAPTER II

PERFORMANCE AND ANALYSIS OF CHOPPER FED D.C. SEPARATELY EXCITED MOTOR

2.1 INTRODUCTION:

In some chopper circuits, the output voltage is either a square wave or can be approximated by a square wave. In some chopper circuits particularly those using load dependent commutation, the output voltage is neither square wave nor can be approximated by square wave without loss of accuracy.

The analysis of a d.c. separately excited motor fed by a chopper with square wave output voltage and time ratio control (TRC) has been described by K. Nitta et al. [2] . The method deals with both the continuous and discontinuous conduction operation of the machine. T.H. Barton [3] has derived the steady state transfer characteristics for this case.

Parimelalagon and Rajagopalan [4] have presented four methods using various approximations for the analysis of a separately excited d.c. motor fed by a chopper with load current dependent commutation (non square output voltage) neglecting discontinuous conduction. Notable

among these methods are the one with the assumption of constant current during commutation and the other with an exact solution of differential equations describing various modes of operation either numerically or graphically. Considerable error was obtained though the second approach, involving a large amount of computation, gave better results. These authors then suggested the use of a resistance value 33% higher than the one obtained by d.c. resistance test and that gave improved accuracy. This analysis suffers from the following limitations.

(i) The effect of source inductance has not been taken into account. The source inductance has considerable effect on the motor performance, because, firstly, it prolongs the free wheeling interval and reduces the effective on interval of chopper, and secondly, it changes the voltage to which the commutating capacitor is charged and thus varies the duration and strength of the commutation pulse.

(ii) The discontinuous conduction has been neglected. The region of discontinuous conduction on the torque-speed plane depends on the chopper operating frequency and the armature circuit inductance. In small size drives,the use of additional inductance is normally avoided because of additional cost (which forms a significant percentage of

total cost of the drive), volume and weight. Due to this, discontinuous conduction is always present. In many low cost choppers, the control range decreases as the frequency of operation is increased. Therefore, if a wide range of control is desired, chopper may have to be operated at low frequency of the order of 200 Hz. In such cases, discontinuous conduction takes place in a considerable region of torque speed plane and therefore the analysis should take the effect of discontinuous conduction into account.

(iii) The armature reaction of the machine has been ignored. Though the effect of armature reaction is small in machines with compensating windings, but in small size machines, compensating windings may not be provided and in that case armature reaction has considerable influence on the motor performance.

(iv) The a.c. component of current, which is only a small percentage of the d.c. component, is not expected to increase the armature resistance value by such a large amount (33% as assumed by the authors). Furthermore, the percentage of a.c. component varies with the load current and the 'mark period ratio' of chopper and therefore if at all appreciable change in resistance occurs it can not be taken to be a constant.

In this chapter, a general method of analysis has been presented which removes the limitations mentioned earlier, by taking into account the effect of source inductance, discontinuous conduction and armature reaction. It assumes constant current during commutation interval, an assumption which is always valid except under very light load conditions. The method allows the realisation of an analytical method involving much less computation time compared to exact solution of differential equations valid for various modes of operation, either numerically or graphically. No such assumption of 33% increase in resistance has been made and the accuracy is quite good. The steady state transfer characteristics of a chopper controller feeding a back e.m.f. load have been given. The effects of chopper commutation pulse and chopper operating frequency on the steady state transfer characteristics have been demonstrated.

2.2 ANALYSIS OF CHOPPER FED D.C. SEPARATELY EXCITED MOTOR WITH SOURCE INDUCTANCE [18]

Figure 2.1 shows a schematic circuit diagram of a d.c. separately excited motor controlled by a chopper with load dependent commutation. L_s is the inductance of source. The chopper used is a 2 thyristor chopper with load dependent commutation. There are many other chopper circuits employing

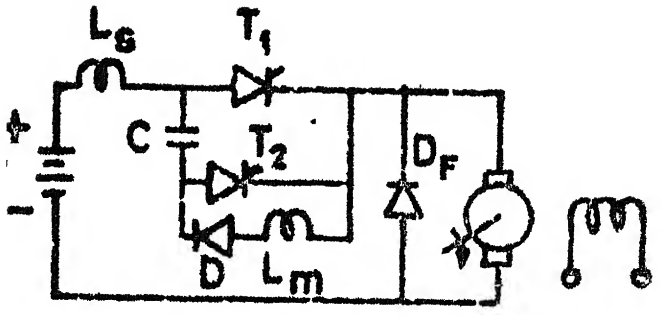

g. 2.1 Chopper Controlled D.C. separately excited motor.

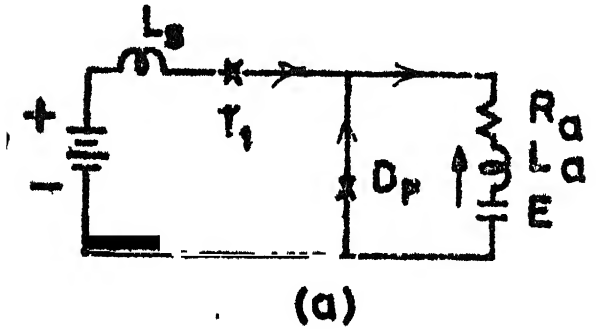

(a)

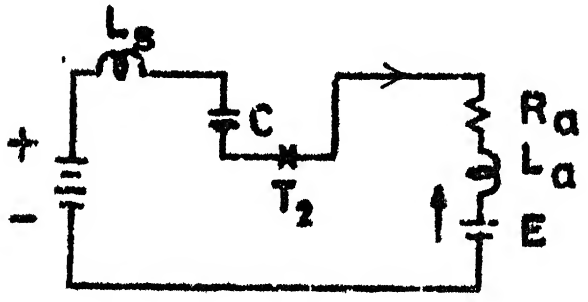

(b)

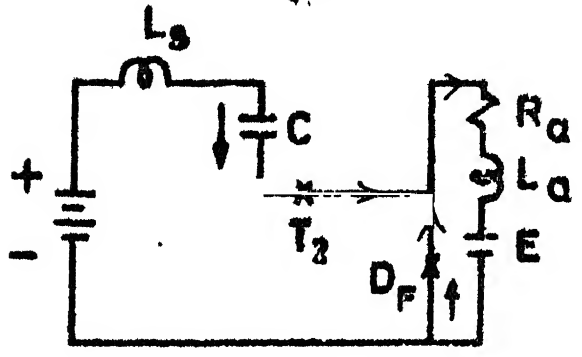

(c)

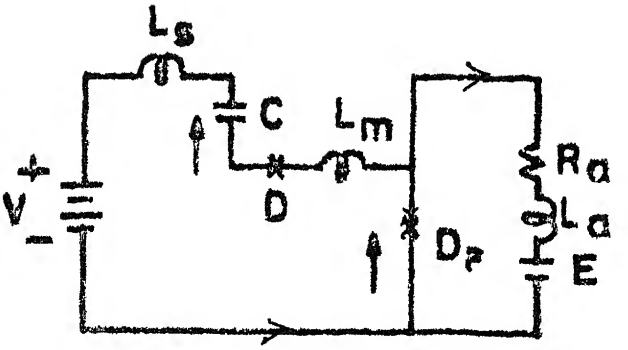

(d)

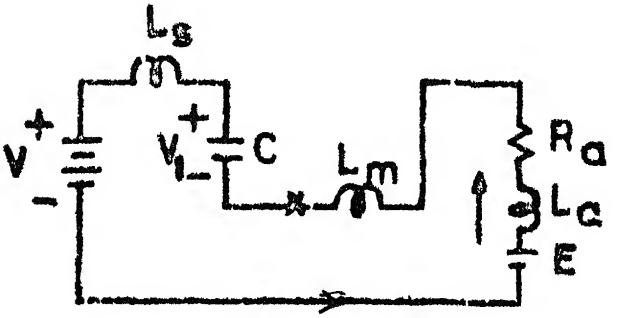

(e)

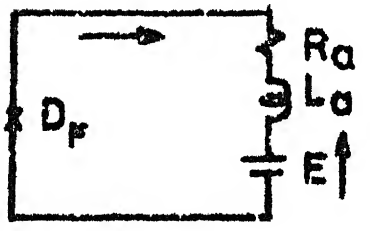

(f)

Fig. 2.2 Equivalent Circuits of Chopper Controlled D.C. Separately Excited Motor.

load dependent commutation. However, the basic approach developed here for 2 thyristor chopper of Fig. 2.1 can be employed for any other chopper with load dependent commutation.

The induced back e.m.f. of a d.c. machine is given by

$$e = K_e \phi . \omega = f(i_f . i_a) . \omega = K . \omega \qquad (2.1)$$

i_f = constant.

In absence of armature reaction, the e.m.f. coefficient K will be a constant. But due to armature reaction flux, K will be a function of i_a. In case of chopper controlled d.c. motors, the armature current i_a fluctuates between a maximum and a minimum level and as a result of this, the performance equations are nonlinear. For the purpose of analysis, $K(i_a)$ can be taken to be equal to $K(I_{av})$. The analysis is then carried out based on the following assumptions:

i) the thyristors and diodes are ideal switches;

ii) the resistances and inductances are constants;

iii) under a specific operating condition, the motor speed is constant [illegible] constant.

iv) during commutation, the armature current remains constant.

2.2.1 Continuous Conduction:

Duty Interval $(0 \leq t \leq \delta T)$

This interval starts with the firing of the main thyristor T_1 as shown in Figure 2.1. Prior to this, under steady state condition, the armature current was free wheeling through the free wheeling diode D_F. Due to the presence of source inductance, the source current i_s linearly rises and it reaches the value I_{a1} after an interval of μT. At this instant, the source current and the motor current are equal and therefore, free wheeling stops. The equivalent circuit is shown in Figure 2.2(a). The idealised voltage and current wave forms are shown in Figure 2.3. The differential equations describing this mode are given by

$$L_s \cdot \frac{di_s}{dt} = V \quad \text{for } 0 \leq t \leq \mu T \qquad (2.2)$$

with $i_s(0) = 0$ and $i_s(\mu T) = I_{a1}$ (say)

From equation (2.2),

$$i_s = \left(\frac{V}{L_s}\right).t$$

$$\therefore \mu = (I_{a1}/V.T.).\ L_s \qquad (2.3)$$

At $t = \mu T$, the free wheeling stops and the armature current rises exponentially and the differential equation is given by

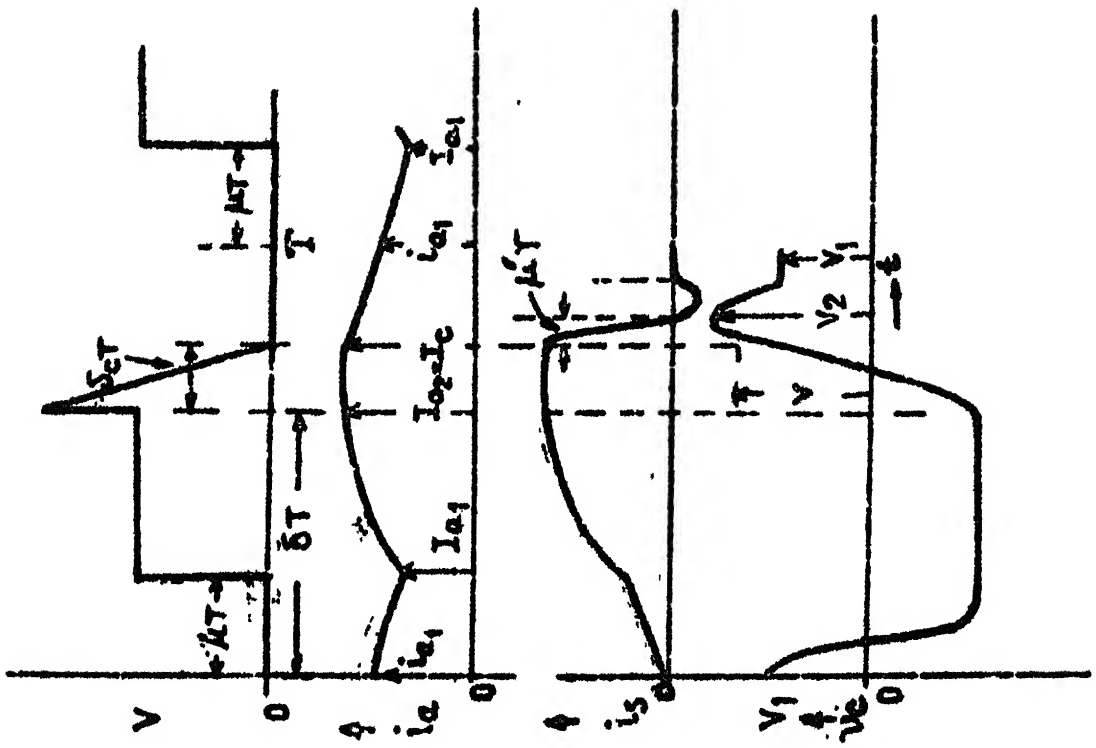

Fig. 2.3 Idealised voltage and current wave forms of chopper-fed d.c. separately excited motor.

$$V = (L_a+L_s).\frac{di_a}{dt} + R.i_a + E \quad \text{for} \quad \mu T \leq t \leq \delta T \tag{2.4}$$

with $i_a(\mu T) = I_{a1}$

The solution is

$$i_a = \frac{V-E}{R}\left[1-e^{-(t-\mu T)/T'_a}\right] + I_{a1}.e^{-(t-\mu T)/T'_a} \tag{2.5}$$

where, $T'_a = \frac{L_s+L_a}{R}$ and $R = R_a+R_s$

At $t = \delta T$, $i_a(\delta T) = I_{a2}$(say)

$$\therefore I_{a2} = \frac{V-E}{R}\left[1-e^{-(\delta-\mu)T/T'_a}\right] + I_{a1}.e^{-(\delta-\mu)T/T_a'} \tag{2.6}$$

If the source resistance is small, then we can take $R_a \approx R$.

II. Commutation Interval.

This interval starts with the turning on of the auxiliary thyristor T_2. It is assumed that the commutating capacitor which was charged previously to a voltage of $-V_1$, turns off the main thyristor immediately. The interval $\delta_c T$ during which the capacitor gets charged linearly from a voltage $-V_1$ to V, on the assumption of constant current during commutation at the level $i_a=I_{a2}$, is given by

$$\delta_c = \frac{(V + V_1).C}{I_{a2}.T} \qquad (2.7)$$

The equivalent circuit describing this mode is shown in Figure 2.2(b).

III. Free Wheeling Interval I·

This interval begins when the commutating capacitor C is charged to a voltage +V and the free wheeling diode is forward biased and it begins to conduct. But due to the presence of source inductance L_s, the capacitor C contimues to be charged. The equivalent circuit is shown in Figure 2.2(c). The differential equation after neglecting the voltage drop due to source resistance, is given by

$$V = L_s \cdot \frac{di_c}{dt} + \frac{1}{C}\int_0^t i_c.dt \text{ with } i_c\,((\delta + \delta_c)T) = I_{a2}$$

The solution of i_c is given by

$$i_c = I_{a2} \cos \gamma_o (t - \delta' T)$$

where, $\gamma_o = \frac{1}{\sqrt{L_s.C}}$ and $\delta' = (\delta + \delta_c)$

This mode ends when i_c=0 which is given by

$$\mu' = \frac{\pi}{2\gamma_o T} \qquad (2.8)$$

The maximum voltage V_2 to which the capacitor gets charged is given by

$$V_2 = V + \frac{1}{C} \int_{\delta' T}^{(\delta' + \mu')T} i_c \, dt = I_{a2} \cdot \sqrt{\frac{L_s}{C}} + V \qquad (2.9)$$

IV. Free Wheeling Interval II

This mode starts when the capacitor current i_c in the previous mode has become zero and the capacitor has been charged to a voltage $V_2 > V$. The over charged capacitor C now discharges partially through the source and the free wheeling diode. The equivalent circuit describing this mode is shown in Figure 2.2(d). The differential equation is given by

$$(L_s + L_m) \frac{di_c}{dt'} + \frac{1}{C} \int_0^{T'} i_c \, dt' = V - V_2 \qquad (2.10)$$

where t' is the time measured from the beginning of the present mode. The solution of i_c is given by

$$i_c = \frac{V - V_2}{\sqrt{(L_s + L_m)/C}} \cdot \sin \gamma_o' t'$$

where, $\gamma_o' = \frac{1}{\sqrt{(L_s + L_m) \cdot C}} \approx \frac{1}{\sqrt{L_s \cdot C}} = \gamma_o$ as $L_m \ll L_s$

This mode ends when $i_c = 0$ or at the beginning of the next cycle whichever is earlier. The voltage across the capacitor at the end of this interval is given by

$$v_c = V_1 = (V-V_2) - (L_s+L_m) \left.\frac{di_c}{dt'}\right|_{t'=\tau'}$$

when $i_c = 0$, V_1 is minimum and is given by

$$V_1 = V - \sqrt{(L_s+L_m)/C} \cdot I_{a2} \qquad (2.11)$$

From equation (2.11) it is found that the capacitor voltage available for commutation is reduced by the source inductance and larger is the motor current, more is the reduction in capacitor voltage provided the capacitor gets enough time to discharge. Thus, the source inductance may adversely affect the commutation capability. The armature current starts free wheeling at $t = (\delta + \delta_c)T$. The differential equation is

$$L_a \cdot \frac{di_a}{dt} + R_a \cdot i_a = -E$$

with $i_a(\delta'T) = I_{a2}$ and the armature current is given by

$$i_a = -\frac{E}{R_a}(1-e^{-(t-\delta'T)/T_a}) + I_{a2} \cdot e^{-(t-\delta'T)/T_a} \qquad (2.12)$$

The free wheeling of i_a continues upto $t=T+\mu T$. The armature current at the end of free wheeling is given by

$$I_{a1} = -\frac{E}{R_a}\left(1-e^{-(1-\delta'+\mu)T/T_a}\right) + I_{a2} \cdot e^{-(1-\delta'+\mu)T/T_a} \qquad (2.13)$$

From equations (2.6) and (2.13) by elimination of variables,

$$I_{a1} = -\frac{E}{R_a} + \frac{V}{R_a}\left[\frac{1-e^{(\delta-\mu)T/T_a'}}{1-e^{(1-\delta_c)T/T_a - a(\delta-\mu)}}\right] \qquad (2.14)$$

$$I_{a2} = -\frac{E}{R_a} + \frac{V}{R_a}\left[\frac{1-e^{-(\delta-\mu)T/T_a'}}{1-e^{-(1-\delta_c)T/T_a + a(\delta-\mu)}}\right] \qquad (2.15)$$

where, $a = \left(\frac{T}{T_a} - \frac{T}{T_a'}\right)$

Substituting I_{a1} from equation (2.14) into equation (2.3) one gets,

$$\mu = \frac{L_s}{T.R_a}\left[-\frac{E}{V} + \frac{1-e^{(\delta-\mu)T/T_a'}}{1-e^{(1-\delta_c)T/T_a - a(\delta-\mu)}}\right]$$

Expanding the terms containing $e^{-\mu(T/T_a')}$ and $e^{a\mu}$ in terms of their power series and then neglecting all higher order terms greater than two, yields a quadratic in μ as

$$A'\mu^2 + B'\mu + C' = 0$$

where,

$$A' = -a.e^{(1-\delta_c)T/T_a - a\delta} - \frac{L_s.a^2}{2T.R_a}\left(\frac{E}{V}\right).e^{(1-\delta_c)T/T_a - a.\delta} + \frac{L_s}{2T.R_a}\cdot\left(\frac{T}{T_a'}\right)^2 e^{\delta T/T_a}$$

$$B' = (1-e^{(1-\delta_c)T/T_a - a\delta}) - \frac{L_s}{TR_a}\left(\frac{E}{V}\right).a.e^{(1-\delta_c)T/T_a - a.\delta} - \frac{T}{T_a}\cdot\frac{L_s}{TR_a}\cdot e^{\delta T/T_a'}$$

$$C' = \frac{L_s}{TR_a}\left[\frac{E}{V}\left(1-e^{(1-\delta_c)T/T_a - a.\delta}\right)-\left(1-e^{\delta T/T_a'}\right)\right]$$

$$\text{or,}\quad \mu_{1,2} = -\frac{B'}{2A'} \pm \frac{\sqrt{B'^2-4A'.C'}}{2A'} \qquad (2.16)$$

Usually μ is a small quantity unless L_s is large and in that case μ is approximately given by

$$\mu = -\frac{C'}{B'} = \frac{-\frac{E}{V}\left(1-e^{(1-\delta_c)T/T_a - a.\delta}\right)+\left(1-e^{\delta T/T_a}\right)}{\frac{T.R_a}{L_s}.\left(1-e^{(1-\delta_c)T/T_a - a.\delta}\right)-\frac{E}{V}.a.e^{(1-\delta_c)T/T_a - a.\delta} - \frac{T}{T_a'}.e^{\delta T/T_a'}} \qquad (2.17)$$

The commutation interval $\delta_c T$ is determined as follows. Substituting the values of V_1 and I_{a2} from equation (2.11) and (2.15) into equation (2.7) and then expanding the terms containing $e^{\delta_c T/T_a}$ in terms of its power series and neglecting all higher order terms greater than two, yields a quadratic in δ_c as

$$A.\delta_c^2 + B.\delta_c + C = 0 \qquad (2.18)$$

where,

$$A = \left[\frac{E}{V}.\left(\frac{T}{T_a}\right)e^{-T/T_a+a(\delta-\mu)} + \frac{C.R_a}{T_a}\left(\frac{T}{T_a}\right).e^{-T/T_a+a(\delta-\mu)} + \frac{E}{V}.\frac{1}{y_o T_a}.\left(\frac{T}{T_a}\right).e^{-T/T_a+a(\delta-\mu)}\right]$$

$$B = \left[-\frac{E}{V}\left(1-e^{-T/T_a+a(\delta-\mu)}\right)+\left(1-e^{-(\delta-\mu)T/T_a}\right)+\frac{E}{V}\cdot \right.$$

$$\left. \frac{1}{\gamma_o T_a}\cdot e^{-T/T_a+a(\delta-\mu)} + \frac{2C.R_a}{T_a}\cdot e^{-T/T_a+a(\delta-\mu)} \right]$$

$$C = \left(e^{-T/T_a+a(\delta-\mu)}-1\right).\left(\frac{2C.R_a}{T}+\frac{E}{V}\cdot\frac{1}{\gamma_o T}\right)]$$

$$\therefore \delta_{c1,2} = -\frac{B}{2A} \pm \frac{\sqrt{B^2-4AC}}{2A} \qquad (2.19)$$

The expressions for μ and δ_c as shown in equations (2.17) and (2.19) are interdependent. As a first step, δ_c can be determined from equation (2.19) ignoring μ. Next, this value of δ_c is used to calculate the value of μ from equation (2.17) and the corrected value of δ_c is again recalculated with that value of μ.

The load voltage and current waveforms for continuous conduction have been shown in Figure 2.3. The average armature current is given by

$$I_{av} = \frac{1}{T}\left[\int_{\mu T}^{T} i_a.dt + I_{a2}\cdot\delta_c T + \int_{(\delta+\delta_c)T}^{(1-\delta-\delta_c+\mu)T} i_a.dt\right]$$

Under continuous conduction, the average armature current can also be conveniently found out from the expression

$$I_{av} = \frac{V(\delta - \mu) - E(1 - \delta_c)}{R_a} + \frac{C(V+V_1)}{T}$$

Substituting the values of V_1 and I_{a2} from equations (2.11) and (2.15) into above equation,

$$I_{av} = \frac{V(\delta - \mu) - E(1 - \delta_c)}{R_a} + \frac{2CV}{T} - \frac{I_a}{\gamma_o T} \qquad (2.20)$$

The electromagnetic developed torque is given by

$$T_e = K(I_{av}).I_{av} \qquad (2.21)$$

The motor speed is given by

$$\omega_{av} = \omega = \frac{E}{K(I_{av})} \qquad (2.22)$$

2.2.2 Discontinuous Conduction:

I. Duty Interval $(0 \leq t \leq \delta T)$

The differential equation describing this mode is given by

$$V-E = (L_s+L_a).\frac{di_a}{dt} + R_a i_a \text{ with } i_a(o) = 0$$

$$i_a = \frac{V-E}{R_a}(1-e^{-t/T_a'}) \qquad (2.23)$$

At $t = \delta T$,

$$I_{a2} = \frac{V-E}{R_a}(1-e^{-\delta T/T_a'}) \qquad (2.24)$$

II. Commutation Interval: $\delta T \leq t \leq (\delta + \delta_c)T$

Assuming that the main thyristor T_1 has already been turned off, the load current entirely flows through the commutating thyristor T_2. The differential equation is given by

$$(L_s+L_a)\frac{di_a}{dt} + R_a i_a + \frac{1}{C}\int_o^t i_a\,dt = V-E+V_1$$

where, $v_c(o) = -V_1$.

The solution of this equation after neglecting the voltage drop due to resistance is

$$i_a = \frac{I_{a2}}{\sin \phi_i} \cdot \sin [\gamma_o' \cdot (t-t_1) + \phi_1] \qquad (2.25)$$

where,

$$\gamma_o' = \frac{1}{\sqrt{(L_s+L_a)C}} \quad \text{and} \quad \phi_i = \tan^{-1}\left[\frac{\gamma_o'(L_s+L_a).I_{a2}}{V_1+V-E}\right]$$

The commutation interval $\delta_c T$ is given by

$$\delta_c T = \frac{1}{\gamma_o'}\left[\cos^{-1}\left\{\cos \phi_1 - \left(\frac{V+V_1}{I_{a2}}\right).\sin \phi_1 \cdot \gamma_o' \cdot \delta_c\right\} - \phi_1\right]$$

Now, due to source inductance, the capacitor C will be charged to a voltage $V_2 > V$. The differential equation describing this mode is given by

$$L_s \cdot \frac{di_s}{dt} + \frac{1}{C}\int i_c.dt = V \text{ with } v_c(o)=V \text{ and } i_c(o) = I'_{a2}$$

The solution for i_c is given by

$$i_c = I'_{a2} \cdot \cos \gamma_o [\, t-(\delta+\delta_c)T \,]$$

where, $I'_{a2} = \frac{I_{a2}}{\sin \phi_i} \cdot \sin(\gamma_o' \cdot \delta_c T + \phi_i)$

and $$\gamma_o = \frac{1}{\sqrt{L_s \cdot C}} \qquad (2.26)$$

This mode ends when $i_c=0$ at $t-(\delta+\delta_c)T = \frac{\pi}{2}$. Now, the over charged capacitor will discharge partially through the supply and free wheeling diode and the current is given by

$$i_c = \frac{V_2-V}{\sqrt{(L_m+L_s)/C}} \sin \gamma_o'' t' \qquad (2.27)$$

where $\gamma_o'' = \frac{1}{\sqrt{(L_s+L_m)C}}$, and t' is measured from the instant discharging of C takes place. This mode ends when $i_c=0$ which gives

$$\gamma_o'' \cdot \lambda' T = \pi$$

or, $\lambda' = \frac{\pi}{\gamma_o'' \cdot T} \approx \frac{\pi}{\gamma_o T}$ as $L_m \ll L_s$.

III. Free Wheeling Interval: $(\delta + \delta_c)T \leq t \leq (\gamma)T$

The armature current starts free wheeling at $t = \delta' T$, i.e. when the commutating capacitor has been

charged to +V and the free wheeling diode is forward biased. The differential equation describing this mode is given by

$$L_a \frac{di_a}{dt} + R_a . i_a = -E \text{ with } i_a(\delta' T) = I'_{a2} \text{ (say)}$$

The armature current is given by

$$i_a = -\frac{E}{R_a}(1-e^{-t'/T_a}) + \frac{V-E}{R_a}(1-e^{-\delta T/T'_a}).e^{-t'/T_a} \cdot \frac{\sin(\gamma'_o \delta_c T+\phi_1)}{\sin \phi_i} \qquad (2.28)$$

where, $t' = t - \delta' T$.

Let at $t = \gamma T$, the armature current i_a become zero. Substituting $i_a=0$ in equation (2.28) yields

$$\gamma = \delta' - \frac{T_a}{T} \text{Log}_e \left[\frac{(E/V) \cdot \sin \phi_i}{(E/V).\sin \phi_i + (1-\frac{E}{V}).(1-e^{-\delta T/T'_a}) \sin(\gamma'_o \delta_c T+\phi_i)} \right] \qquad (2.29)$$

Under discontinuous conduction, I_{av} is given by

$$I_{av} = \frac{V.\delta - (\gamma - \delta_c)E}{R_a} + \frac{C(V+V_1)}{T} \qquad (2.30)$$

IV. Reverse Armature Current Interval

This mode exists if the armature current has reached

zero value at $t = \gamma T$. The commutating capacitor C will again discharge through the source, the motor armature circuit, L_m and D. The equivalent circuit is shown in Figure 2.2(e). The capacitor will discharge only if $E + V_1 > V$.

The differential equation describing this mode is

$$(L_a+L_s+L_m)\frac{di_c}{dt'} + R_a i_c + \frac{1}{C}\int_0^{t'} i_c.dt' = E-V+V_1$$

where, $v_c(o) = V_1$ and $i_c(o) = 0$.

The solution for i_c after neglecting the voltage drop across R_a is

$$i_c = I_m \cdot \sin \omega_o t' \qquad (2.31)$$

where, $t' = (t-\gamma T)$, $I_m = \dfrac{E+V_1-V}{\sqrt{(L_a+L_s+L_m)/C}}$ and

$$\omega_o = 1/\sqrt{(L_a+L_s+L_m).C}.$$

The final voltage across the capacitor is then given by

$$V_1' = (E+V_1-V) - (L_s+L_a+L_m)\left.\frac{di_c}{dt'}\right|_{t'=(1-\gamma)T} \qquad (2.32)$$

If this mode occurs and sufficient time is available for C to discharge, there is a strong possibility of commutation

failure in the next cycle. The value of V_1 in equation (2.30) is unknown and it can be determined approximately as follows. For a given δ, I_{a2} is determined from equation (2.24) and then V_1 is determined from equation (2.11).

The steady state electromagnetic torque is given by equation (2.21) and the speed is given by equation (2.22). When discontinuous conduction just fails to occur (i.e. minimum i_a=0), γ= 1 and the critical value of $(\frac{E}{V})_{cr}$ above which discontinuous conduction occurs, can be determined from equation (2.29) for a given δ by trial.

2.3 ANALYSIS WITHOUT SOURCE INDUCTANCE.

The analysis in this case is carried out on the basis of assumptions mentioned in Section 2.2.

2.3.1 Continuous Conduction:

I. Duty Interval $(0 \leq t \leq \delta T)$

This interval starts with the firing of the main thyristor T_1. The differential equation describing this mode is given by equation (2.4) with μ= 0. The armature current is given by equation (2.5) after substituting μ= 0. The armature current I_{a2} at the end of this interval is given by equation (2.6) with μ= 0 and $T'_a = T_a$.

II. Commutation Interval. $\delta T \leq t \leq (\delta+\delta_c)T$

This interval starts when commutating thyristor T_2 is turned on and on the assumption that the main thyristor is immediately turned off and the entire load current flows through the commutating capacitor and remains constant at the level $i_a=I_{a2}$. The interval $\delta_c T$ during which the capacitor is charged from -V to V is given by equation (2.7) with $V_1=V$. This interval ends when C is charged to V.

III. Free Wheeling Interval: $(\delta+\delta_c)T \leq t \leq (1-\delta-\delta_c)T$

This interval starts when C has been charged to V and i_c has become zero. The equivalent circuit is shown in Fig. 2.2(f).

The expression for armature current is given by equation (2.12). The armature current I_{a1} at the end of this interval is given by equation (2.13) after substituting $\mu = 0$. The expressions for I_{a1} and I_{a2} obtained after elimination of variables,are given by equations (2.14) and (2.15) respectively with $a = 0$ and $\mu = 0$.

The commutation interval $\delta_c T$ is given by equation (2.19). The expressions for A,B and C in this case are obtained after noting that $V_1 = V$. Thus from equation (2.7),

$$A = \frac{E}{V}\left(\frac{T}{T_a}\right) e^{-T/T_a} + \frac{CR_a}{T_a}\left(\frac{T}{T_a}\right) \cdot e^{-T/T_a}$$

$$B = -\frac{E}{V}(1-e^{-T/T_a}) + (1-e^{-\delta T/T_a}) + \frac{2CR_a}{T_a} e^{-T/T_a}$$

$$C = -\frac{2CR_a}{T}(1-e^{-T/T_a}).$$

2.3.2 Discontinuous Conduction

I. Duty Interval : $0 \leq t \leq \delta T$

The armature current during this mode is given by equation (2.23) with $T_a' = T_a$. The armature current I_{a2} at the end of this interval is given by equation (2.24) with $T_a' = T_a$.

II. Commutation Interval: $\delta T \leq t \leq (\delta + \delta_c)T$

The current during commutation is given by equation (2.25) with $L_s = 0$ and $V_1 = V$. The commutation interval $\delta_c T$ is given by

$$\delta_c T = \frac{1}{\gamma_2}\left[\cos^{-1}(\cos \phi_i - \frac{2V}{I_{a2}} \cdot \sin \phi_i \cdot \gamma_2 \cdot C) - \phi_i\right] \qquad (2.33)$$

The current at the end of this interval I_{a2}' is given by

equation (2.26) with $\gamma_2 = \frac{1}{\sqrt{L_a \cdot C}}$ and $\phi_i = \tan^{-1}\left[\frac{\gamma_2 \cdot L_a \cdot I_{a2}}{2V-E}\right]$.

III. Free Wheeling Interval: $(\delta + \delta_c)T = t = \gamma T$

The current i_a during this interval is given by equation (2.12). The armature current i_a becomes zero at $t = \gamma T$. Substituting $i_a = 0$ corresponding to $t = \gamma T$ in equation (2.12) yields,

$$\gamma = \delta' + \frac{T_a}{T} \log_e \left[\frac{V}{E} + \left(1 - \frac{V}{E}\right) \cdot e^{-\delta T/T_a}\right] \qquad (2.34)$$

The average armature current I_{av} is given by equation (2.30) with $V_1 = V$. The critical value of $\left(\frac{E}{V}\right)_{cr}$ below which conduction becomes continuous can be found out by trial solution of equation (2.34) by substituting $\gamma = 1$ for a given value of δ.

IV. Reverse Armature Current Interval: $T \leq t \leq (1-\gamma)T$

This interval exists if the armature current has already reached zero value at $t = \gamma T$. The equivalent circuit representing this mode of operation is given by Figure 2.2(e) with $L_s = 0$ and $V_1 = V$. If sufficient time is available, the commutating capacitor will get discharged to a low value and commutation failure may occur in this case also. The current i_a in this case is given by equation (2.31) with $L_s = 0$ and V_1 being replaced by V.

This mode continues until the beginning of the next cycle. If this mode of operation continues for sufficient time, the commutating capacitor may discharge completely and commutation failure will take place in the next cycle. The voltage on the capacitor at the end of this mode is given by

$$v_{c_f} = V - \frac{1}{C} \int_0^{t'} I_m . \sin \Omega_o t' . dt'$$

$$= V + \frac{I_m}{C . \Omega_o} \left\{ \cos \Omega_o (1 - \gamma) T - 1 \right\}$$

The analysis presented in Sections 2.2 to 2.3 are also applicable for a square wave output chopper except that commutation intervals are absent.

2.4 CHOPPER AS A CONTROLLER FEEDING A BACK E.M.F. LOAD

The chopper is used as a controller in high performance d.c. motor speed control systems. The incremental gain, of the chopper is an important factor in the design of control system employing chopper-fed d.c. motors. The steady state transfer function of a chopper can be defined [3] as the relationship between the mean output voltage v_o delivered to the load by the chopper and the chopper control voltage v_c.

$$\frac{v_o}{V} = \frac{\text{Average voltage across the load}}{\text{Input voltage of chopper}} = G = \text{Open loop gain.}$$

The 'normalised gain' is defined as

$$F = \left(\frac{V_o/V}{V_c/V_{cm}} \right) = \frac{G}{\delta} \qquad (2.35)$$

where,

$$\frac{V_c}{V_{cm}} = \frac{\text{Available control voltage of chopper}}{\text{Available maximum control voltage of chopper}} = \delta$$

I. Chopper with load current dependent commutation

For continuous conduction, open loop gain is given by,

$$\text{'open loop gain'} = \frac{E + I_{av}.R}{V} = G$$

Substituting the value of I_{av} from equation (2.20) into above, yields,

$$G = (\delta - \mu) + \frac{E}{V} \cdot \delta_c + \left(\frac{2CR}{T} - \frac{R}{\gamma_o T.V} \right) \qquad (2.36)$$

In the absence of source inductance, $\mu = 0$ and $\frac{R}{\gamma_o T.V}$ term is absent.

The normalised p.u. gain $= \left(\frac{V_o/V}{V_c/V_{cm}} \right)$

$$= 1 - \left(\frac{\mu}{\delta} \right) + \frac{E}{V} \cdot \left(\frac{\delta_c}{\delta} \right) + \frac{2CR}{T.\delta} - \frac{R}{\gamma_o T. \delta.V} \qquad (2.37)$$

The 'incremental gain' is defined as,

$$G_{in} = \frac{\Delta G}{\Delta \delta}$$

For discontinuous conduction, the open loop gain is obtained by substituting the value of I_{av} from equation (2.30) into the expression for G, as

$$G = \delta + \frac{E}{V}(1 - \gamma + \delta_c) + \frac{C.R}{T}(1 + \frac{V_1}{V}) \qquad (2.38)$$

If there is no source inductance, then the terms containing μ and γ_o in equations (2.36) and (2.37) will be absent. For discontinuous conduction case, V_1 is taken equal to V in equation (2.38) assuming that the mode IV operation in Section 2.3.2 is insignificant.

II. Chopper with square wave output voltage:

The 'open loop gain' G in this case is given by equation (2.36) with $\delta_c = 0$ and the terms containing γ_o and C absent for continuous conduction. For discontinuous conduction, G is given by equation (2.38) with $\delta_c = 0$ and the terms containing C absent.

The incremental open loop gain $= \frac{\Delta G}{\Delta \delta} = G_{in} = 1.0$ for continuous conduction.

and $G_{in} = 1 - \frac{E}{V}(\frac{d\gamma}{d\delta})$ for discontinuous conduction.

2.5 PERFORMANCE AND EXPERIMENTAL VERIFICATION

Experiments were carried out on a d.c. separately excited motor using a two thyristor load current commutated

chopper as shown in Figure 2.1. The particulars of the test motor are given below:

Rating : 220V, D.C., $\frac{1}{2}$ H.P., 1500 r.p.m.

The parameters found from static test are

L_a = armature inductance = .088H (at rated current)

R_a = armature resistance = 4.13 ohms (hot)

L_m = .0005 H

L_s = source inductance = 0.040H (unsaturated d.c. value)

The source consisted of a 220V, D.C. 3 KW separately excited generator. The armature circuit inductances were measured using a well known bridge method described by C.V. Jones [17]. The back e.m.f. coefficient $K(I_a)$ is approximately taken to be equal to $K(I_{av})$. $K(I_{av})$ is determined from the internal characteristic of the motor. Thus $K(I_{av})$ includes armature reaction effect.

The torque-speed characteristics of the test motor were calculated for a chopper operating frequency of 400 Hz using equations (2.17), (2.19), (2.20), (2.21) and (2.22) taking the effect of source inductance into account. Figure 2.4 shows the calculated and experimental chnacteristics. There is a satisfactory agreement between the calculated and the measured curves. Calculations were also done neglecting the

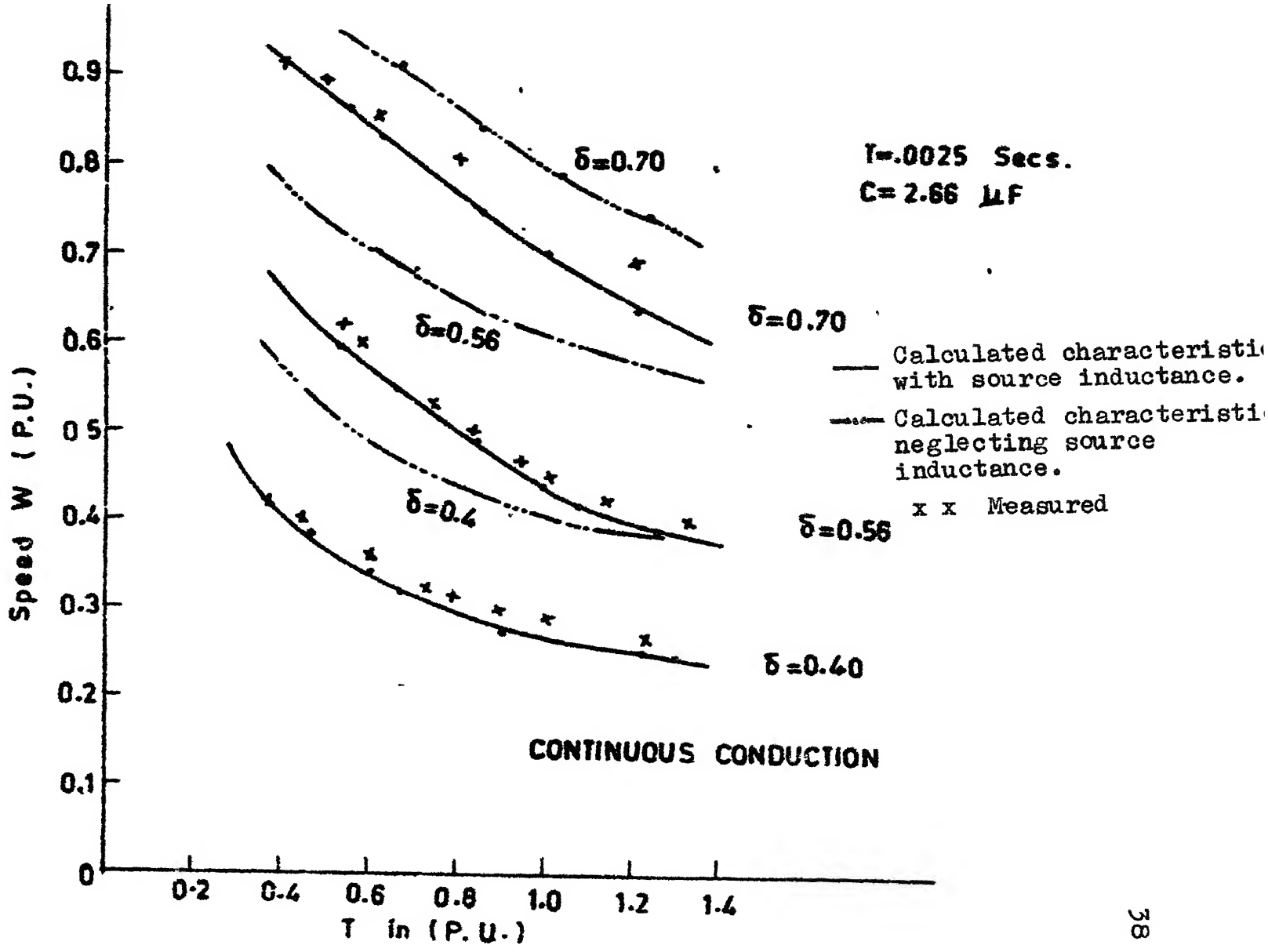

Fig. 2.4 Speed-torque characteristics (L_s = .04H)

effect of source inductance and using equation (2.19), with $\mu = 0$ and $\frac{1}{\gamma_o T}$ term absent, and equations (2.21) and (2.22). The calculated torque-speed characteristics without taking the effect of source inductance into account, are also shown in Figure 2.4. The difference between the two characteristics is quite significant. The decrease in effective on interval of chopper due to source inductance reduces average voltage across motor terminals. Higher is the load current greater is the reduction in motor terminal voltage for a given δ. As a result of this, droop in torque speed characteristics is more. This shows that the predicted curves will be in considerable error if source inductance is neglected. It is also found that for this chopper operating frequency of 400 Hz, discontinuous conduction did not occur in the presence of source inductance. Figure 2.5 shows the characteristics at 400 Hz when a buffer condenser bank of 8000 μF was used at the source terminals. The characteristics are also calculated using equations (2.19), (2.20), (2.21) and (2.22) without taking the effect of source inductance, in which case $\mu = 0$ and the terms containing γ_o are absent. In this case, however, discontinuous conduction was clearly noticeable and the experimental and theoretical boundaries of discontinuous conduction have been shown in Figure 2.5.

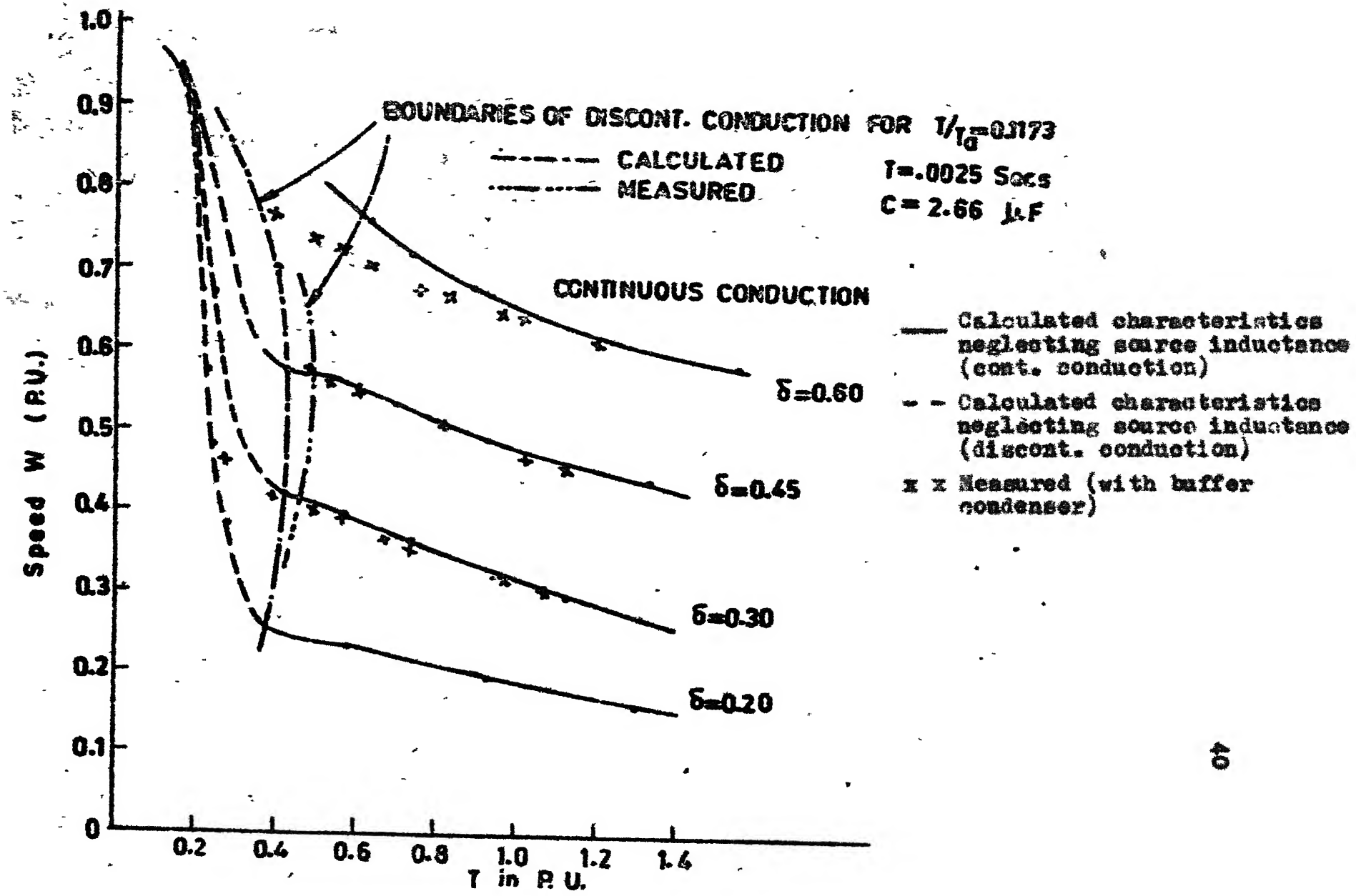
BOUNDARIES OF DISCONT. CONDUCTION FOR T/Tq=0.3173
CALCULATED
MEASURED
T=.0025 Secs
C= 2.66 μF
CONTINUOUS CONDUCTION
δ=0.60
δ=0.45
δ=0.30
δ=0.20
Speed W (P.U.)
T in P.U.
1.0
0.9
0.8
0.7
0.6
0.5
0.4
0.3
0.2
0.1
0
0.2
0.4
0.6
0.8
1.0
1.2
1.4
Calculated characteristics neglecting source inductance (cont. conduction)
Calculated characteristics neglecting source inductance (discont. conduction)
x x Measured (with buffer condenser)

The theoretical boundary of discontinuous conduction was calculated from equation (2.34). The close agreement between measured characteristics and those predicted neglecting the source inductance shows that the use of a buffer condenser neutralizes the effect of source inductance.

Figure 2.6 shows the torque speed characteristics of the machine for a chopper operating frequency of 250 Hz. in the presence of a source inductance of 40 mH. With the same commutation circuit parameters, commutation difficulties were encountered at this low frequency operation because of two reasons: firstly, due to increase in value of I_{a2} and secondly due to reverse armature current conduction (mode IV operation during discontinuous conduction) which provided enough time for C to discharge. Commutation failure occurred for $\delta > 0.5$. Commutation failure also took place for $\delta = 0.31$ at high speed under discontinuous conduction (due to mode IV operation). It is also observed that the boundary of discontinuous conduction has shifted further to the right on the torque speed plane, i.e. increased the region of discontinuous conduction. Figure 2.7 shows the measured torque speed characteristics of the motor at 250 Hz when the buffer condenser bank was connected across the

Fig. 2.6 Speed torque characteristics in presence of armature inductance (T_a = .004 sec).

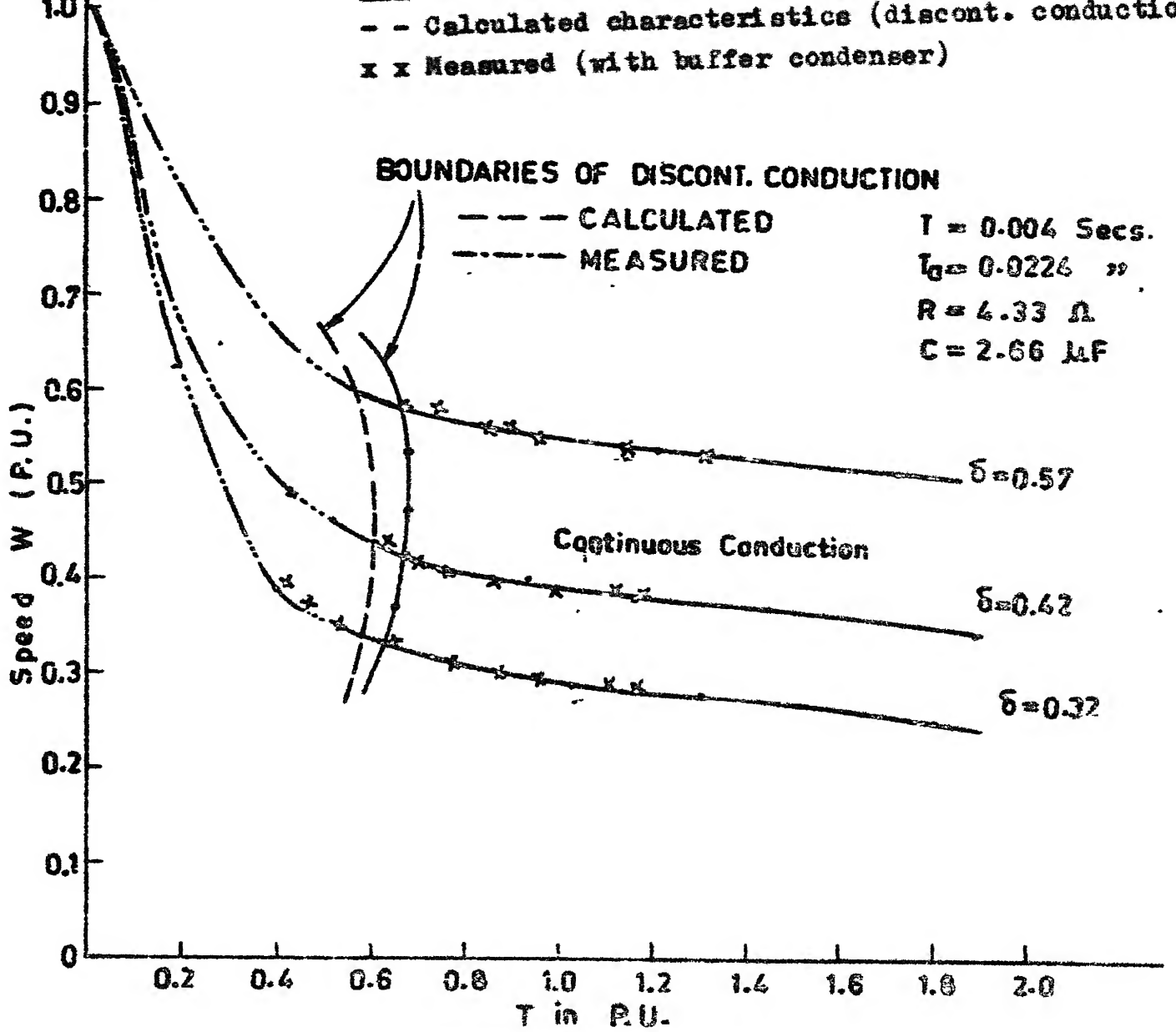

Fig. 2.7 Speed-torque characteristics (with buffer condenser, T = .004 sec)

source. Commutation difficulties were also observed in this case for $\delta = .31$ at high speed under discontinuous conduction due to mode IV operation. The characteristics were then calculated ignoring source inductance. The close agreement between the experimental and calculated curves shows that the use of a suitable buffer condenser bank neutralizes the effect of source inductance. Comparing these characteristics with those of Figure 2.6 shows that the region of discontinuous conduction has increased and speed regulation in continuous conduction region has become better. Comparison of Figures 2.5 and 2.7 indicates that the use of a high frequency eliminates discontinuous conduction or reduces it to a narrow region. Fig. 2.8 shows the variation of open loop gain $(\frac{V_o}{V})$ with $(\frac{V_c}{V_{cm}})$ for the load current commutated chopper with C= 2.66 μF and $(\frac{T}{T_a})=0.1173$. The calculations were done using equations (2.37), (2.38) without taking the effect of source inductance. The line corresponding to $\frac{E}{V} = 0$ represents the boundary of discontinuous conduction for an ideal square wave chopper without any source inductance. It is found that the boundary of discontinuous conduction shifts to the left of $\frac{E}{V} = 0$ line for a load current commutated chopper, i.e. it reduces the region of discontimuous conduction. It is

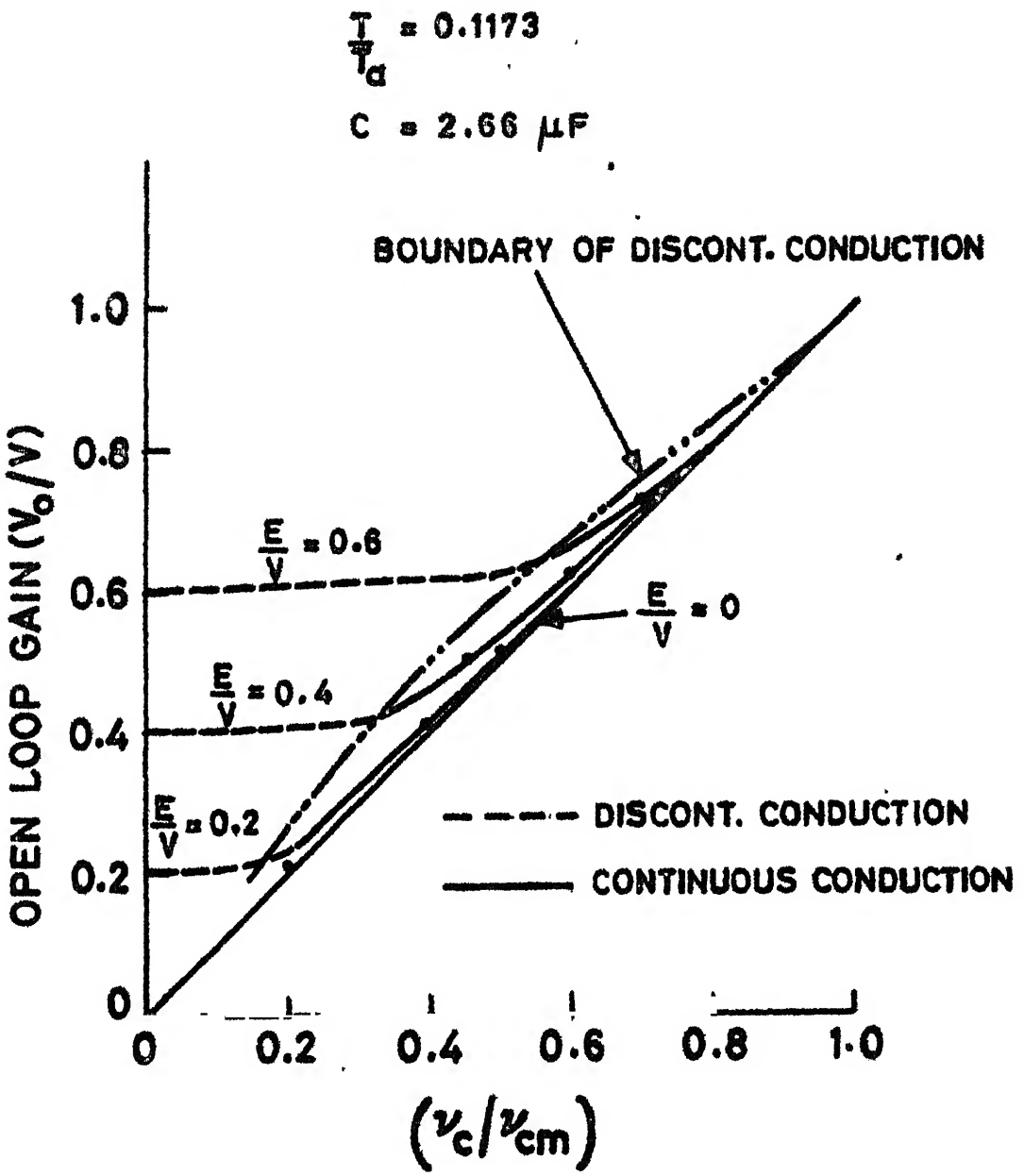

Fig. 2.8 Open loop gain vs. chopper control voltage.

also found that the 'incremental gain' $\frac{dG}{d\delta}$ is very small in the region of discontinuous conduction and it is near about unity in the continuous conduction region. If considerable amount of source inductance be present, then 'open loop gain' reduces during continuous conduction as it is evident from equation (2.36).The corresponding incremental gain $\frac{dG}{d\delta}$ also reduces due to source inductance.

2.6 CONCLUSIONS

The following important conclusions are drawn from the above study:

1. The method of analysis presented here is general in the sense that it takes into account the effect of source inductance, chopper commutation interval, armature reaction and discontinuous conduction. There is close agreement between predicted and experimental performance.

2. Source inductance has considerable effect on the motor torque-speed curves. The droop in speed becomes larger and the region of discontinuous conduction is reduced. Since the commutating capacitor may charge to a voltage less than the source voltage, chopper commutation failure may take place if commutation capacitor value is selected neglecting the source inductance. The use of buffer

condenser bank at the source terminal, neutralizes the effect of source inductance, thus increasing the region of discontinuous conduction and reducing the drop in speed.

3. If the current zero interval stays for a long time, commutation capacitor may discharge and commutation failure may occur.

4. The operation of chopper at low frequencies increases the region of discontinuous conduction on the torque-speed plane. For reliable prediction of machine performance, discontinuous conduction should be taken into account.

5. The open loop gain of a chopper controlled d.c. motor system decreases due to source inductance. The chopper commutation interval increases the open loop gain. The incremental gain $\frac{dG}{d\delta}$ is very small under discontinuous conduction.

CHAPTER III

PERFORMANCE AND ANALYSIS OF CHOPPER FED D.C. SEPARATELY EXCITED MOTOR UNDER REGENERATIVE BRAKING

3.1 INTRODUCTION

One of the important features of chopper control is that it permits the regenerative braking of the machine down to a very low speed thus improving the over all efficiency of the drive. This chapter presents a study of regenerative braking of chopper fed d.c. separately excited motor.

G. Kimura and M. Shioya [7] have described a graphical technique for analysis of regenerative braking of a d.c. separately excited motor fed by a chopper with square wave output voltage. Their method does not take into account the effect of source inductance, chopper commutation interval and armature reaction which have considerable effect on the braking performance.

In the present chapter, initially a method of analysis is presented for chopper with square wave output voltage. The expressions have been derived for braking torque, regenerated power and efficiency of regeneration. The effect of filter inductor on the boundary of discontinuous conduction, current

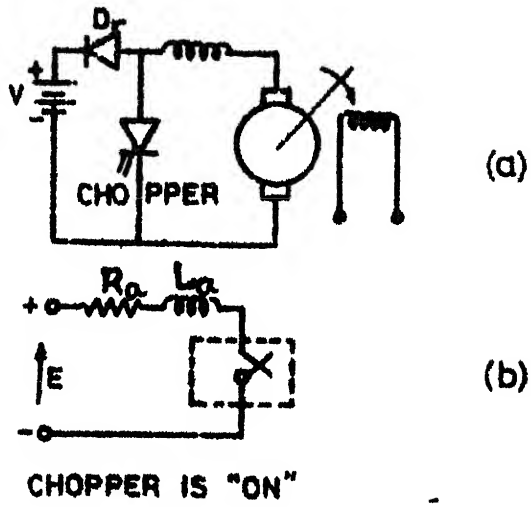

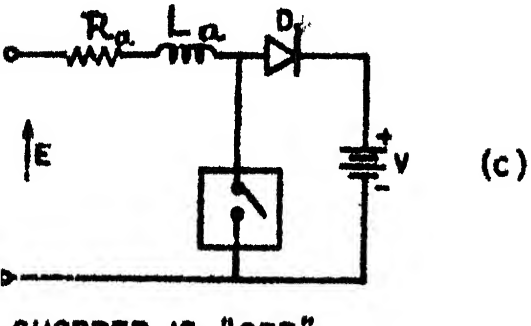

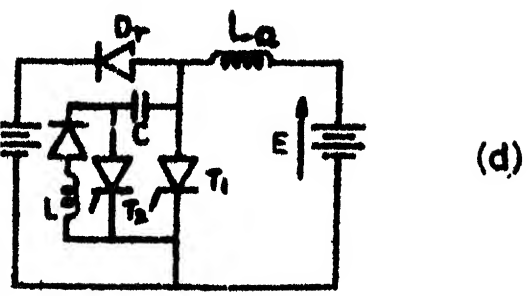

Fig. 3.1 Regenerative braking of chopper controlled d.c. separately excited motor.

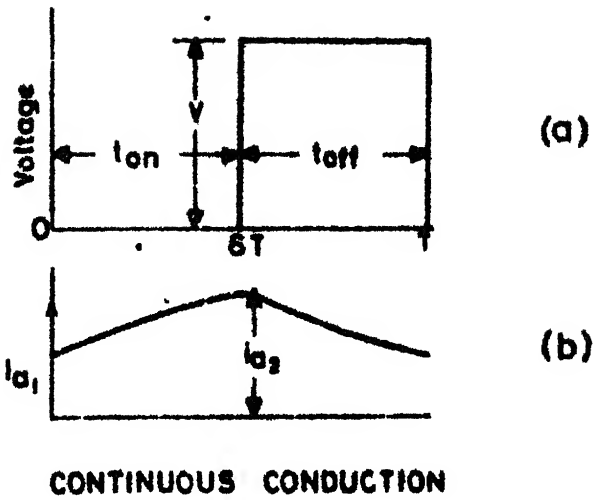

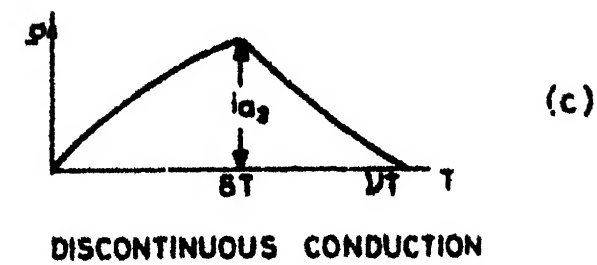

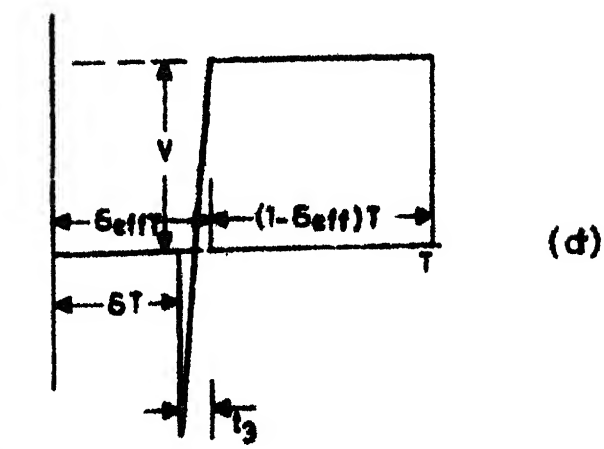

Fig. 3.2 Chopper output voltage and armature current wave forms

ripple, regenerated power and efficiency of regeneration have been considered and a method is presented for the choice of a suitable value of filter inductance. Later, the analysis and performance have been presented for chopper with load dependent commutation (with non-square output voltage), incorporating the effect of source inductance, commutation pulse and armature reaction.

A basic scheme for a separately excited motor controlled by a chopper under regenerative braking is shown in figure 3.1(a). D_r is the diode that provides the path for regenerative current to flow against the supply voltage V. The equivalent circuits under ideal conditions are shown in Figures 3.1(b) and 3.1.(c). The idealised output voltage and current waveforms of the chopper under regenerative braking mode have been shown in Figures 3.2(a) and 3.2(b) respectively. Figure 3.2(c) shows the armature current waveform under discontinuous conduction. In some chopper circuits, the output voltage is neither a square wave nor can be approximated by a square wave. In case of chopper with load current dependent commutation as shown in Figure 3.1(d), the output voltage waveform is neither a square wave nor can it be approximated by a square wave without loss of accuracy. The armature current is not a smooth d.c. but contains ripples superimposed on the d.c.

component. During on period, the motor is like a short circuited generator and during off period, it forces current against the supply. In both these modes, the motor produces braking torque. Depending upon the motor speed, δ and (T/T_a) ratio, the armature current may be discontinuous. Large ripples and discontinuous conduction give rise to poor machine performance and commutation problems.

3.2 ANALYSIS WHEN FED BY A CHOPPER WITH SQUARE WAVE OUTPUT VOLTAGE [19]

The output voltage and current waveforms for such a chopper has been shown in Figures 3.2(a) to 3.2(c). In a separately excited d.c. motor, the induced e.m.f. is given by

$$E = K_e \cdot \phi \cdot \omega_{av} = K \cdot \omega_{av} \qquad (3.1)$$

In equation (3.1), K will be a constant in the absence of armature reaction. In the presence of armature reaction, K will vary with armature current. In case of chopper, armature current fluctuates between maximum and minimum values. The average effect of armature reaction will be taken into account by considering K to be a function of average value of current I_{av}. Thus,

$$K = f(I_{av}) \qquad (3.2)$$

706205

The analysis is carried out based on the assumptions (i), (ii) and (iii) in Section 2.2 of Chapter II.

3.2.1 Continuous Conduction

I. Duty Interval: ($0 \leq t \leq \delta T$)

The equivalent circuit describing this mode is shown in Figure 3.1(b). The differential equation describing this mode is

$$E = R_a \cdot i_a + L_a \cdot \frac{di_a}{dt} \qquad (3.3)$$

with initial condition $i_a(0) = I_{a1}$.

The solution of i_a is given by

$$i_a = \frac{E}{R_a} (1 - e^{-t/T_a}) + I_{a1} \cdot e^{-t/T_a} \qquad (3.4)$$

II. Regeneration Interval: ($\delta T \leq t \leq T$)

The equivalent circuit describing this mode is shown in Figure 3.1(c). The differential equation describing this mode is

$$E = R_a \cdot i_a + L_a \frac{di_a}{dt} + V \qquad (3.5)$$

with $i_a(\delta T) = I_{a2}$.

The solution of i_a is given by

$$i_a = \frac{E-V}{R_a} (1-e^{-t/T_a}) + I_{a2} \cdot e^{-t/T_a} \qquad (3.6)$$

In the steady state, from equations (3.4) and (3.6), we get,

$$I_{a2} = \frac{E}{R_a}\left(1-e^{-\delta T/T_a}\right) + I_{a1}\cdot e^{-\delta T/T_a} \qquad (3.7)$$

and

$$I_{a1} = \frac{E-V}{R_a}\left(1-e^{-(1-\delta)T/T_a}\right) + I_{a2}\cdot e^{-(1-\delta)T/T_a} \qquad (3.8)$$

From equations (3.7) and (3.8), by elimination of variables, we get,

$$I_{a2} = \frac{E}{R_a} - \frac{V}{R_a}\cdot\frac{1-e^{(1-\delta)T/T_a}}{1-e^{T/T_a}} \qquad (3.9)$$

$$I_{a1} = \frac{E}{R_a} - \frac{V}{R_a}\cdot\frac{1-e^{-(1-\delta)T/T_a}}{1-e^{-T/T_a}} \qquad (3.10)$$

$$\text{current ripple} = \Delta i_f = \frac{I_{a2}-I_{a1}}{2}$$

$$= \frac{V}{2R_a}\left[\frac{1-e^{-(1-\delta)T/T_a}}{1-e^{-T/T_a}} - \frac{1-e^{(1-\delta)T/T_a}}{1-e^{T/T_a}}\right] \qquad (3.11)$$

Equation (3.11) shows that the ripple is independent of E. The maximum value of ripple is given by δ_m corresponding to $\frac{d}{d\delta}(\Delta i_f) = 0$, which yields a value of $\delta_m = 0.5$.

$$\text{The maximum ripple} = \frac{V}{2R_a}\left[\frac{e^{0.5\,T/T_a}-1}{e^{0.5T/T_a}+1}\right] \qquad (3.12)$$

$$\frac{(\Delta i_f)_{max}}{\frac{V}{2R_a}} = \text{Normalised maximum ripple} = \frac{e^{0.5T/T_a} - 1}{e^{0.5T/T_a} + 1} \qquad (3.13)$$

3.2.2 Discontinuous Conduction.

In this case, the chopper operates in three distinct modes of operation, namely, duty interval, regeneration interval and current zero interval.

I. Duty Interval : $(0 \leq t \leq \delta T)$

Since for this interval the initial value of i_a will be zero, then from equation (3.4),

$$i_a = \frac{E}{R_a}(1-e^{-t/T_a}) \qquad (3.14)$$

II. Regeneration Interval: $(\delta T \leq t \leq \gamma T)$

Noting that I_{a2} is the value of i_a at the end of duty interval, we get from equation(3.6),

$$i_a = \frac{E-V}{R_a}(1-e^{-t/T_a}) + e^{-t/T_a} \cdot \frac{E}{R_a}(1-e^{-\delta T/T_a}) \qquad (3.15)$$

Let i_a become zero at $t = \gamma T$ measured from the begining of the duty interval, then from equation (3.15),

$$\frac{E-V}{R_a}(1-e^{-(\gamma-\delta)T/T_a}) + \frac{E}{R_a}(1-e^{-\delta T/T_a}).e^{-(\gamma-\delta)T/T_a} = 0 \qquad (3.16)$$

Solving for γ from equation (3.16) yields,

$$\gamma = \delta + \frac{T}{T_a} \log_e \left[\frac{E.\, e^{-\delta T/T_a} - V}{E-V}\right]$$

The average value of armature current can conveniently be calculated from

$$I_{av} = \frac{\gamma E - (\gamma - \delta)V}{R_a} \qquad (3.17)$$

The critical $(\frac{E}{V})_{cr}$ representing the boundary between continuous and discontinuous conduction is obtained by letting $\gamma = 1$ in equation (3.16) as

$$(\frac{E}{V})_{cr} = \frac{1-e^{-(1-\delta)T/T_a}}{1-e^{-T/T_a}} \qquad (3.18)$$

From equation (3.18),

$$(1-\delta) = -\frac{T}{T_a} \log_e \left[1-(\frac{E}{V})_{cr}.(1-e^{-T/T_a})\right] \qquad (3.19)$$

Now, $(\frac{E}{V})_{cr} = \frac{K.\omega_c}{V}$, where ω_c is the speed below which discontinuous conduction occurs for a given δ. Further, during continuous conduction

$$I_{av} = \frac{E-(1-\delta)V}{R_a} \qquad (3.20)$$

and at the point of transition to discontinuous conduction

$$I_{av} = \frac{K\omega_c - (1-\delta)V}{R_a} \qquad (3.21)$$

Substituting for $(1-\delta)$ from equation (3.19) into equation (3.21),

$$I_{av} = \frac{K\omega_c}{R_a} + \frac{V}{R_a}.\left(\frac{T_a}{T}\right)\log_e\left[1 - \frac{K\omega_c}{V}(1-e^{-T/T_a})\right]$$

T_{av} = average torque $= K.I_{av}$

$$= \left(\frac{K^2.V}{R_a}.\frac{\omega_c}{V}\right) + \frac{V}{R_a}.K.\left(\frac{T}{T_a}\right).$$

$$\log_e\left[1 - \frac{\omega_c}{V/K}(1-e^{-T/T_a})\right]$$

or, $\dfrac{T_{av}}{\left(\frac{V}{R_a}.K\right)} = T_p$ = normalised p.u. torque

$$= \omega_p + \frac{T_a}{T}.\log_e\left[1 - \omega_p(1-e^{-T/T_a})\right] \qquad (3.22)$$

where, $\frac{V}{K} = \omega_o$ = No load speed

$$\frac{\omega_c}{\omega_o} = \omega_p = \text{p.u. speed}$$

The equation (3.22) gives a boundary between continuous and discontinuous conduction on the normalised speed ω_p and normalised torque T_p plane for various values of $\frac{T}{T_a}$ ratio

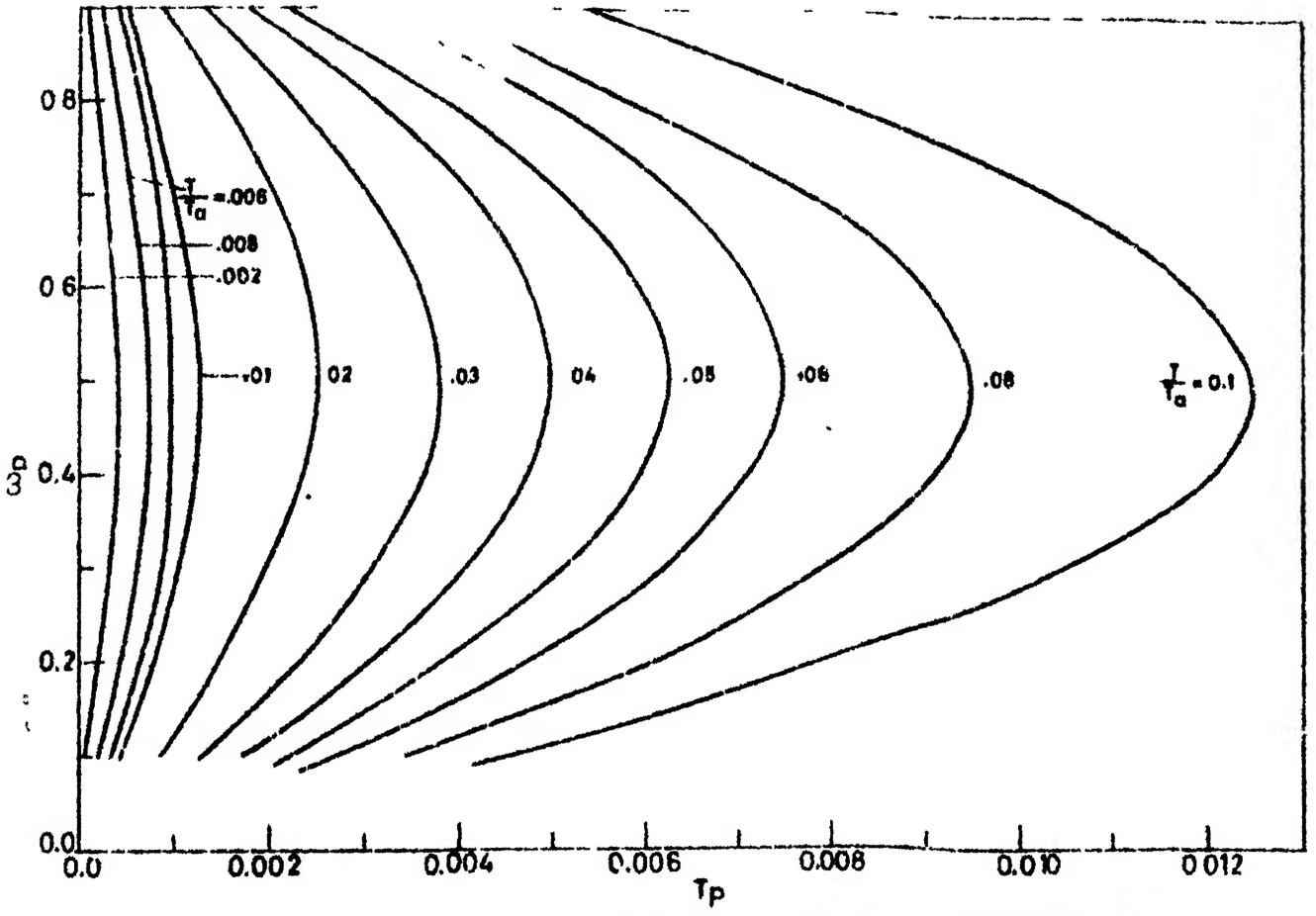

Fig. 3.3 Boundaries between discontinuous and continuous conduction on normalised torque-speed plane for various values of T/T_a.

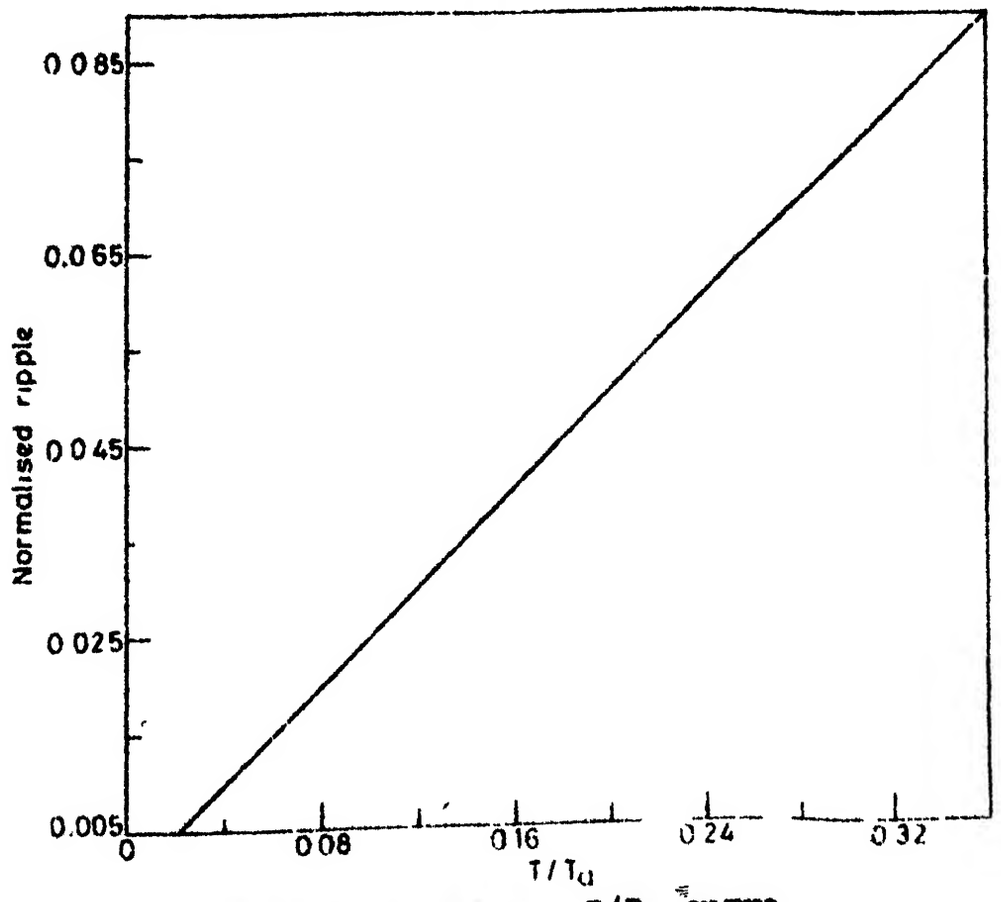

Fig. 3.4 Normalised ripple vs. T/T_a curve.

as shown in Figure 3.3. In order to eliminate discontinuous conduction, one should select that value of $(\frac{T}{T_a})$ which gives the boundary between continuous and discontinuous conduction to the left of the curve. Now maximum ripple is obtained from Figure 3.4 to check whether it is within the permissible value or not.

3.2.3 Expression for Braking Power and Efficiency of Regeneration

The braking power consists of the power lost in armature circuit resistances producing dynamic braking and the regenerative power that is fed back to the supply.

P_{em} = Total electromagnetic power developed by the machine during a cycle of period T.

$$= \frac{1}{T}\left[\int_0^{\delta T} E.i_a.dt + \int_{\delta T}^{T} E.i_a.dt\right] = E.I_{av} \qquad (3.23)$$

P_{rg} = Regenerative braking power

$$= E.I_{av} - I_{rms}^2 \cdot R_a \qquad (3.24)$$

Let P_{rdy} denote the dynamic braking loss $= I_{r.m\ s}^2.R_a$ (3.25)

Also for continuous conduction

$$P_{rg} = \frac{V}{T} \int_0^{(1-\delta)T} \cdot i_a.dt \qquad (3.26)$$

Substituting i_a from equation (3.6) into equation (3.26) and performing the integration yields,

$$P_{rg} = V\left[\frac{E-V}{R_a}(1-\delta)+\frac{T_a}{T}.\left(\frac{E-V}{R_a}\right)\left(e^{-(1-\delta)T/T_a}-1\right)\right.$$
$$\left.-\left\{\frac{E}{R_a}-\frac{V}{R_a}.\frac{1-e^{(1-\delta)T/T_a}}{1-e^{T/T_a}}\right\}\left(\frac{T_a}{T}\right).\left(e^{-(1-\delta)T/T_a}-1\right)\right] \qquad (3.27)$$

For discontinuous conduction, P_{rg} is obtained by substituting i_a from equation (3.15) into equation (3.26) and performing the integration, thus

$$P_{rg} = \frac{V(E-V)}{R_a}.(\gamma-\delta)+\frac{T_a}{T}\left(e^{-(\gamma-\delta)T/T_a}-1\right).\left(\frac{E.V}{R_a}e^{-\delta T/T_a}-\frac{V^2}{R_a}\right) \qquad (3.28)$$

The net braking torque T_{br} is given by,

$$T_{br} = \frac{E.I_{av}}{\omega} \qquad (3.29)$$

The efficiency of regeneration can be defined as

$$\eta_{rg} = \frac{P_{rg}}{P_{em}} = \frac{P_{rg}}{E.I_{av}} \qquad (3.30)$$

For continuous conduction, equation (3.27) can be rewritten as,

$$P_{rg} = \frac{V^2}{R_a}\left[\left(\frac{E}{V}-1\right).(1-\delta)+\frac{T_a}{T}.\frac{e^{(1-\delta)T/T_a}+e^{\delta T/T_a}-e^{T/T_a}-1}{1-e^{T/T_a}}\right] \qquad (3.31)$$

Now substituting for I_{av} from equation (3.20) and for P_{rg} from equation (3.31) into equation (3.30), yields

$$\eta_{rg} = \left[(\omega_r - 1).(1-\delta) + \frac{T_a}{T}\left\{\frac{e^{(1-\delta)T/T_a} + e^{\delta T/T_a} - e^{T/T_a} - 1}{(1 - e^{T/T_a})}\right\}\right]$$

$$\div \quad [\omega_r^2 - (1-\delta)\omega_r] \qquad (3.32)$$

where, $\omega_r = \frac{E}{V}$.

Equation (3.32) shows that for a given δ and ω_r, effieiency of regeneration depends on $(\frac{T_a}{T})$. Equations (3.20), (3.23) and (3.31) show that while braking power P_{em} is independent of $(\frac{T_a}{T})$, the regenerative power does depend on $(\frac{T_a}{T})$ and therefore depends on the chopping frequency and on the value of filter inductance. For discontinuous conduction, equation (3.28) can be rewritten as,

$$P_{rg} = \frac{V^2}{R_a}\left[(\omega_r - 1).(\gamma - \delta) + \frac{T_a}{T}.(e^{-(\gamma-\delta)T/T_a} - 1).(\omega_r.e^{-\delta T/T_a} - 1)\right]$$

(3.33)

The effieiency of regeneration η_{rg} is obtained from equation (3.30) on substitution from equations (3.17) and (3.33) as

$$\eta_{rg} = \frac{(\omega_r - 1).(\gamma - \delta) + \frac{T_a}{T}.(e^{-(\gamma-\delta)T/T_a} - 1).(\omega_r.e^{-\delta T/T_a} - 1)}{\omega_r^2 - (\gamma - \delta)\omega_r}$$

(3.34)

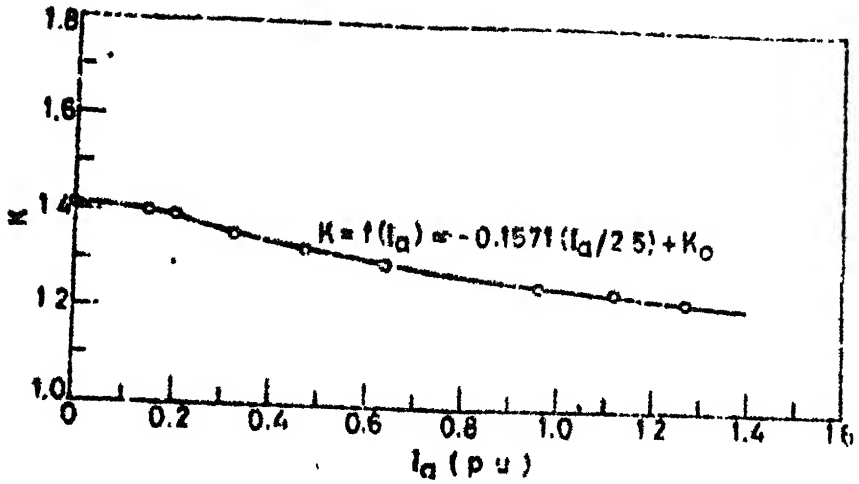

Fig. 3.5 Motor back e.m.f. coefficient K vs. armature current I_a.

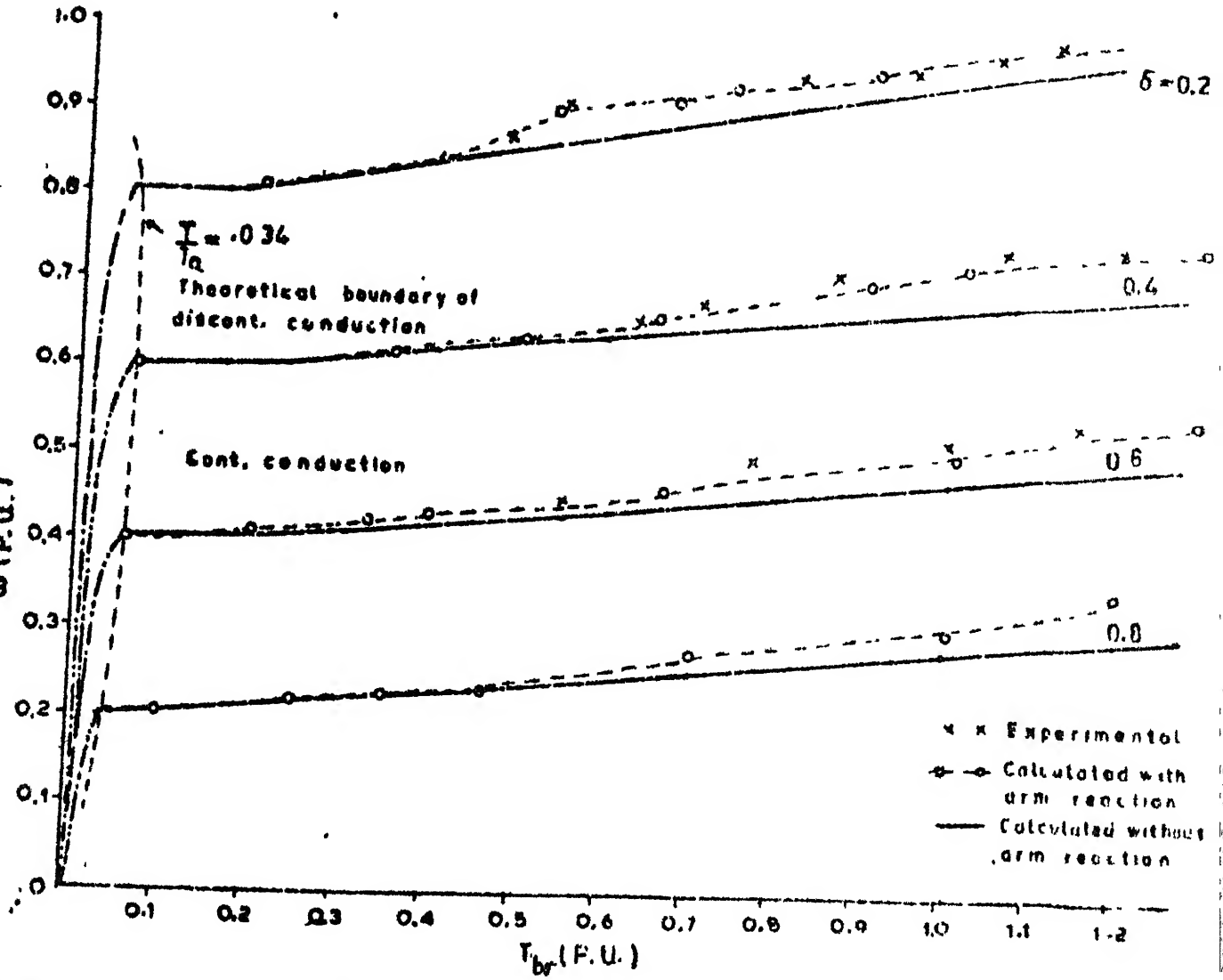

Fig. 3.6 Speed vs. Braking torque curves for various values of duty ratio .

Equations (3.17), (3.33) and (3.34) reveal that for a given value of δ and ω_r, generated power, regenerated power and efficiency of regeneration depend on $\frac{T}{T_a}$ and therefore on the chopping frequency and filter inductance.

3.2.4 Performance and Experimental Verification:

Tests were carried out on a d.c. separately excited motor whose details are given in Section 2.5 of Chapter II. The variation of machine e.m.f. coefficient K as a function of armature current I_a is shown in Figure 3.5. For practical purposes, K for the test machine can conveniently be represented by straight line approximation for higher values of I_a under constant field, i.e.,

$$K = -m \left(\frac{I_a}{I_A}\right) + K_o \qquad (3.35)$$

where m is the slope of the straight line, I_A is the rated current and K_o is a constant. In case of chopper control, I_{av} will replace I_a. The calculated curves of braking torque T_{br} versus speed ω are shown in Figure 3.6 for various values of δ. The measured values of torque and speed using an approximately square wave chopper are also shown in Figure 3.6. Discontinuous conduction was found to be almost absent for this value of $\frac{T}{T_a} = 0.034$. The calculated results

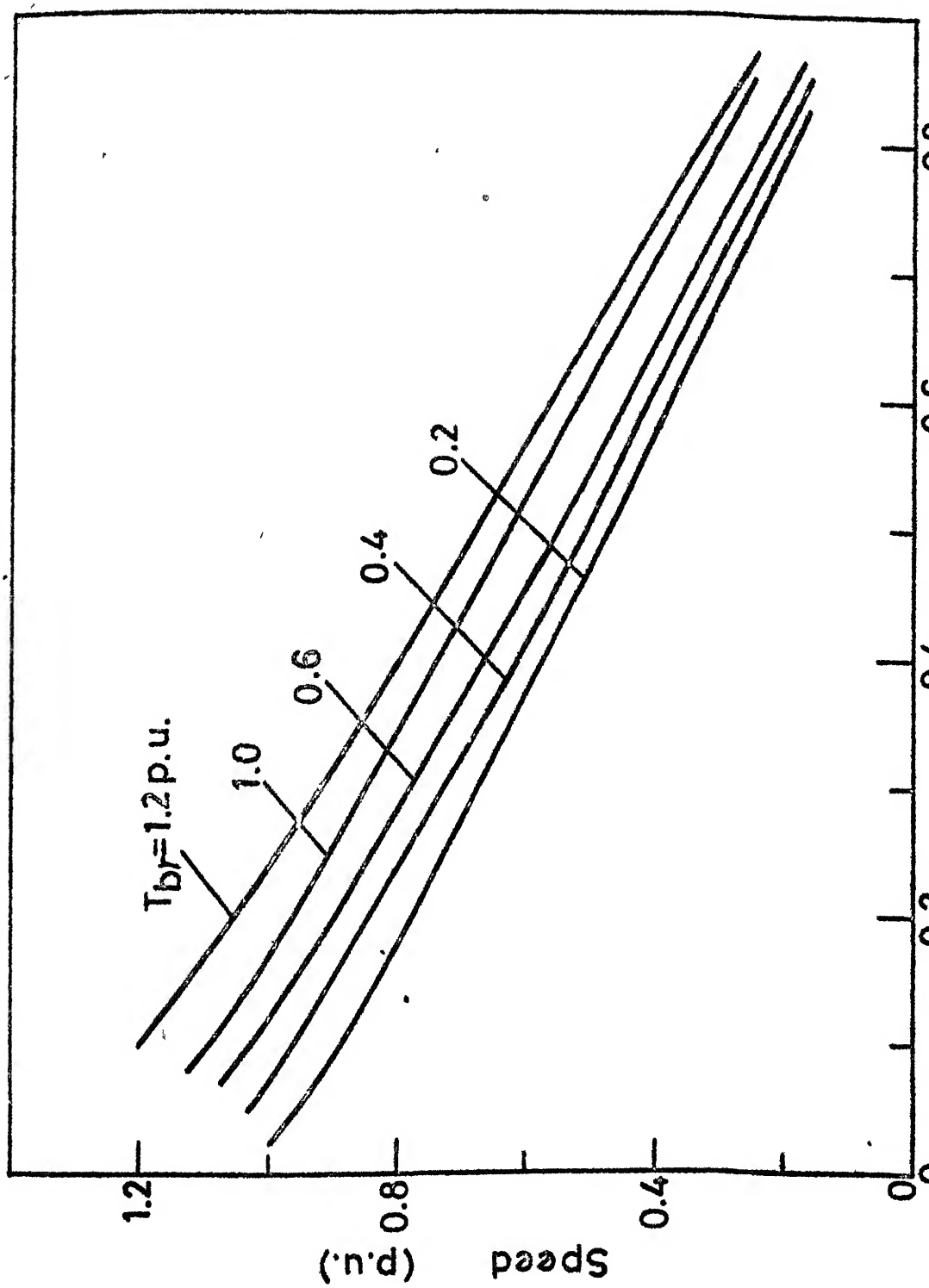

Fig. 3.7 Speed vs. duty ratio curves for constant braking torque.

closely agree with the experimental results after taking into account the effect of armature reaction on the value of K as shown by the relationship (3.35).

The curves in Figure 3.7 shows the relationship between δ and ω for constant braking torques. These curves suggest suitable closed loop control strategy to be adopted for producing constant braking torques under varying machine speed. The curves in Figure 3.8 show the relationship between P_{rg} and ω for different values of δ and for different values of $\frac{T}{T_a}$. The values of P_{rg} were calculated using equation (3.27). The machine speed was calculated from the equation

$$\omega = \frac{E}{K(I_{av})}$$

$K(I_{av})$ was obtained from equation (3.35). The curves show that armature reaction reduces the value of P_{rg} for a fixed machine speed by a considerable amount. It is also seen that P_{rg} reduces as δ increases and P_{rdy} increases with δ as expected. From the value of P_{rdy}, one can calculate the effective value of armature current $I_{r.m.s.}$. The 'form factor' = $\frac{I_{r.m.s.}}{I_{av}}$ is not a fixed quantity but varies with δ as well as with $(\frac{T}{T_a})$. For sufficiently high values of filter inductance, the average and effective values of armature current are almost equal.

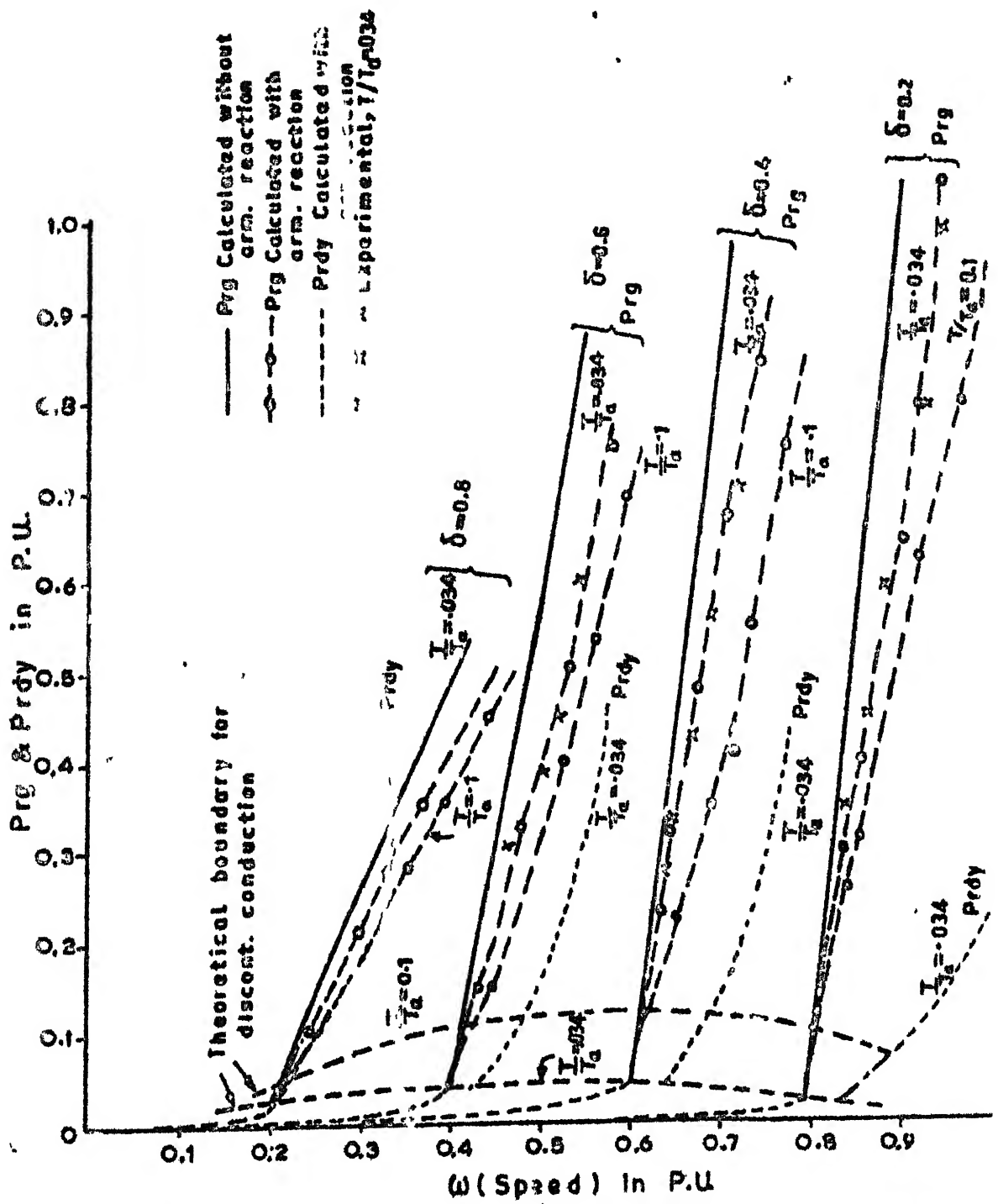

Fig. 3.8 P_{rg} vs. speed curves for various values of T/T_a.

The computed curves of P_{rg} versus ω for $(\frac{T_a}{T}) \geq 20$ with a fixed value of δ are almost same and have been shown by a single curve for clarity. The computed curves of P_{rg} for $\frac{T_a}{T} = 10$ show that P_{rg} decreases as $(\frac{T_a}{T})$ decreases for a fixed value of speed. This is due to increase in ripple in the armature current. The variation of P_{rg} with $\frac{T_a}{T}$ for given values of speed corresponding to a fixed value of δ is shown in Figure 3.9. The nature of the curves reveal that P_{rg} decreases appreciably for values of $\frac{T_a}{T} < 10$. For sufficiently low values of $\frac{T_a}{T}$, the conduction may be discontinuous in a wide region of the speed-torque plane. It is seen from Figure 3.9 that for $\frac{T_a}{T} \geq 20$, there is practically no change in the value of P_{rg} for a given δ and fixed speed. This corresponds to values of maximum normalised ripple ≤ 0.012. Thus, the value of $\frac{T_a}{T} = 20$ can be considered optimum as it gives nearly maximum regenerative power and it also reduces the armature current ripple to fairly low value. The efficiency of regeneration η_{rg} was calculated using equation (3.32) for various values of $\frac{T}{T_a}$ ratio for given values of ω_r and δ. The curves in Figure 3.10 show that for fixed value of δ and ω_r, η_{rg} is almost constant for $\frac{T}{T_a} > 5$ and η_{rg} decreases rapidly for $\frac{T_a}{T} < 2$. Thus the value of $(\frac{T_a}{T}) = 20$ also permits the realisation of maximum value of regenerated power if the increase in losses due to increase in filter inductance is neglected.

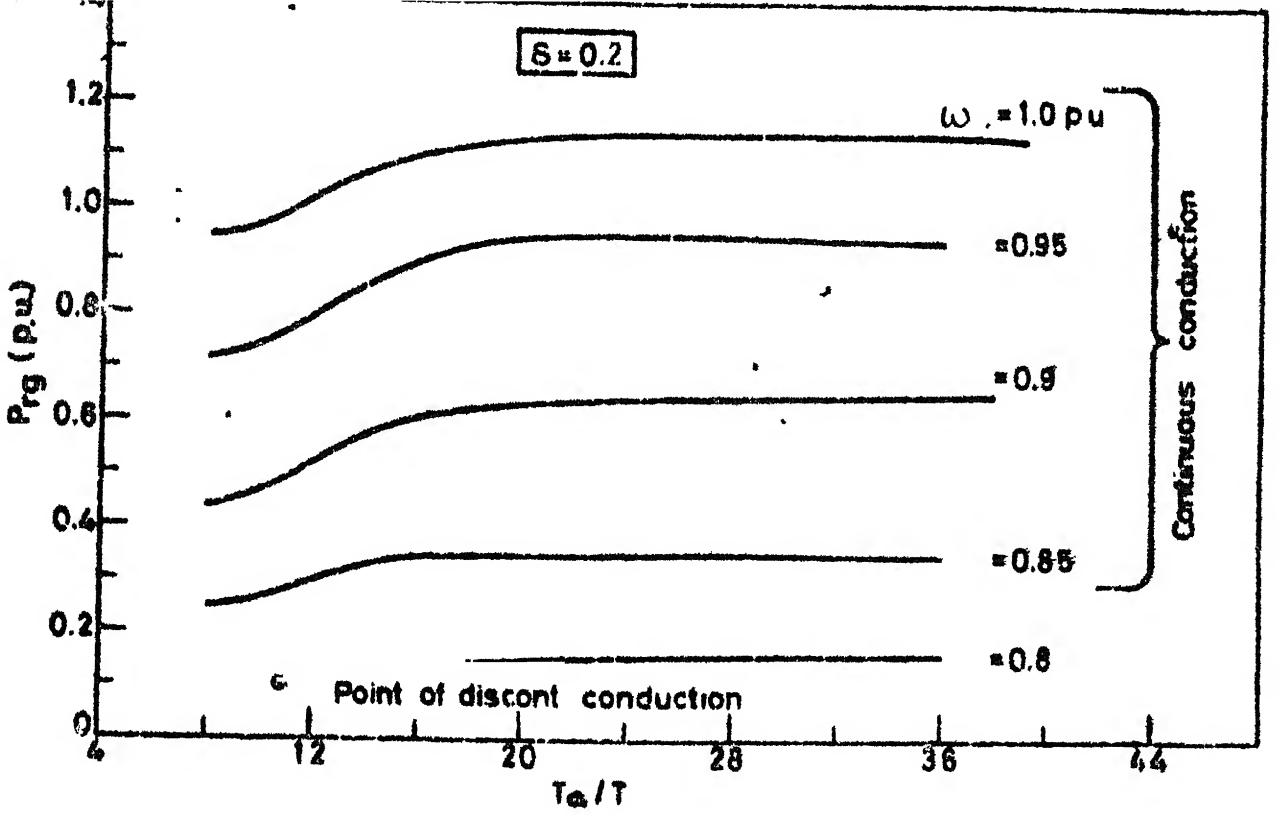

Fig. 3.9 P_{rg} vs. T_a/T curves for various values of speed.

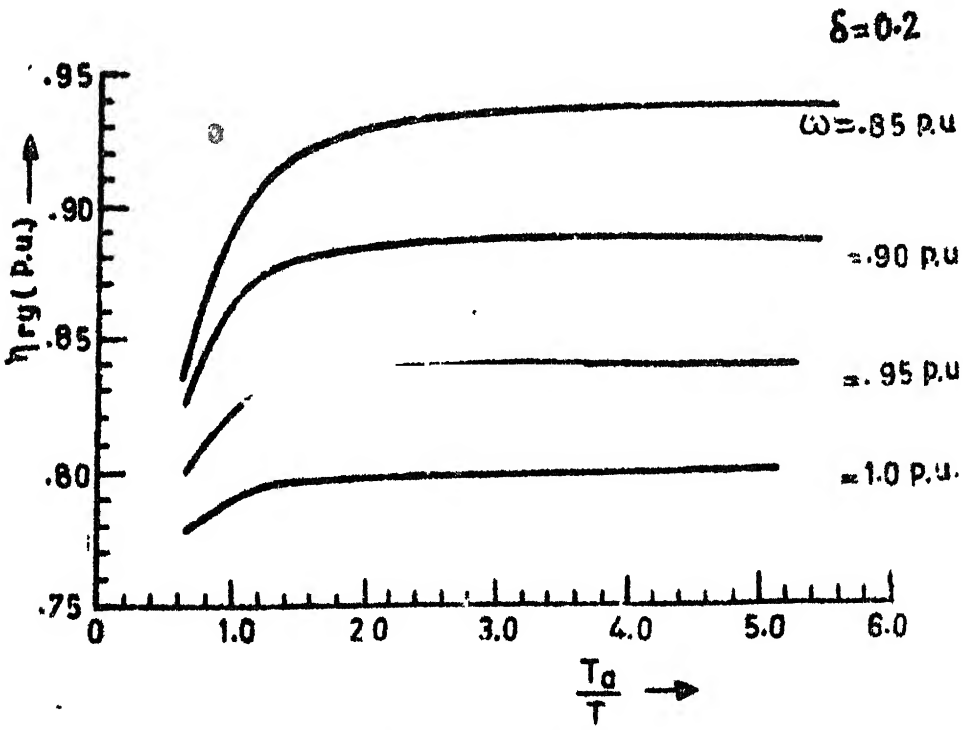

Fig. 3.10 Efficiency of Regeneration (η_{rg}) vs. T/T_a curves for various values of speed.

3.3 ANALYSIS WHEN FED BY CHOPPER WITH LOAD DEPENDENT COMMUTATION.

Figure 3.1(d) shows the circuit representation of a typical load current commutated chopper controlled d.c. separately excited motor under regenerative braking. In addition to the assumptions described in Section 3.2, it is also assumed that during commutation interval, the load current remains constant. Initially, source inductance will be neglected. There are three distinct modes of operation, namely, duty interval, commutation interval and regeneration interval.

3.3.1 Continuous Conduction

I. Duty Interval: $(0 \leq t \leq \delta T)$

This mode begins with the turning on of the main Thyristor T_1 and continues until the auxiliary thyristor T_2 is turned on. The differential equation describing this mode is given by equation (3.3) and i_a is given by equation (3.4). The equivalent circuit is shown in Figure 3.11(a).

II. Commutation Interval : $(\delta T \leq t \leq (\delta + \delta_c)T)$

This interval starts when the auxiliary thyristor T_2 is turned on. On the assumption of constant current during commutation, the commutation interval $(\delta_c T)$ during which the

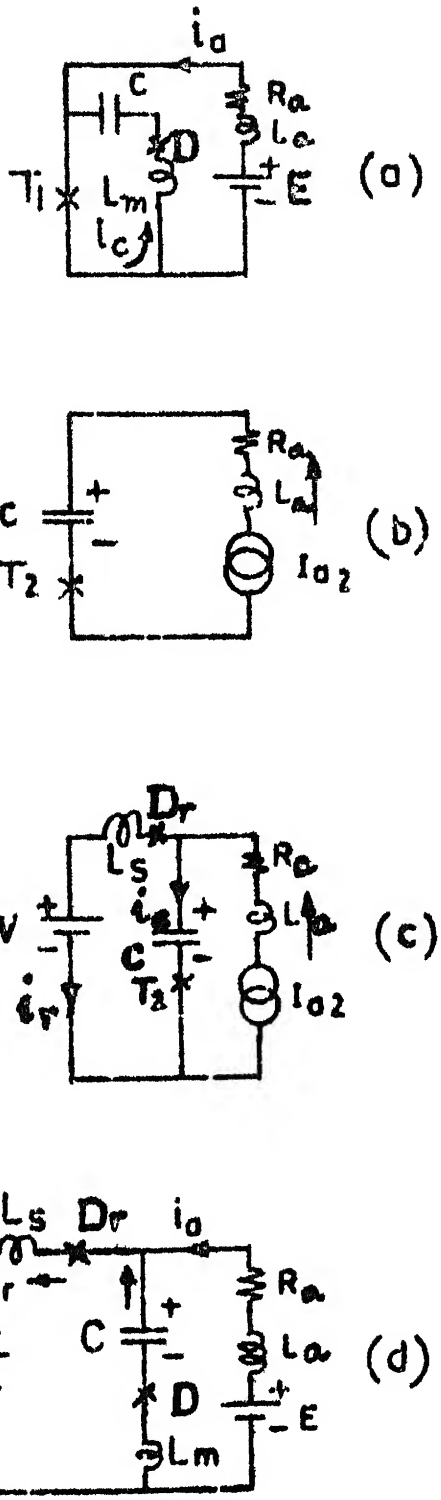

Fig. 3.11 Chopper Equivalent Circuits.

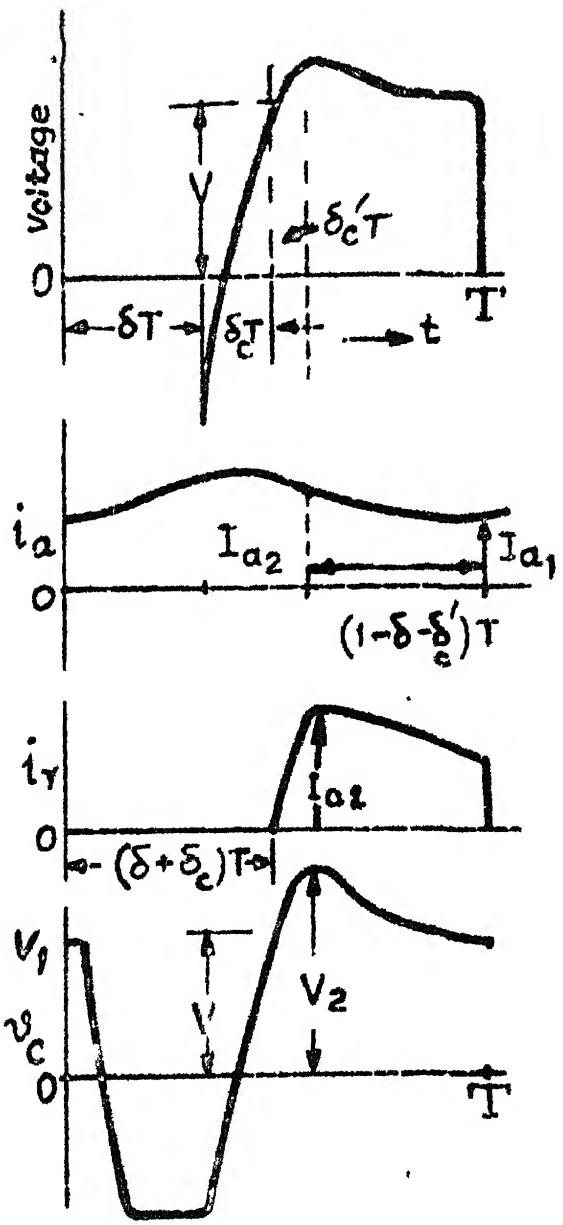

Fig. 3.12 Idealised Chopper Output Voltage and Current Wave forms.

commutating capacitor gets charged from a voltage -V to +V is given by

$$\delta_c = \frac{2C.V}{I_{a2}.T} \qquad (3.36)$$

The equivalent circuit for this mode is shown in Figure 3.11(b).

III. Regeneration Interval: $(\delta + \delta_c)T \leq t \leq T$

This mode starts as soon as the commutating capacitor C is charged to +V thus D_r is forward biased and current is forced against the source giving regeneration. The equivalent circuit describing this mode is shown in Figure 3.1(c). The differential equation describing this mode is given by equation (3.5) and i_a is given by equation (3.6). The expressions for I_{a1} and I_{a2} are obtained from equations (3.7) and (3.8) taking equation (3.36) into account as,

$$I_{a2} = \frac{E}{R_a} - \frac{V}{R_a} \cdot \frac{1-e^{(1-\delta')T/T_a}}{1-e^{(1-\delta_c)T/T_a}} \qquad (3.37)$$

$$I_{a1} = \frac{E}{R_a} - \frac{V}{R_a} \cdot \frac{1-e^{-(1-\delta')T/T_a}}{1-e^{-(1-\delta_c)T/T_a}} \qquad (3.38)$$

where, $\delta' = (\delta + \delta_c)$.

In the above equations, δ_c is unknown. It can be determined from equation (3.36) as follows.

Substituting the value of I_{a2} from equation (3.37) into equation (3.36), one gets,

$$\delta_c = \frac{2CR}{T} \cdot \frac{1-e^{(1-\delta_c)T/T_a}}{(\frac{E}{V}-1)-\frac{E}{V}\cdot e^{(1-\delta_c)T/T_a} + e^{(1-\delta')T/T_a}} \qquad (3.39)$$

Now, expanding the terms containing $e^{-\delta_c \frac{T}{T_a}}$ in terms of its power series, yields a quadratic in δ_c after neglecting all terms containing 3rd and higher powers in δ_c, as,

$$A.\ \delta_c^2 + B.\ \delta_c + C = 0 \qquad (3.40)$$

where,

$$A = [\frac{T}{T_a} \cdot \frac{E}{V} \cdot e^{T/T_a} - \frac{T}{T_a} \cdot e^{(1-\delta)T/T_a} + \frac{CR_a}{T_a} \cdot e^{T/T_a}]$$

$$B = \frac{E}{V} \cdot (1-e^{T/T_a}) - (1-e^{(1-\delta)T/T_a}) - \frac{2CR_a}{T_a} \cdot e^{T/T_a}$$

$$C = -\frac{2CR_a}{T} \cdot (1-e^{T/T_a})$$

Now,

$$\delta_{c1,2} = -\frac{B}{2A} \pm \frac{\sqrt{B^2-4A.C}}{2A} \qquad (3.41)$$

For a given $\frac{E}{V}$, the positive realistic value of δ_c is obtained from equation (3.41). The steady state average current I_{av} under continuous conduction is given by,

$$I_{av} = [\frac{E}{V}(1-\delta_c)-(1-\delta')]\frac{V}{R_a} + \frac{2.C.V}{T} \qquad (3.42)$$

The developed electromagnetic torque is given by equation (3.29). The p.u. normalised ripple is given by

$$\text{p.u. normalised ripple} = \frac{I_{a2}-I_{a1}}{(\frac{V}{R_a})} = \left[\frac{1-e^{-(1-\delta')T/T_a}}{1-e^{-(1-\delta_c)T/T_a}} - \frac{1-e^{(1-\delta')T/T_a}}{1-e^{(1-\delta_c)T/T_a}}\right] \qquad (3.43)$$

Unlike in the case of chopper with square wave, the p.u. normalised ripple is dependent on the machine back e.m.f. E and hence the speed because δ_c is dependent on $(\frac{E}{V})$ as seen in equation (3.41).

3.3.2 Discontinuous Conduction:

I. Duty Interval : $0 \leq t \leq \delta T$

The equivalent circuit is shown in Figure 3.11(a). For this interval, the armature current i_a is given by equation (3.14) and the value of I_{a2} at the end of this interval is given by

$$I_{a2} = i_a(\delta T) = \frac{E}{R_a}(1-e^{-\delta T/T_a}) \qquad (3.44)$$

II. Commutation Interval : $\delta T \leq t \leq (\delta + \delta_c)T$

On the assumption of constant current during commutation, the commutation interval is given by equation (3.36). The equivalent circuit is given by Figure 3.11(b). Substituting I_{a2} from equation (3.44) into equation (3.36), yields

$$\delta_c = \frac{1}{T} \cdot \frac{2\,C.V.R_a}{E.(1-e^{-\delta T/T_a})} \qquad (3.45)$$

The equation (3.45) is valid except for very light load condition. In that case, a more accurate analysis will be to solve the exact differential equation given by,

$$L_a \frac{di_c}{dt} + R_a.i_c + \frac{1}{C}\int_{\delta T}^{(\delta+\delta_c)T} i_c.dt = E-V \qquad (3.46)$$

where the initial condition is $i_c(0^+) = I_{a2}$.

Neglecting the voltage drop across the resistance, the solution for i_c is given by,

$$i_c = \frac{I_{a2}}{\sin \phi_1}\left\{\sin \omega_o'((t-\delta T)+\phi_i)\right\} \qquad (3.47)$$

where $\phi_i = \tan^{-1}\dfrac{\omega_o' L_a.I_{a2}}{2V-E}$

and

$$\gamma'_o = \frac{1}{\sqrt{L_a \cdot C}}$$

The interval $\delta_c T$ during which the capacitor gets charged from -V to +V is then obtained from,

$$v_c(\delta_c T) = V = \frac{1}{C} \int_o^{\delta_c T} i_c \, dt'$$

where, $t' = (t - \delta T)$

or,

$$\delta_c = \frac{1}{\gamma'_o T} \left[\cos^{-1} \left\{ \cos \phi_i - \frac{(2V)}{I_{a2}} \cdot \sin \phi_i \cdot \gamma'_o \cdot C \right\} - \phi_i \right] \tag{3.48}$$

Equation (3.48) provides a more accurate estimation of commutation interval under light load conditions.

III. Regeneration Interval : $(\delta + \delta_c)T \leq t \leq \gamma T$

This mode starts when C has been charged to +V and diode D_r is forward biased. The armature current will flow against the supply producing regenerative braking. The equivalent circuit is shown in Figure 3.1(c). The differential equation is given by,

$$L_a \frac{di_a}{dt} + R_a i_a = E - V \quad \text{with } i_a(0) = I_{a2}$$

The solution of i_a is given by equation (3.15). The armature

current becomes zero at $t = \gamma T$. Substituting $i_a = 0$ for $t = \gamma T$, yields

$$\gamma = \delta' + \frac{T_a}{T} \log_e \left[\frac{E.e^{-\delta T/T_a} - V}{E - V} \right] \qquad (3.49)$$

The average armature current I_{av} can be calculated from

$$I_{av} = \frac{(\gamma - \delta_c)E - (1 - \delta')V}{R_a} + \frac{2CV}{T} \qquad (3.50)$$

The critical value of $(\frac{E}{V})$ below which discontinuous conduction occurs is obtained from equation (3.49) by substituting $\gamma = 1$. Thus,

$$\left(\frac{E}{V} \right)_{cr} = \frac{K \cdot \omega_c}{V} = \left[\frac{1 - e^{-(1-\delta')T/T_a}}{1 - e^{-(1-\delta_c)T/T_a}} \right] \qquad (3.51)$$

As seen by equation (3.51), critical speed is a function of δ and δ_c where δ_c is not known. The boundary of discontinuous conduction is obtained from equation (3.51) by trial. First, for a given δ, a suitable value of δ_c is chosen and the corresponding $(\frac{E}{V})$ is calculated from equation (3.51). The corresponding values of torque and speed are calculated. If the calculated point does not lie on the torque speed characteristic for continuous conduction, another value of δ_c is chosen and the calculations are repeated.

The expression for braking power under continuous conduction is given by equation (3.27) with δ replaced by δ'. Under discontinuous conduction, the regenerative power is given by equation (3.28) with δ replaced by δ'. The braking torque is given by equation (3.29). The efficiency of regeneration is given by equation (3.30).

3.3.3 Analysis in Presence of Source Inductance.

With the assumptions mentioned in Section 3.2 and further assuming constant current during commutation interval, the analysis is carried out for continuous conduction as follows

I. Duty Interval : $(0 \leq t \leq \delta T)$

The equivalent circuit is shown in Figure 3.11(a). The differential equation is given by equation (3.3) and armature current is given by equation (3.4). The current I_{a2} at the end of this interval is given by equation (3.7).

II. Commutation Interval:$(\delta T \leq t \leq (\delta + \delta_c)T)$

The equivalent circuit is shown in Figure 3.11(b). On the assumption of constant current during commutation, the interval ($\delta_c T$) during which the commutating capacitor gets charged from a voltage of $-V_1$ to $+V$ is given by $\delta_c = C(V+V_1)/I_{a2}T$. In the presence of source inductance, V_1 may be greater or less than V depending upon the circuit parameters.

III. Regenerative Interval I:($0 \leq t' \leq \delta_c' T$)

This interval starts when the commutating capacitor C has been charged to +V and the diode D_r is forward biased. Due to the presence of source inductance L_s, the entire armature current can not be transferred immediately to the supply but it rises slowly and during this interval, a part of the load current flows through the commutating capacitor which overcharges it to a voltage $V_2 > V$. The charging process stops when $i_c=0$. It can be assumed that, the armature current remains constant at I_{a2} during this interval, an assumption which is always valid when there is a large inductance connected in the armature circuit. The equivalent circuit describing this mode is shown in Figure 3.11(c).

The equations describing this mode are,

$$i_a = I_{a2} = i_r + i_c \tag{3.52}$$

and

$$L_s \cdot \frac{di_r}{dt'} + V = \frac{1}{C} \int_0^{t'} i_c \cdot dt' + v_c(o) \tag{3.53}$$

where, $v_c(o) = V$ and $i_c(o) = I_{a2}$

and t' is the time redefined from the beginning of this mode. The solution for i_c is obtained from (3.52) and (3.53), as,

$$i_c = I_{a2} \cdot \cos \gamma_o t' \tag{3.54}$$

The regenerative current i_r is obtained from equation (3.52) after substituting i_c from equation (3.54) as

$$i_r = I_{a2} (1-\cos \gamma_o t') \qquad (3.55)$$

where, $\gamma_o = \frac{1}{\sqrt{L_s \cdot C}}$,

The condenser will continue to charge until $i_c=0$. This gives $\delta_c' = \frac{\pi}{2\gamma_o T}$. The voltage to which the condenser is charged is given by,

$$V_2 = V + \frac{1}{C} \int_0^{\delta_c' T} i_c . dt' \qquad (3.56)$$

The maximum value of V_2 occurs corresponding to $\delta_c' = \frac{\pi}{2\gamma_o T}$, which yields,

$$V_2 = V + \sqrt{\frac{L_s}{C}} \cdot I_{a2} \qquad (3.57)$$

If the value of γ_o is such that i_c does not become zero before the beginning of the next cycle, then the next two modes of operation are absent.

IV. Regenerative Interval II: $(0 \leq t' \leq \beta T)$

This interval starts immediately after the condenser current i_c has reached zero in the previous mode and the entire armature current flows against the supply producing regenerative braking. The capacitor C being overcharged, it discharges partially against the supply mains and also through the armature circuit loop. The equivalent circuit describing this mode is shown in Fig. 3.11(d). The partial discharge of C will continue until $i_c = 0$ or the beginning

f the next cycle whichever is earlier. The equations escribing this mode are,

$$i_a - i_r = i_c$$

oop I : $$L_a \frac{di_a}{dt'} + R_a i_a + \frac{1}{C} \int_0^{t'} i_c \cdot dt' + L_m \cdot \frac{di_c}{dt'} = E - V_2$$

oop II : $$-L_m \cdot \frac{di_c}{dt'} - \frac{1}{C} \int_0^{t'} i_c \, dt' + L_s \cdot \frac{d}{dt'} (i_a - i_c) = V_2 - V$$

nitial conditions are, $i_a(o) = I_{a2}$, $v_c(o) = V_2$ and $i_c(o) = 0$. Where t' is the time measured from the beginning of this mode. Taking Laplace's transform, the expression for $I_c(s)$ is given by

$$I_c(s) = \frac{(L_a s + R_a) \cdot \left\{ \frac{V_2 - V}{s} + L_s \cdot I_{a2} \right\} - L_s \cdot s \left(\frac{E - V_2}{s} + L_a \cdot I_{a2} \right)}{-(L_a s + R_a) \left\{ (L_s + L_m) s + \frac{1}{Cs} \right\} - L_s \cdot s \left(\frac{1}{Cs} + L_m s \right)} \qquad (3.58)$$

If the voltage drop across resistance R_a is neglected, then the time domain solution of i_c obtained by taking inverse transform of equation (3.58) is given by

$$i_c(t') = -I_{max} \sin \gamma_1 t' \qquad (3.59)$$

where, $$I_{max} = \frac{V_2(L_a + L_s) - V \cdot L_a - L_s \cdot E}{\sqrt{L_a L_s + L_a L_m + L_s \cdot L_m}} \cdot \sqrt{\frac{C}{L_a + L_s}}$$

and $\gamma_1 = \sqrt{\frac{(L_a L_s)}{(L_a L_s + L_a L_m + L_m L_s) C}}$

The final voltage V_1 on the condenser is given by

$$V_1 = V_2 + \frac{1}{C} \int_0^{\beta T} -I_{max} \cdot \sin \gamma_1 t' \, dt'$$

$$= V_2 + \frac{I_{max}}{C \gamma_1} \left[\cos \gamma_1 \beta T - 1 \right] \qquad (3.60)$$

The armature current during this interval is given by,

$$L_a \frac{di_a}{dt'} + R_a i_a + L_s \cdot \frac{di_r}{dt'} + V = E \qquad (3.61)$$

with $i_a(o) = i_r(o) = I_{a2}$

and $i_r = (i_a - i_c)$.

Now, substituting the value of i_c from equation (3.59) in to equation (3.61), yields,

$$i_a(t') = \frac{E-V}{R_a} (1 - e^{-\alpha_1 t'}) + I_{a2} e^{-\alpha_1 t'} + \left(\frac{L_s}{L_s + L_a}\right) \cdot \alpha_1 \cdot \gamma_1 \cdot I_{max} \left(\frac{e^{-\alpha_1 t'}}{\alpha_1^2 + \gamma_1^2}\right)$$

$$- \left(\frac{L_s}{L_s + L_a}\right) \cdot \frac{\gamma_1 \cdot I_{max}}{\alpha_1^2 + \gamma_1^2} \left(\alpha_1 \cos \gamma_1 t' + \gamma_1 \cdot \sin \gamma_1 t' \right).$$

where $\alpha_1 = \frac{R_a}{L_a + L_s} = \frac{1}{T'_a}$.

Since $\gamma_1^2 \gg \alpha_1^2$, so $\frac{\alpha_1}{\alpha_1^2 + \gamma_1^2}$ is a very small quantity and hence, it can be neglected. Again, γ_1 being a large quantity, the armature current can approximately be written as,

$$i_a(t') = \frac{E-V}{R_a}(1-e^{-\alpha_1 t'}) + I_{a2}.e^{-\alpha_1 t'} \qquad (3.62)$$

The current at the end of this interval is then given by,

$$I'_{a2} = i_a(\beta T) = \frac{E-V}{R_a}(1-e^{-\alpha_1 . \beta T}) + I_{a2}.e^{-\alpha_1 . \beta T} \qquad (3.63)$$

V. Regenerative Interval III: $(0 \leq t' \leq (1-\delta-\delta_c-\delta'_c-\beta)T)$

This interval starts when the condenser current i_c has reached zero value in the previous mode. If i_c does not become zero before the turning on of the main thyristor in the next cycle, this mode does not exist. The equivalent circuit is shown in Fig. 3.11(d) with diode D in blocked state.

The differential equation is given by,

$$(L_s+L_a)\frac{di_a}{dt'} + R_a.i_a = E-V$$

with $i_a(o) = I'_{a2}$

The solution of i_a is given by

$$i_a = \frac{E-V}{R_a}(1-e^{-\alpha_1 t'}) + I'_{a2}.e^{-\alpha_1 t'} \qquad (3.64)$$

The armature current at the end of this interval is

$$i_a(T)=I_{a1} = \frac{E-V}{R_a}\left\{1-e^{-(1-\delta'')T/T_a'}\right\} + I'_{a2} \cdot e^{-(1-\delta'')T/T_a'} \qquad (3.65)$$

where, $\delta'' = (\delta+\delta_c+\delta'_c+\beta)$, $\alpha_1 = \frac{R_a}{L_a+L_s}$

Substituting the value of I'_{a2} from equation (3.63) into equation (3.65) yields,

$$I_{a1} = \frac{E-V}{R_a}\left\{1-e^{-\beta\frac{T}{T_a'}} - (1-\delta'')T/T_a'\right\} + I_{a2}.e^{-\beta\frac{T}{T_a'}} -(1-\delta'')T/T_a' \qquad (3.66)$$

By elimination of variables from equations (3.7) and (3.66) gives,

$$I_{a2} = \frac{E}{R_a} - \frac{V}{R_a}\left[\frac{1-e^{(1-\delta_c-\delta_c')T/T_a'-\delta(T/T_a')}}{1-e^{(1-\delta_c-\delta_c')T/T_a'+a.\delta}}\right] \qquad (3.67)$$

$$I_{a1} = \frac{E}{R_a} - \frac{V}{R_a}\left[\frac{1-e^{-(1-\delta_c-\delta_c')T/T_a'+\delta(T/T_a')}}{1-e^{-(1-\delta_c-\delta_c')T/T_a'-a.\delta}}\right] \qquad (3.68)$$

$$\text{The normalised p.u. ripple} = \frac{I_{a2}-I_{a1}}{\frac{V}{R_a}} = \left[\frac{e^{(1-\delta-\delta_c-\delta_c')T/T_a'}-1}{1-e^{(1-\delta_c-\delta_c')T/T_a'+a.\delta}}\right] + \left[\frac{1-e^{-(1-\delta-\delta_c-\delta_c')T/T_a'}}{1-e^{-(1-\delta_c-\delta_c')T/T_a'-a.\delta}}\right] \qquad (3.69)$$

The average armature current is given by,

$$I_{av} = \frac{1}{T}\left[\int_0^{\delta T} i_a\,dt + I_{a2}(\delta_c+\delta_c') + \int_0^{\beta T} i_a\,dt' + \int_0^{(1-\delta-\delta_c-\delta_c'-\beta)T} i_a.\,dt'\right] \qquad (3.70)$$

The value of δ_c in the above equations is unknown and it can be determined as follows:

First, the value of V_1 is determined from equation (3.60) after substituting the values of I_{max} and γ_1, thus,

$$V_1 = V_2 \cos \gamma_1 \beta T + \frac{L_a . V}{L_a + L_s} . (1-\cos(\gamma_1 . \beta T)) + \frac{L_s E}{L_a + L_s} (1-\cos(\gamma_1 . \beta T))$$

Substituting the value of V_2 from equation (3.57), the minimum possible value of V_1 corresponding to $\gamma_1 \beta T = \pi$, is

$$V_1 = \left(\frac{L_a - L_s}{L_a + L_s}\right) V + \frac{2L_s}{L_a + L_s} . E - \sqrt{\frac{L_s}{C}} . I_{a2} \qquad (3.71)$$

Substituting V_1 from equation (3.71) into $\delta_c = \frac{C(V+V_1)}{I_{a2}}\frac{}{T}$ gives,

$$\delta_c = \frac{2CV}{I_{a2}T} \left[\frac{L_a + L_s (E/V)}{L_a + L_s} \right] - \frac{1}{\gamma_o T} \qquad (3.72)$$

where, $\gamma_o = \frac{1}{\sqrt{L_s . C}}$

Substituting I_{a2} from equation (3.67) into equation (3.72) and then expanding the terms containing $e^{-(\delta_c)T/T_a'}$ in terms of its power series and then neglecting all higher order terms in δ_c greater than two, yields a quadratic in δ_c as,

$$A' \delta_c^2 + B' \delta_c + C' = 0$$

where,

$$A' = \frac{E}{V}\left(\frac{T}{T_a'}\right) e^{(1-\delta_c')T/T_a'+a\delta} - \left(\frac{T}{T_a'}\right) \cdot e^{(1-\delta-\delta_c')T/T_a'}$$

$$- \frac{1}{2\gamma_o T_a'}\left(\frac{E}{V}\right)\left(\frac{T}{T_a'}\right) \cdot e^{(1-\delta_c')T/T_a + a\cdot\delta}$$

$$+ \frac{CR_a}{T_a'}\left(\frac{L_a+L_s\, E/V}{L_a+L_s}\right)\cdot\left(\frac{T}{T_a'}\right) e^{(1-\delta_c')T/T_a' + a\cdot\delta}$$

$$B' = \frac{E}{V}\left(1-e^{(1-\delta_c)T/T_a'+a\cdot\delta}\right)-\left(1-e^{(1-\delta-\delta_c')T/T_a}\right)$$

$$+ \frac{1}{\gamma_o T_a'}\left(\frac{E}{V}\right) \cdot e^{(1-\delta_c')T/T_a' + a\cdot\delta} - \frac{1}{\gamma_o T_a'}\cdot e^{(1-\delta-\delta_c')T/T_a'}$$

$$- \frac{2CR}{T_a'}\left(\frac{L_a+L_s\, E/V}{L_a+L_s}\right) \cdot e^{(1-\delta_c')T/T_a' + a\cdot\delta}$$

$$C' = - \frac{2CR}{T}\left(\frac{L_a+L_s\, E/V}{L_a+L_s}\right)\cdot\left(1-e^{(1-\delta_c')T/T_a'+a\cdot\delta}\right)$$

$$+ \frac{1}{\gamma_o T}\left\{\frac{E}{V}\left(1-e^{(1-\delta_c')T/T_a'+a\cdot\delta}\right)-\left(1-e^{(1-\delta-\delta_c')T/T_a}\right)\right\}$$

The feasible value of δ_c is then calculated from

$$\delta_{c1,2} = - \frac{B'}{2A'} \pm \frac{\sqrt{B'^2 - 4A'C'}}{2A'}$$

If the commutating capacitor C does not get enough time to discharge to the minimum value of V_1 before the begining

of the next cycle, then mode .V does not exist and the commutation interval ($\delta_c T$) in that case can be calculated assuming $V_1=V$ and the expressions for A',B',C' given above can be used with terms containing γ_o absent and $(\frac{L_a+L_s(E/V)}{L_a+L_s})$ being replaced by unity. The expression for regenerative power P_{rg} is given by

$$P_{rg} = \frac{V}{T}\left[\int_0^{\delta_c' T} I_{a2}\,(1-\cos \gamma_o t')dt' + \int_0^{\beta T} (i_a - i_c)dt' + \int_0^{(1-\delta-\delta_c-\beta)T} i_a\,dt'\right] \qquad (3.73)$$

The electromagnetic braking torque is given by equation (3.29).

Under discontinuous conduction, the armature current i_a given by equation (3.64) becomes zero at $t = \gamma T$, where t is measured from the beginning of the chopping cycle (i.e. mode I). Substituting the value of I'_{a2} from equation (3.63) into equation (3.64) and putting $i_a=0$ at $t' =(\gamma - \delta'')T$, gives the value of γ, the point where discontinuous conduction occurs.

$$\gamma = \delta'' + (\frac{T'_a}{T})\log_e \left[\frac{(1-\frac{E}{V})(1+e^{-\beta\frac{T}{T_a}}) + \frac{E}{V}e^{-\beta\frac{T}{T'_a}}\cdot(1-e^{-\delta T/T_a})}{(1-\frac{E}{V})}\right] \qquad (3.74)$$

where, $\delta'' = (\delta + \delta_c + \delta'_c + \beta)$.

It is evident from equation (3.74), that, chances of discontinuous conduction in the presence of appreciable source inductance are remote, specially for high frequency operation.

3.3.4 Performance and Experimental Verification.

For the test machine, whose particulars have already been given in Section 2.5 of Chapter II, it is found that the parameters are such that δ_c' is quite high ($\delta_c' = \frac{\pi}{2\gamma_o T}$) and β is also high ($\beta = \frac{\pi}{\gamma_1 T}$) for the chopper operating frequency of 400 Hz. As a result of this, the regenerative interval III is absent and the commutating capacitor C does not get enough time to discharge to a voltage below the supply voltage. The idealised voltage and current wave forms are shown in Figure 3.12. In this case, the commutation interval ($\delta_c T$) can be determined without much loss of accuracy from equation (3.36) and, using the expressions for A',B',C' derived earlier in Section 3.3.3 in which the terms containing γ_o are dropped and the term $\frac{L_a+L_s(E/V)}{L_a+L_s}$ is replaced by unity. The average armature current is calculated from the expression obtained below. after integrating the R.H.S. of equation (3.70) and ignoring the last term:

$$I_{av} = \frac{E}{R_a}.\delta + (\frac{T_a}{T})\frac{E}{R_a}\,(e^{-\delta T/T_a} - 1) + I_{a1}.(\frac{T_a}{T}).(1 - e^{-\delta T/T_a})$$

$$+ I_{a2}(\delta_c + \delta_c') + \frac{E-V}{R_a}(1 - \delta - \delta_c - \delta_c') + \frac{E-V}{R_a}(\frac{T_a'}{T})$$

$$.(e^{-(1-\delta-\delta_c-\delta_c')T/T_a'} - 1) + I_{a2}(\frac{T_a'}{T}) .$$

$$(1 - e^{-(1-\delta-\delta_c-\delta_c')T/T_a'}) \qquad (3.75)$$

The expression for regenerative power is obtained after integrating R.H.S. of equation (3.73) dropping the last term. Thus,

$$P_{rg} = \frac{V}{T}\,[I_{a2}(\delta_c'T - \frac{\sin\gamma_o\,\delta_c'T}{\gamma_o})] + \frac{V(E-V)}{R_a}(1 - \delta - \delta_c - \delta_c')$$

$$+ V(\frac{E-V}{R_a}) .(\frac{T_a'}{T}).(e^{-(1-\delta-\delta_c-\delta_c')T/T_a'} - 1)$$

$$+ I_{a2}.V(\frac{T_a'}{T}).(1 - e^{-(1-\delta-\delta_c-\delta_c')T/T_a'}) \qquad (3.76)$$

For the purpose of test, a 220V, 3 KW, 1500 r.p.m., d.c. separately excited generator was used as a source. The armature of the generator was found to have an inductance of 40 mH (d.c.). The chopper operating frequency was 400 Hz. An external choke having an inductance of 300 mH was used in the armature circuit of the motor for regeneration. Discontinuous conduction was found to be absent. Figure 3.13 shows typical calculated torque-speed characteristics using

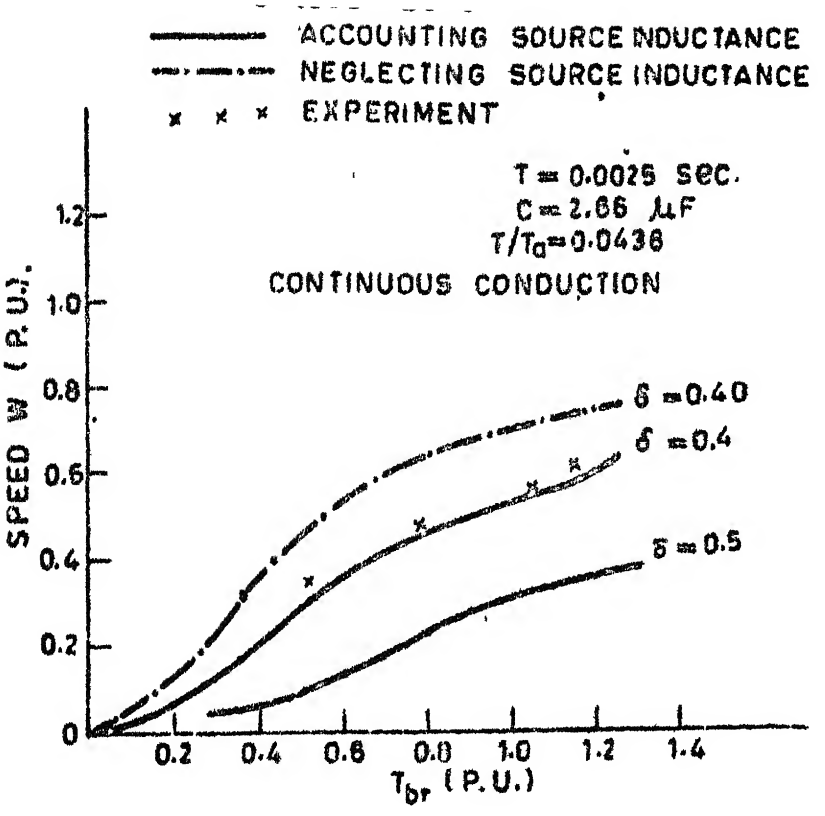

Fig. 3.13 Speed vs. braking torque characteristics in presence of source inductance (L_s = .04H).

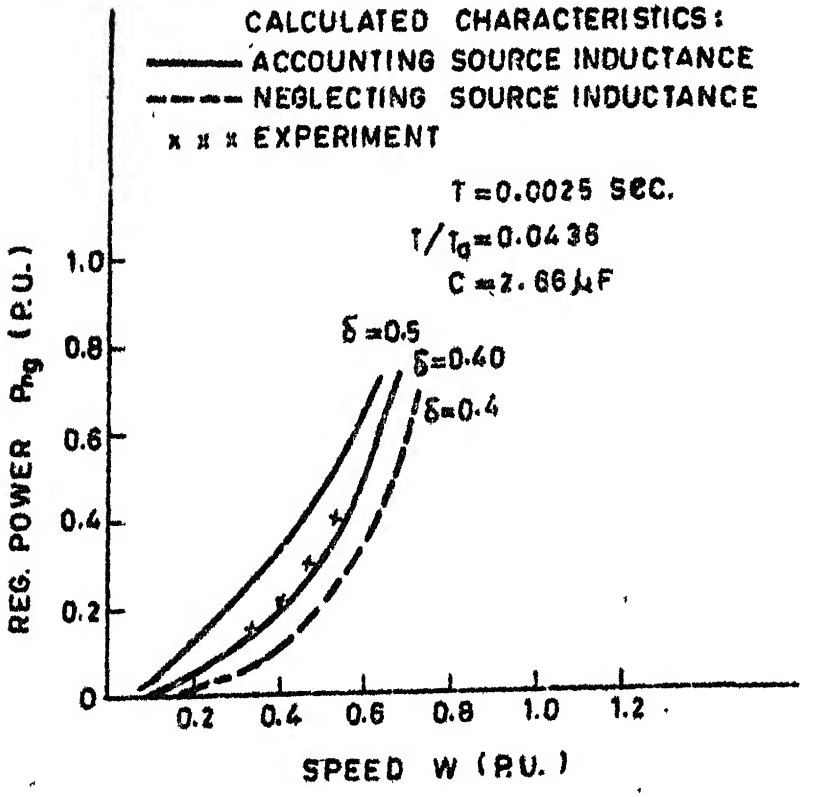

Fig. 3.14 Reg. power (P_{rg}) vs. speed characteristics in presence of source inductance (L_s = .04H)

equations (3.75) and (3.79) along with the measured points under regenerative braking mode for $\delta = 0.4$ and 0.5 respectively. The predicted results agree well with the experimental ones. It is also seen, that, considerable error is introduced if the source inductance is not taken into account. The effect of source inductance is to reduce regenerated braking torque. It was found that regenerative braking practically failed for values of $\delta > 0.57$ at this value of chopper operating frequency. Figure 3.14 shows the corresponding calculated and measured speed versus regenerative power characteristics. Experimental results agree well with the calculated characteristics. Figure 3.15 shows the calculated torque speed characteristics without considering the source inductance for fixed values of δ using the analysis presented in Section 3.3. Experimental results obtained after putting a filter capacitor (Buffer condenser) of 8000 μF at the source terminals are also shown in Figure 3.15. The corresponding speed versus regenerative power characteristics are shown in Figure 3.16. The experimental results using buffer condenser at the source terminals are also shown in Figure 3.16. These figures indicate that the use of a suitable buffer condenser bank at the source terminals neutralizes the effect of source inductance.

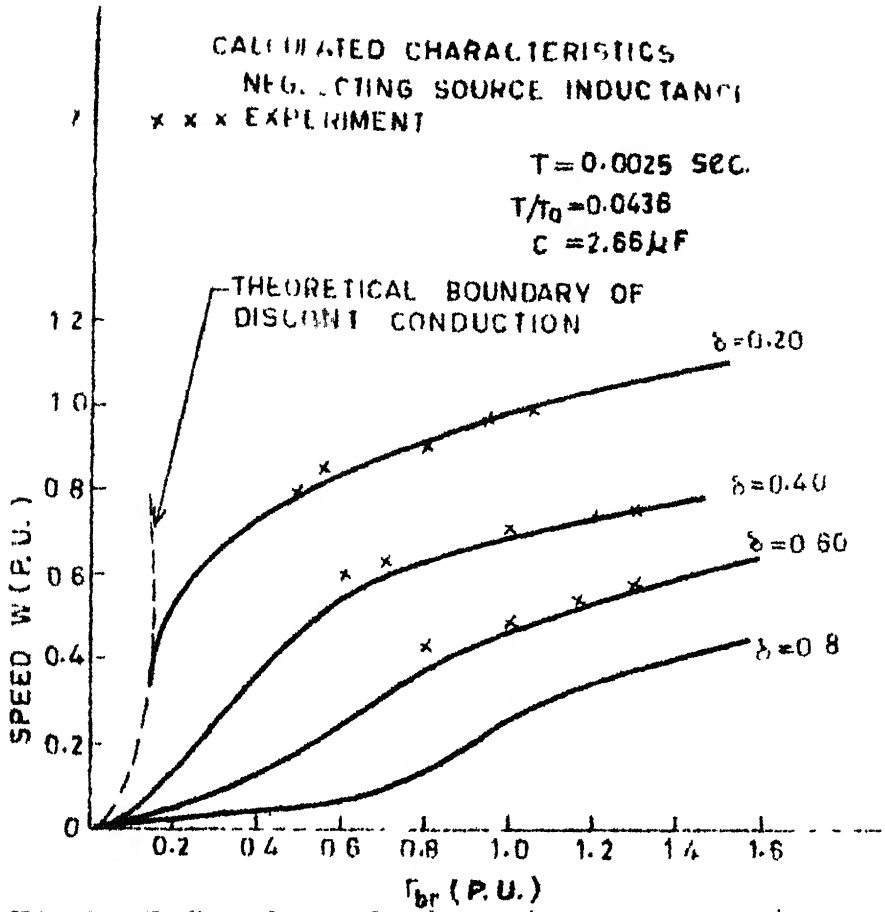

Fig.3.15 Speed vs. braking torque characteristics (with buffer condenser)

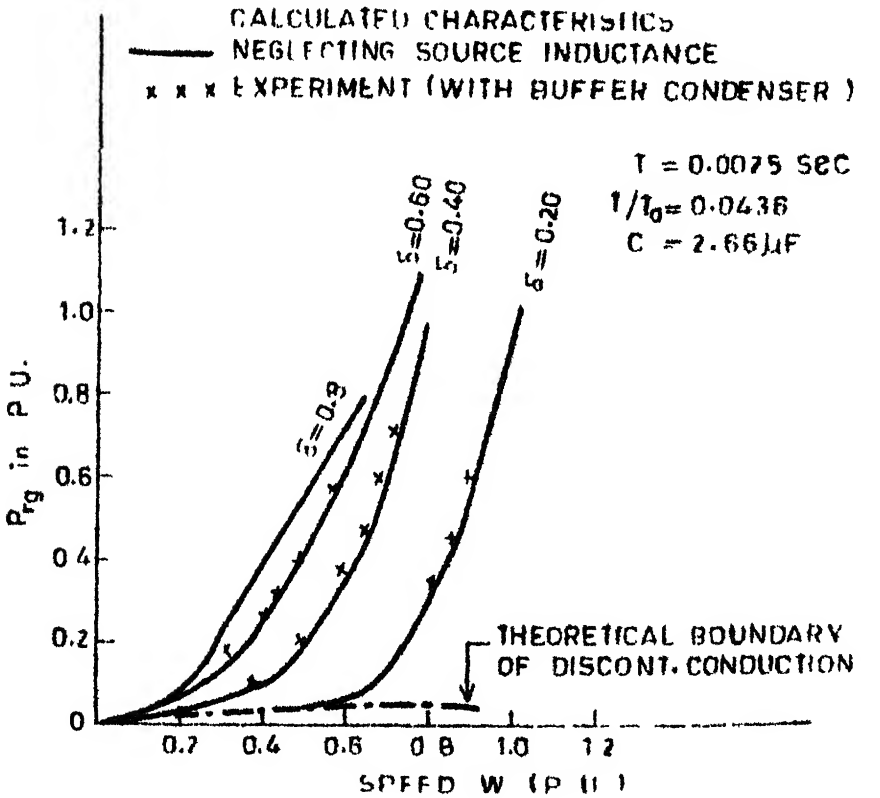

Fig.3.16 Regenerative power vs. speed characteristics (with buffer condenser)

3.4 CONCLUSIONS:

The following important conclusions can be drawn from the above study.

1. The method of performance calculation presented here is general and can be used for choppers with load current dependent commutation with non square output voltage and also for choppers with square wave output voltage. The analysis takes the effect of source inductance into account. There is a close agreement between predicted and experimental results.

2. The source inductance has considerable effect on the braking performance of the motor, the regenerated power decreases for the same value of duty ratio and speed.

3. In the presence of source inductance, the commutating capacitor initially charges to a value greater than the source voltage. Subsequently it discharges and if enough time is available, it will discharge to a voltage less than the source voltage; greater is the load current less is the voltage to which C is finally charged. If commutating capacitor is chosen neglecting source inductance, commutation failure may occur. The expressions derived can be used to select a suitable value of capacitor in presence of source inductance assuring reliable commutation.

4. The region of discontinuous conduction can be reduced to a narrow region by suitably choosing a $\frac{T}{T_a}$ ratio with the help of normalised torque T_p versus normalised speed ω_p curves of Figure 3.3. The constraints regarding the maximum permissible current ripple can be checked from Figure 3.4. These nomograms have been plotted in normalised co-ordinates and therefore can be employed for regenerative braking of any d.c. separately excited motor.

In case of chopper with load dependent commutation, the boundary of discontinuous conduction calculated using equation (3.51) for the same $\frac{T}{T_a}$ ratio, lies slightly to the left of the boundary obtained from the normalised boundary for square wave case. Therefore, the normalised boundaries of discontinuous conduction given in Figure 3.3 can also be used to select a conservative value of T/T_a ratio for eliminating discontinuous conduction in chopper with load dependent commutation.

5. The effect of source inductance, chopper commutation interval and armature reaction of the machine should be taken into account for accurate prediction of machine performance.

CHAPTER IV

PERFORMANCE AND ANALYSIS OF CHOPPER FED D.C. SERIES MOTOR

4.1 INTRODUCTION

The analysis of chopper fed d.c. series motor is complicated due to the presence of nonlinearities such as saturation of magnetic circuit and armature reaction effect. Moreover, eddy currents are induced in the field cores due to time varying excitation current. These eddy currents influence the building up or decay of air gap flux. P.W. Franklin [8] has given an analysis for a current limit controlled chopper-fed d.c. series motor taking nonlinearity of the magnetic circuit by straight line approximation. Dubey and Shepherd [9] have developed an analytical technique for analysis of series motors controlled by a square wave chopper. Mellitt and Rashid [10] and Damle and Dubey [11] have developed computer based analysis of series motors controlled by choppers with load current dependent commutation taking the nonlinearity of magnetic circuit by piece wise linear technique. Dubey [12] has extended the analytical technique described in reference [9] to the case of a nonsquare output voltage chopper with load current dependent commutation. Ranade and Dubey [20] have reported that

though this method gave satisfactory results for the calculation of steady state speed torque curves, large amount of error was obtained in prediction of ripple in armature current. None of these methods have taken into account the effect of armature reaction, eddy currents and the effect of source inductance on the performance of chopper fed d.c. series motors.

In this chapter, first of all a modelling of series motor has been done taking into account the effects of magnetic saturation, armature reaction and eddy currents. Next an analysis has been done for a square wave chopper. Then, the analysis has been extended to a load current commutated chopper taking into account all the nonlinearities mentioned above. The source inductance has also been taken into account. The calculated results agree well with the experimental.

4.2 MODELLING OF D.C. SERIES MACHINE

For analysising the performance of d.c. series machine, a good mathematical model of the machine should be made which is valid for dynamic as well as for steady state operating conditions.

4.2.1 Effect of Magnetic Saturation

It is well known, that, in a saturated magnetic circuit,

the rise of current is relatively faster than in the case of nonsaturated magnetic circuit. This is due to decrease of self inductance with saturation. Again, if there are ripples in the current, as is usually the case with chopper fed d.c. series machine, incremental inductance has to be considered and its value also reduces with saturation of the magnetic circuit. The relationship between the flux produced and excitation current is given by

$$\phi = K_1' \cdot i_f \tag{4.1}$$

where,

$$K_1' = f(i_f) \tag{4.2}$$

Equation (4.1) effectively represents the B-H characteristics of d.c. machines. Under saturated condition, the field flux may be represented by Frolich's equation

$$\phi = \frac{k_1 \cdot i_f}{(k_2 + i_f)} \tag{4.3}$$

where k_1 and k_2 are constants to be determined from the saturation characteristic of the machine. The main drawback of equation (4.3) is that, it departs quite widely around the low induction region. To overcome this, an empirical relationship has been suggested here in the form

$$\phi = \frac{C \cdot i_f}{(k_2 + i_f)} + D \cdot \log_e \left(\frac{k_2 + i_f}{k_2} \right) \tag{4.4}$$

The constants C and D may be suitably chosen to yield satisfactory results as,

$$C = k' \left\{ 1 - \frac{1}{D_1} \left(1 - \frac{1}{I_o}\right) \right\} \text{ and } D = \frac{k'}{I_o \cdot D_1}$$

where, k' and D_1 are constants and I_o may conveniently be chosen as the rated current. The expression for d.c. self inductance follows on differentiation of equation (4.4) as,

$$L = N \cdot \frac{d\phi}{di_f} = \left[\frac{k_3}{(k_2+i_f)^2} + \frac{k_3(i_f - I_o)}{I_o \cdot D_1 (k_2+i_f)^2} \right] \qquad (4.5)$$

The measurements of self inductances of d.c. machines for different values of steady-state current, were done using a well known bridge method described by C.V. Jones [17] The method developed by Mellitt and Rashid [21] can also be used to measure inductances of machines. The measured self inductances versus current curves for three typical d.c. machines whose particulars are given in Appendix B are shown in Figures 4.1(a) to 4.1(c). Figures 4.1(a) to 4.1(c) clearly show, that, equation (4.5) gives a better representation than equation (4.3). The empirical formulation for self inductance given by relationship (4.5)

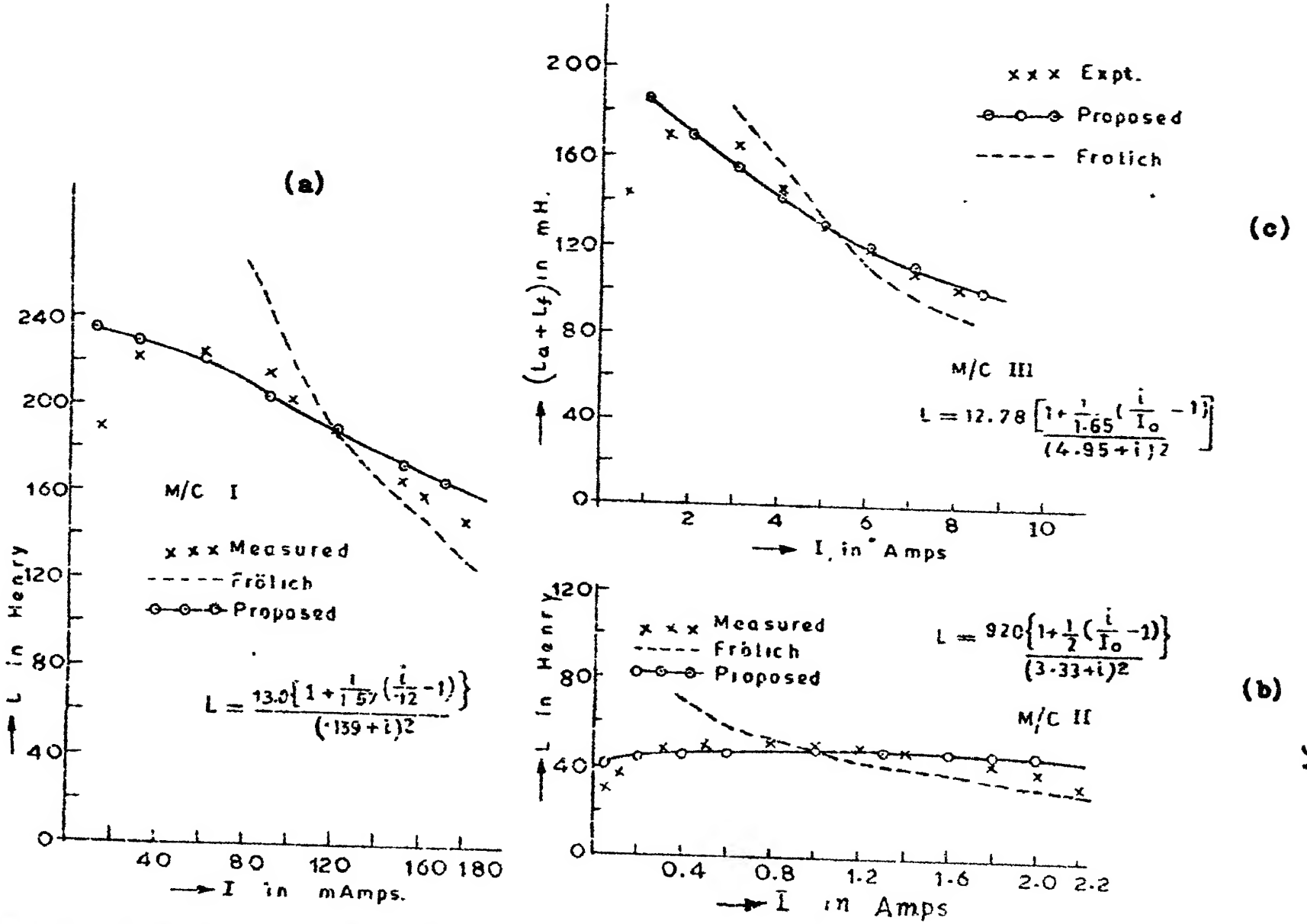

Fig. 4.1 Variation of Self Inductance of d.c. machine with saturation

enables one to represent the d.c. machine self inductance satisfactorily. The equation due to step voltage input to the field windings is given by,

$$V - R.i_f - N \frac{d\phi}{di_f} \cdot \frac{di_f}{dt} = 0 \qquad (4.6)$$

$$\text{with } i_f(o) = 0$$

The equation corresponding to the case when the field winding is short circuited, is given by,

$$R.i_f + L_f(i_f) \frac{di_f}{dt} = 0$$

$$\text{with } i_f(o) = I_{fo} \qquad (4.7)$$

where, $L_f(i_f) = N \cdot \frac{d\phi}{di_f}$

Equations (4.6) and (4.7) are first order nonlinear differential equations and they are solvable numerically using classical Runge-Kutta method of order four.

4.2.2 Representation of Armature Reaction

It is well known, that, when the armature of the machine carries current, the armature reaction flux affects the main air gap-flux and thus, the back e.m.f. coefficient K is not a constant and it may be represented as,

$$K = f(i_f, i_a) \qquad (4.8)$$

The values of K are obtained from the internal characteristic of the machine.

4.2.3 Effect of Eddy currents Induced in the Magnetic Circuit on the Armature Induced e.m.f.

The flux distribution inside a magnetic core excited by a time varying flux is given by Maxwell's equations. Eddy currents are induced inside the pole cores, yoke and armature laminations due to time varying excitation current. These eddy currents produce short duration magnetic fluxes which damp the building up or decay of the air gap flux. A detailed analysis for flux distribution inside a torroidal core due to a step input excitation has been given by N. Keshavamurthy and P.K. Rajagopalan [22] and it has been shown that it is possible to derive an equivalent circuit model to represent the eddy current effect as shown in Figure 4.2. The dynamic equivalent circuit of a d.c. machine field may also be represented by the circuit shown in Figure 4.2. The parameters of the equivalent circuit have to be identified from experimental data.

4.2.4 Experimental Investigation of Eddy currents on Armature Induced e.m.f.

To estimate the effects of eddy currents on the armature induced e.m.f., recordings were taken for measuring

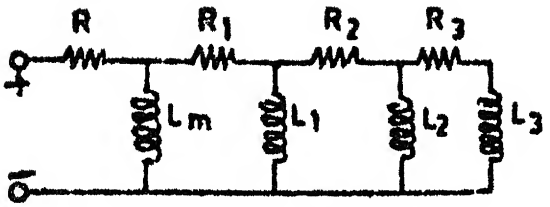

Fig. 4.2 Dynamic Equivalent Circuit of d.c. machine field.

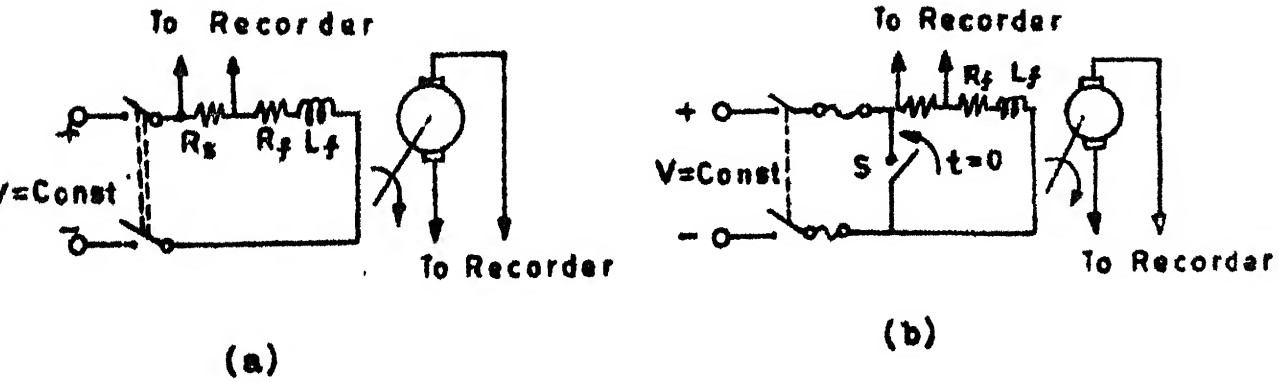

Fig. 4.3 Experimental arrangement for recording step input dynamic response.

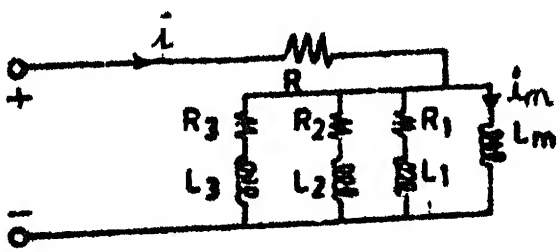

Fig. 4.5 Modified dynamic equivalent circuit.

the dynamic field current and the armature induced e.m.f. for step input voltage to the field and also due to free wheeling of field current. The experimental arrangements are shown in Figures 4.3(a) and 4.3(b) respectively. The Figures 4.4(a) to 4.4(c) show the typical dynamic characteristics for three test machines whose particulars are given in Appendix B.

It has been observed that in machine with laminated pole and solid yoke (M/C IV), and in machine with both laminated pole and laminated yoke (M/C III), the influence of eddy currents on the dynamic armature induced e.m.f. is considerably less than in the case of machine with both solid pole and solid yoke (M/C II).

4.2.5 Identification of Dynamic Circuit Parameters from Transient Step Response.

The network model shown in Figure 4.2 to represent the dynamic behaviour of the air gap flux may further be simplified as shown in Figure 4.5. In this model, R and L_m are the actual resistance and self inductance of the field circuit of the d.c. machine respectively. The branches in parallel to L_m represent the eddy current effects. The actual air gap flux is given by i_m rather than i flowing from mains under dynamic conditions. For a d.c. machine, it is sufficient to consider only three branches in parallel

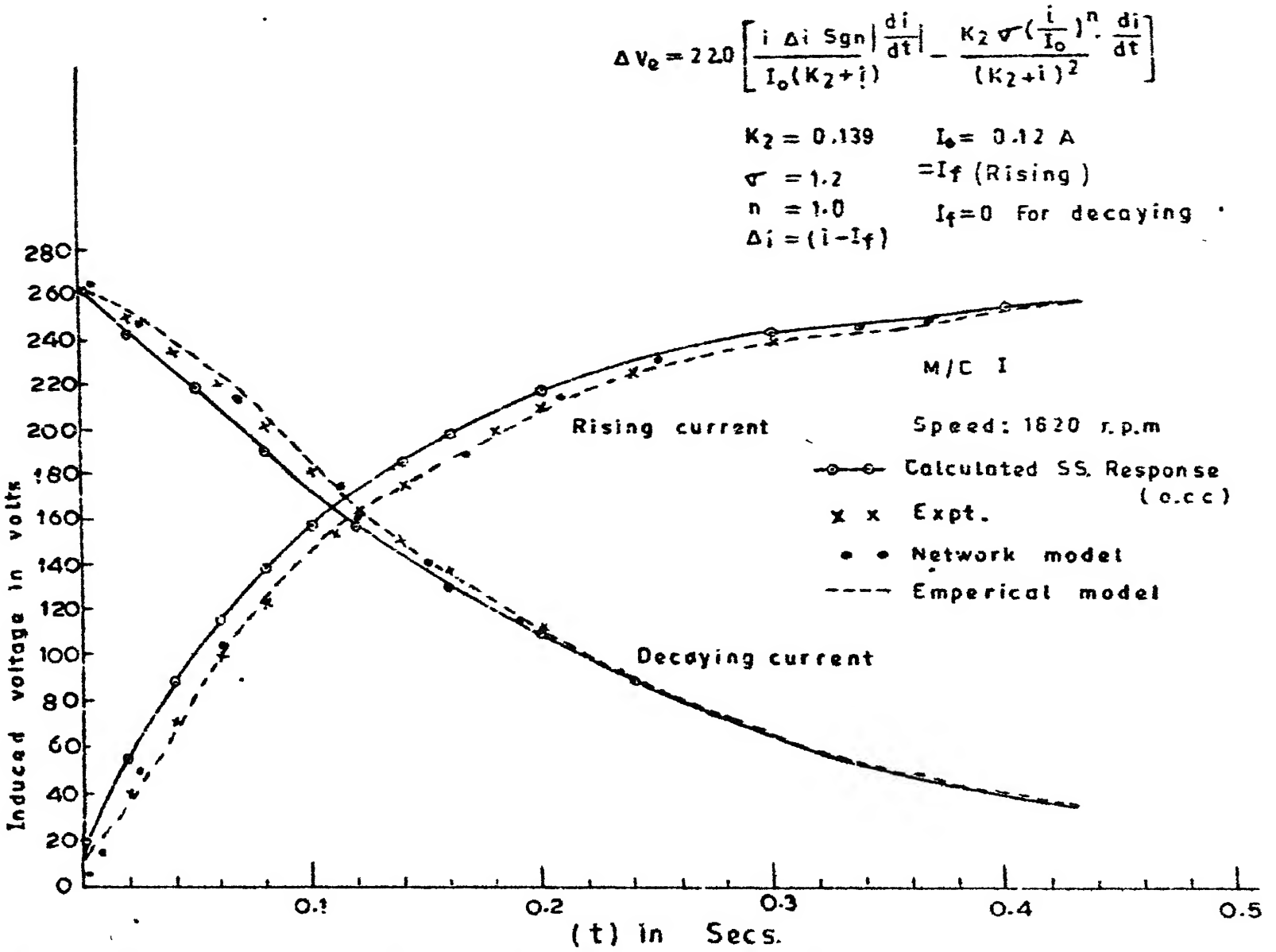

Fig. 4.4(a) Dynamic Response of Armature induced e.m.f. due to step input to the field.

$$\Delta V_e = 94\left[\frac{i.\Delta i\,Sgn\frac{di}{dt}}{(K_2+i)} - \frac{K_2\,\sigma\,(\frac{i}{I_0})^n\cdot\frac{di}{dt}}{(K_2+i)^2}\right]$$

$n = 0.7 \qquad I = 0.9\,A$

$\sigma = 1.2 \qquad K_2 = 3.33$

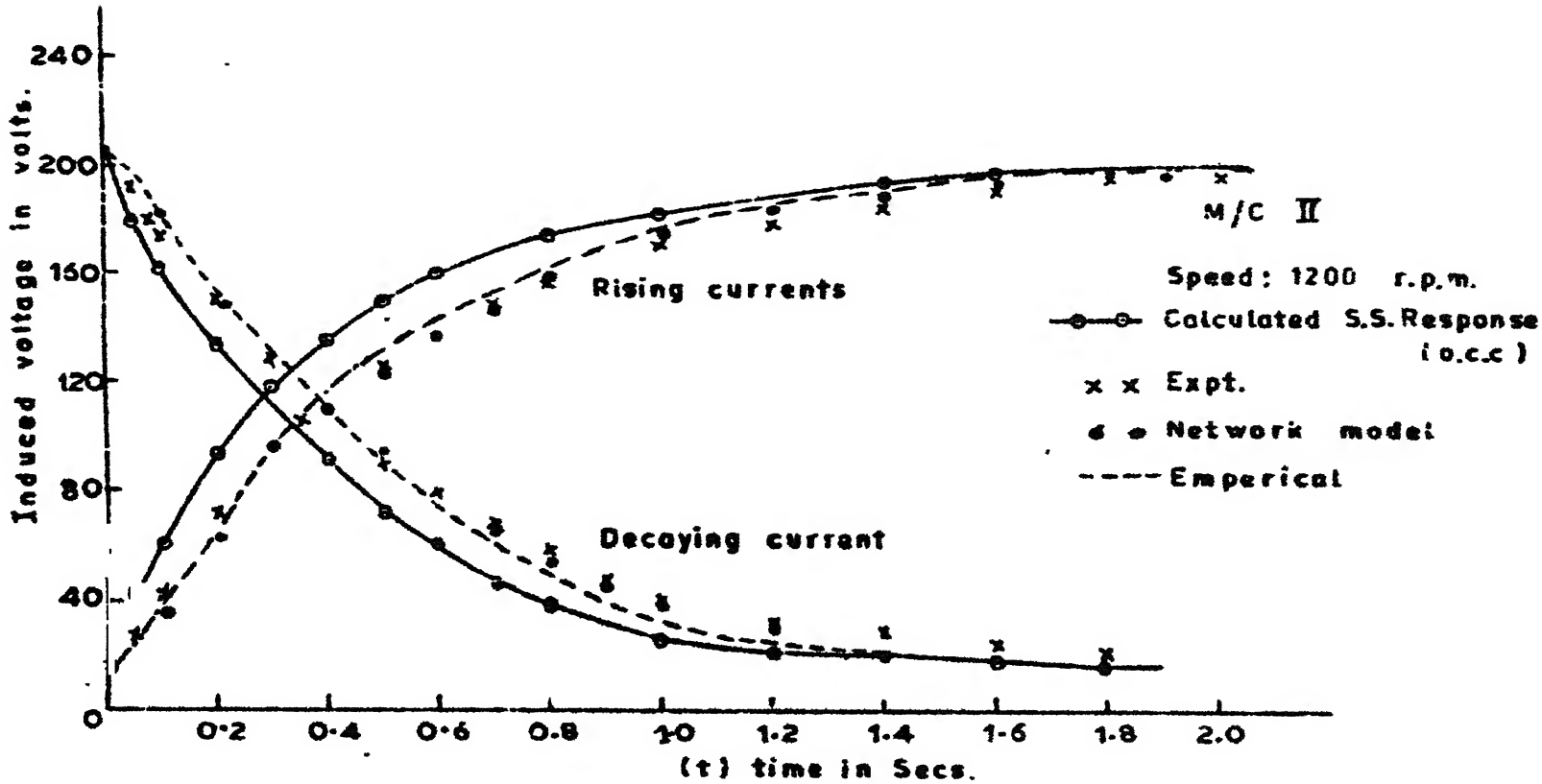

Fig. 4.4(b) Dynamic Response of Armature induced e.m.f. due to step input to the field.

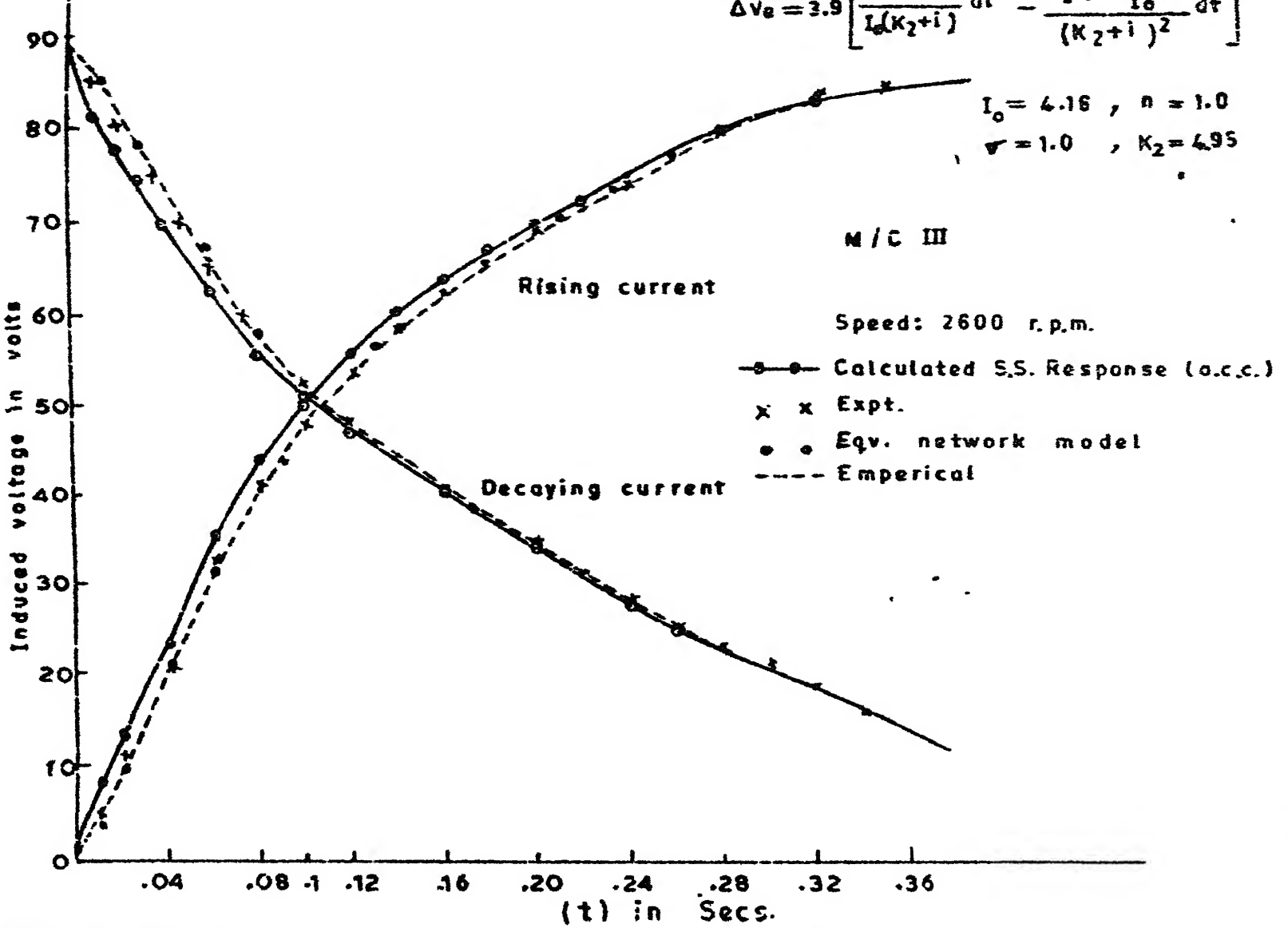

Fig. 4.4(c) Dynamic Response of Armature induced e.m.f. due to step input to the field.

to get satisfactory results in most cases. The excitation current i_m is dominated by three time constants $\frac{1}{\lambda_1}$, $\frac{1}{\lambda_2}$ and $\frac{1}{\lambda_3}$. Then i_m due to step input voltage can approximately be expressed as,

$$i_m(t) = I_o \left[1 - A_1 . e^{-\lambda_1 t} - A_2 . e^{-\lambda_2 t} - A_3 e^{-\lambda_3 t} \right] \qquad (4.9)$$

where I_o is the final steady state current. The eddy current time constants are of very short durations. On the assumption that $\frac{1}{\lambda_1} \gg \frac{1}{\lambda_2} \gg \frac{1}{\lambda_3}$, the roots λ_1, λ_2 and λ_3 can be found out by the well known method of determination of prominent time constants from the plot of dynamic error $e(t) = (1 - \frac{i_m}{I_o})$ on a logarithmic scale versus time. The largest time constant $\frac{1}{\lambda_1}$ is determined from the slope of the tangent which is asymptotic to the curve. Then, the error between the actual plot and the tangent line are plotted in the same manner to determine $\frac{1}{\lambda_2}$ and the same procedure is repeated for determination of $\frac{1}{\lambda_3}$. Once these approximate roots are determined graphically, the constants A_1, A_2 and A_3 can be estimated from experimental data using a 'Least Square Error Criteria' whose formulation is given in Appendix B. Although, the constants A_1, A_2 and A_3 can also be determined graphically, appreciable error will be involved if the experimental data are inaccurate. After the roots

λ_1, λ_2 and λ_3 and constants A_1, A_2 and A_3 are determined, the parameters of the network model shown in Figure 4.5 can be identified using linear network theory. The calculated dynamic response for the test machines using above approach are shown in Figures 4.4(a) to 4.4(c). It is observed that the dynamic response calculated by this method agrees well with the experimental results except near the origin. The error near the origin can be attributed to the assumption of a less accurate model and errors in experimental data.

4.2.6 Empirical Formulation of Eddy Current on the Armature Induced e.m.f.

The difference between the actual dynamic induced armature e.m.f. due to a step input voltage to the field and the e.m.f. obtained from the machine O.C.C. under steady state condition at constant speed, may be represented by a functional relationship,

$$\Delta V_e = f(i, \frac{di}{dt}).$$

A generalised empirical relationship in the form shown below has been found by trial and error to match the dynamic response characteristics shown in Section 4.2.4.

$$\Delta V_e = \lambda \left(\frac{\omega}{\omega_o}\right).\left[\frac{i.\Delta i \ \mathrm{Sgn}\ \frac{di}{dt}}{I_{fo}(k_2+i)} - \frac{k_2.\sigma.\left(\frac{i}{I_{fo}}\right)^n}{(k_2+i)^2}.\frac{di}{dt}\right] \qquad (4.10)$$

Where, 'Sgn' is the sign of the derivative, $\Delta i = (i - I_o)$, I_o is the final steady state current which is equal to I_{fo} for rising current and $I_o = 0$ for decaying current during free wheeling. k_2 is the Frolich's constant for the machine, σ is a constant dependent on the machine and n is an index dependent on the design of the magnetic circuit. The values of σ and n have to be determined from the experimental dynamic characteristics of the machine. λ is a constant of the machine and $(\frac{\omega}{\omega_o})$ is p.u. speed. The values of the constants σ, λ and the values of the index n determined from the respective dynamic response of the test machines have been shown in the table given in Appendix B. The accuracy of fitting is found to be quite satisfactory. The equation (4.10) thus provides an easy tool to account for the effects of eddy currents on the dynamic machine induced e.m.f. due to step input voltage to the field windings.

4.3 STEADY STATE ANALYSIS OF CHOPPER FED D.C. SERIES MOTOR

The idealised output voltage and current wave forms of a d.c. chopper under continuous conduction has been shown in Figure 4.6(a). The voltage and current wave forms for choppers using load dependent commutation are shown in Figure 4.6(b). The current wave form of a chopper fed d.c.

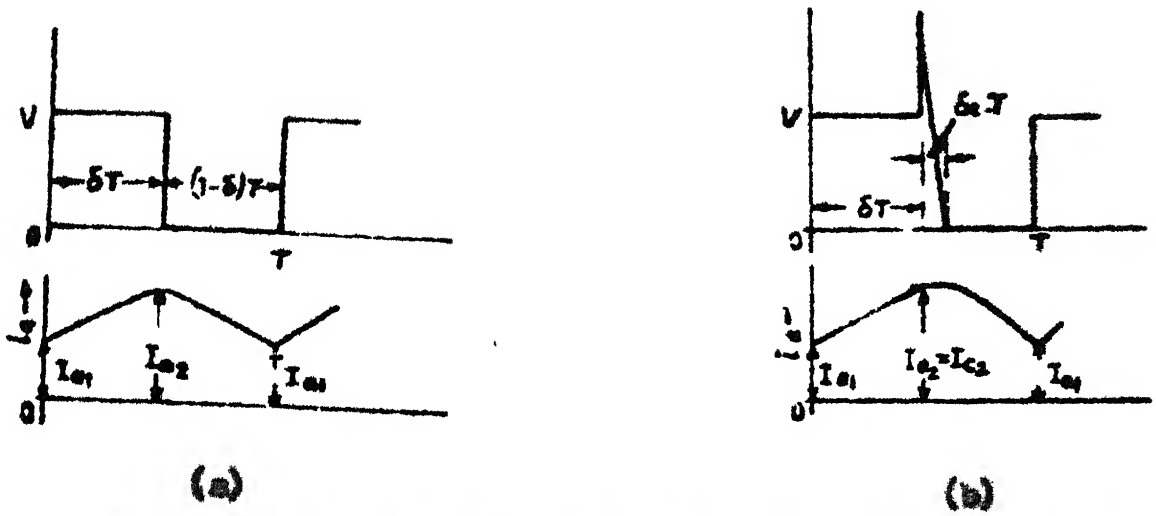

(a) (b)

Fig.4.6 Idealised output voltage and current wave forms.

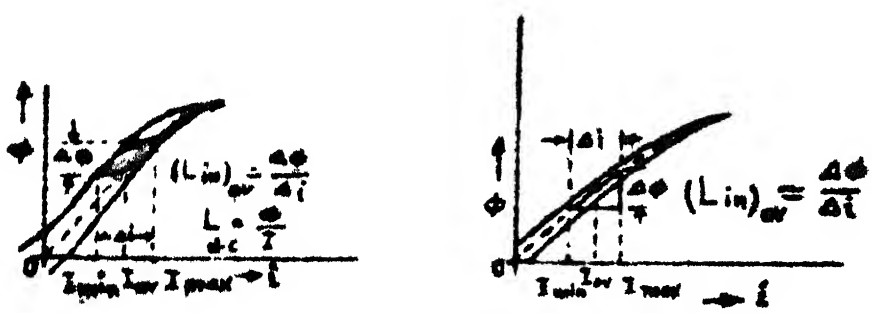

(a) (b)

Fig.4.7 Magnetisation characteristics of d.c. machine magnetic circuit.

series motor fluctuates between a maximum and minimum level and as a result, the motor parameters change with current due to saturation effect and the value of K changes due to armature reaction and saturation. Moreover, eddy currents are induced in the field cores and influence the main field flux. Thus, the performance equations of a chopper-fed series motor are highly nonlinear and it is difficult to solve them. A digital computer simulation of a series motor fed by a square wave chopper has been described by T. Fujimaki et.al[13] taking into account the effect of saturation on the motor inductances and eddy current effect, using the network model of Figure 4.5 with K as constant. In the present work, an attempt has been made to analyse the chopper fed series motor taking into account magnetic saturation, armature reaction and eddy current effects using the empirical relationship of equation (4.10). The quantities in equation (4.10) are redefined and approximated for analysis of chopper-fed series motor as follows.

For rising current, $\frac{\Delta i}{(k_2+i)I_{fo}} = -\frac{(I_{a2} - i_a)}{I_{a2}\cdot(k_2+i_a)}$

and $(\frac{i}{I_{a2}})^n = \left\{\frac{i_a - I_{a1}}{I_{a2}}\right\}^n$.

For falling current during free wheeling,

$$\frac{\Delta_1}{(k_2+i)I_{fo}} = \frac{i_a - I_{a1}}{I_{a2}(k_2+i_a)}$$

and

$$\left(\frac{i}{I_{fo}}\right)^n = \left(\frac{i_a - I_{a1}}{I_{a2}}\right)^n$$

Now i_a is replaced by I_{av} for taking the average effect. Then,

$$-\frac{i_{a2}-i_a}{I_{a2}(k_2+i_a)} \approx -\frac{(I_{a2}-I_{av})}{I_{a2}(k_2+I_{av})} = \frac{(i_p/I_{a2})}{(k_2+I_{av})} = \frac{\alpha}{(k_2+I_{av})}$$

(4.11a)

where, $\alpha = (i_p/I_{a2})$ and i_p = peak value of current ripple and

$$\left(\frac{i_p}{I_{fo}}\right)^n = \left(\frac{i_a - I_{a1}}{I_{a2}}\right)^n \approx \left(\frac{I_{av}-I_{a1}}{I_{a2}}\right)^n = \left(\frac{i_p}{I_{a2}}\right)^n = \alpha^n$$

$$\frac{(i/I_{fo})^n}{(k_2+i)^2} = \frac{(i_p/I_{a2})^n}{(k_2+I_{av})^2} = \frac{\alpha^n}{(k_2+I_{av})^2} \qquad (4.11b)$$

α in the above equations may be suitably chosen and taken as a constant.

The analysis of chopper fed d.c. series motor has been carried out with the following assumptions in addition to the assumptions mentioned in Sec. 2.2 in Chapter II.

(i) The conduction is continuous;

(ii) The motor back e.m.f. coefficient K is assumed to be a function of I_{av} instead of i_a to take into account the effect of saturation and armature reaction;

(iii) The core losses and increase in resistance due to skin effect are neglected;

(iv) The variation of series field and armature inductances due to eddy currents and hysteresis effects are not considered.

4.3.1 Chopper with Square Wave Output Voltage with Negligible Source Inductance

I. Duty Interval: $(0 \leq t \leq T)$

The differential equation describing this mode is

$$L(I_{av}) \frac{di_a}{dt} + R.i_a + K.\omega.i_a + \Delta V_e = V \qquad (4.12)$$

where ΔV_e is the voltage due to eddy currents, R is the total armature circuit resistance and K as defined by equation (4.8) and assumption (ii) above, is a function of I_{av}.

II. Free Wheeling Interval : $(\delta T \leq t \leq T)$

The differential equation describing this mode is

$$L(I_{av}) \frac{di_a}{dt} + R.i_a + K.\omega.i_a + \Delta V_e = 0 \qquad (4.13)$$

Substituting from equations (4.11a) and (4.11b) into equation (4.10) gives,

$$\Delta V_e = \lambda\left(\frac{\omega}{\omega_o}\right).\left[i_a.\ \frac{\alpha.\ \mathrm{Sgn}\ \frac{di_a}{dt}}{(k_2+I_{av})} - \frac{k_2.\sigma.\alpha^n}{(k_2+I_{av})^2}.\ \frac{di_a}{dt}\right] \tag{4.14}$$

Substituting ΔV_e from equation (4.14) into equation (4.12) and (4.13) one gets

$$L_{eq}.\ \frac{di_a}{dt} + i_a.\ R'_{eq} = V \tag{4.15}$$

$$\text{with } i_a(o) = I_{a1} \quad \text{for } 0 \leq t \leq \delta T$$

where,

$$L_{eq} = L(I_{av}) - \frac{\lambda.\left(\frac{\omega}{\omega_o}\right).R_2.\sigma.\alpha^n}{(k_2 + I_{av})^2}$$

$$R'_{eq} = R + K.\omega - \lambda.\frac{\omega}{\omega_o}.\frac{\alpha}{(k_2+I_{av})}$$

and

$$L_{eq}.\ \frac{di_a}{dt} + i_a.R'_{eq} = 0 \tag{4.16}$$

$$\text{with } i_a(\delta T) = I_{a2} \quad \text{for } \delta T \leq t \leq T$$

Equations (4.15) and (4.16) are linear equations for a specified operating condition under steady state. The average steady state machine speed is obtained from

equation (4.15) and (4.16) as

$$\omega_{av} = \omega = \frac{V.\delta - R.I_{av}}{I_{av}\left[K - \frac{\lambda}{\omega_o} \cdot \frac{\alpha}{(k_2+I_{av})}\right]} \qquad (4.17)$$

The electromagnetic torque T_e is given by

$$T_e = \frac{E_{av}.I_{av}}{\omega} \qquad (4.18)$$

4.3.2 Chopper with Nonsquare Output Voltage Wave form due to Load Dependent Commutation and with Negligible source Inductance.

The voltage and current wave forms of a load current commutated chopper are shown in Figure 4.6(b). There are three distinct modes of operation as shown below:

I. Duty Interval: $(0 \leq t \leq \delta T)$

The equations describing this mode of operation are

$$L_{eq} \cdot \frac{di_a}{dt} + i_a.R_{eq} + K'(I_{av})\omega_{av} = V, \qquad (4.19)$$

with $i_a(o) = I_{a1}$ and $K'(I_{av}) = K(I_{av}).I_{av}$

where L_{eq} is defined in Section 4.3.1 and

$$R_{eq} = R - \frac{\lambda(\frac{\omega}{\omega_o}).\alpha}{(k_2+I_{av})}$$

II. Commutation Interval $(\delta T \leq t \leq (\delta + \delta_c)T)$

Assuming constant current during commutation interval,

gives $I_c = I_{a2}$. The commutation interval $\delta_c T$ is given by,

$$\delta_c . T = \frac{2C.V}{I_{a2}} \qquad (4.20)$$

III. Free Wheeling Interval ($(\delta + \delta_c)T \leq t \leq T$)

In this mode, the armature current free wheels through the free wheeling diode and both the main and auxiliary thyristors are off. The equations describing this mode are given by

$$L_{eq} \cdot \frac{di_a}{dt} + i_a . R_{eq} + K'(I_{av}) . \omega_{av} = 0 \qquad (4.21)$$

with $i_a((\delta + \delta_c)T) = I_c = I_{a2}$ and $i_a(T) = I_{a1}$.

The solutions of armature current obtained from equation (4.19), (4.20) and (4.21) are,

$$i_a = \frac{V - K'(I_{av}) \omega_{av}}{R_{eq}} (1 - e^{-t/T_a}) + I_{a1} . e^{-t/T_a}$$

$$\text{for } 0 \leq t \leq \delta T \qquad (4.22)$$

$$i_a = I_c = I_{a2} \quad \text{for } \delta T \leq t \leq (\delta + \delta_c)T$$

and

$$i_a = - \frac{K'(I_{av}) . \omega_{av}}{R_{eq}} (1 - e^{-t'/T_a}) + I_{a2} . e^{-t'/T_a} \qquad (4.23)$$

$$\text{for } 0 \leq t' \leq (1 - \delta - \delta_c')T$$

where $T_a = \frac{L_{eq}}{R_{eq}}$. and $t' = t - \delta T$

From equations (4.20), (4.21) and (4.22) one gets,

$$I_{a1} = \frac{V}{R_{eq}} \cdot \frac{1-e^{\delta T/T_a}}{1-e^{(1-\delta_c)T/T_a}} - \frac{K'(I_{av}).\omega_{av}}{R_{eq}} \qquad (4.24)$$

and

$$I_{a2} = \frac{V}{R_{eq}} \cdot \frac{1-e^{-\delta T/T_a}}{1-e^{-(1-\delta_c)T/T_a}} - \frac{K'(I_{av}).\omega_{av}}{R_{eq}} \qquad (4.25)$$

From equations (4.20) and (4.25), the average motor speed is given by

$$\omega_{av} = \omega = \frac{R_{eq}}{K'(I_{av})} \left\{ \left(\frac{V}{R_{eq}} \cdot \frac{1-e^{-\delta T/T_a}}{1-e^{-(1-\delta_c)T/T_a}} \right) - \frac{2C.V}{\delta_c.T} \right\}$$

$$= \frac{E_{av}}{K'(I_{av})} \qquad (4.26)$$

where, $E_{av} = K'(I_{av}).\omega_{av}$

The average armature current can be determined from

$$I_{av} = \frac{V.\delta - (1-\delta_c)K'(I_{av}).\omega_{av}}{R_{eq}} + \frac{2C.V}{T}$$

$$= \frac{V}{R_{eq}} .\left\{ \delta - (1-\delta_c) \frac{E_{av}}{V} \right\} + \frac{2C.V}{T} \qquad (4.27)$$

The electromagnetic torque is given by equation (4.18).

The values of δ_c for a given $\frac{E_{av}}{V}$ can be determined from equation (4.20) on substitution of I_{a2} from equation (4.25) as follows. The terms containing $e^{-\delta_c T/T_a}$ are expanded in terms of its power series. Neglecting third and higher order terms in δ_c yields a quadratic in δ_c which gives

$$\delta_{c1,2} = -\frac{B}{2A} \pm \frac{\sqrt{B^2-4AC}}{2A} \qquad (4.28)$$

The expressions for A,B, and C are the same as derived in the case of separately excited motor without source inductance in Section 2.3.1 of Chapter II. For known values of $\frac{E_{av}}{V}$ and $\frac{T}{T_a}$, the positive realistic value of δ_c is obtained from above and then I_{av} is calculated from equation (4.27) and the corresponding value of $K'(I_{av})$ is obtained from the internal magnetisation characteristic of the machine which includes both the saturation and armature reaction effect. The machine speed ω is then calculated from equation (4.26).

4.3.3 Calculation of Current Ripple

The normalised current ripple is obtained from equations(4.24) and (4.25) as

$$\frac{I_{a2}-I_{a1}}{\left(\frac{V}{R_{eq}}\right)} = \left[\frac{(1-e^{-\delta T/T_a})}{1-e^{-(1-\delta_c)T/T_a}} - \frac{1-e^{\delta T/T_a}}{1-e^{(1-\delta_c)T/T_a}}\right] \qquad (4.29)$$

In case of chopper with square wave output voltage, expression for normalised ripple is similar to that of equation (4.29) except that $\delta_c=0$.

For calculation of current ripple, incremental inductance should be used instead of the d.c. inductance. Due to presence of ripple in the load current, minihysteresis loops are traced as shown in Figure 4.7(a). The average incremental inductance $(\frac{\Delta\phi}{\Delta i})$ is lower than the d.c. inductance $\frac{\phi}{I}$. If the hysteresis effect is quite small, the incremental inductance can be determined by computing the slope of the mean magnetisation characteristics as shown in Figure 4.7(b). So, the approximate incremental inductance can be obtained by the expression given below.

$$L_{in} = \left[\left(\frac{\Delta\phi}{\Delta i}\right) / \frac{\phi}{I}\right] . \; L(I) \qquad (4.30)$$

The quantity $(\frac{\Delta\phi}{\Delta i})/\frac{\phi}{I}$ can be computed from the mean O.C.C. of the machine for different values of I_a. $L(I_a)$ is the corresponding measured value of d.c. inductance. The equivalent armature circuit time constant T_a has to be

determined taking the effect of eddy currents and the incremental inductance. The effective $(\frac{T}{T_a})$ can be obtained from precalculated nomograms of machines which are calculated as follows. For an assumed $(\frac{\omega}{\omega_0})$ and for a fixed value of coefficient α, L_{eq} and R_{eq} are calculated for various values of I_{av} and plotted.

4.3.4 Effect of Source Inductance on the Performance of Chopper fed d.c. Series Motor.

The source inductance influences the performance characteristics of chopper fed d.c. separately and series excited motors. The analysis in this case, can be carried out in the same way as it was done in the case of separately excited motor in Section 2.2 of Chapter II.

I. Duty Interval: $(0 \leq t \leq \delta T)$

This interval starts with the turning on of main thyristor T_1. The source current can not rise immediately to I_{a1} but rises linearly to I_{a1} after an interval of μT. The armature current continues to free wheel upto $t = \mu T$. The value of μ is given by

$$\mu = (\frac{I_{a1}}{V.T}).L_s \qquad (4.31)$$

where L_s is the source inductance. The armature current is given by

$$i_a = \frac{V-K'(I_{av}).\omega_{av}}{R}\left(1-e^{-(t-\mu T)/T'_a}\right)+I_{a1}.e^{-(t-\mu T)/T'_a} \qquad (4.32)$$

where, $T'_a = \frac{L_s+L_{eq}}{R}$, $R=(R_{eq}+R_s)$

If the source resistance is negligible, then $R=R_{eq}$.

The value of i_a at the end of this interval is

$$I_{a2}=i_a(\delta T)= \frac{V-K'(I_{av}).\omega_{av}}{R}\left(1-e^{-(\delta-\mu)T/T'_a}\right)+I_{a1}.e^{-(\delta-\mu)T/T'_a} \qquad (4.33)$$

II. Commutation Interval: $\delta T \leq t \leq \delta_c T$

The interval ($\delta_c T$) during which the commutating capacitor linearly gets charged from a voltage of $-V_1$ to $+V$, is given by

$$\delta_c T = \frac{(V+V_1).C}{I_{a2}.T} \qquad (4.34)$$

V_1 may be greater or less than V depending upon L_s, L, C and L_m.

III. Free Wheeling Interval: $(\delta+\delta_c)T \leq t \leq (1+\mu)T$

This interval starts when the commutating capacitor C has already been charged to a voltage V and the armature current begins to free wheel. But due to source inductance,

the capacitor C continues to charge. Capacitor current is described by the differential equation

$$V = L_s \cdot \frac{di_c}{dt} + \frac{1}{C}\int i_c \cdot dt$$

$$\text{with } i_c((\delta + \delta_c)T) = I_{a2}$$

The solution of i_c is given by

$$i_c = I_{a2} \cdot \cos \gamma_0 (t - \delta' T) \qquad (4.35)$$

where, $\delta' = (\delta + \delta_c)$ and $\gamma_0 = \frac{1}{\sqrt{L_s \cdot C}}$

This mode ends when $\theta_1 = \frac{\pi}{2\gamma_0 T}$ corresponding to $i_c = 0$. The maximum voltage to which the capacitor gets charged is given by

$$V_2 = I_{a2}\sqrt{\frac{L_s}{C}} + V \qquad (4.36)$$

After this, the condenser C will discharge partially through the source and free wheeling diode. Now

$$(L_s + L_m) \cdot \frac{di_c}{dt} + \frac{1}{C}\int i_c \, dt = V$$

$$\text{with } v_c(o) = V_2 \text{ and } i_c(o) = 0$$

The solution of i_c is given by

$$i_c = \frac{V - V_2}{\sqrt{(L_s + L_m)/C}} \sin \gamma_0'(t - \lambda') \qquad (4.37)$$

where,

$$\gamma_o' = \frac{1}{\sqrt{(L_s+L_m)C}}, \quad \lambda' = (\delta' + \theta_1)T$$

The minimum possible voltage on C occurs when $i_c=0$ which yields

$$V_1 = V - \sqrt{(L_s + L_m)/C} \cdot I_{a2} \tag{4.38}$$

The armature current starts free wheeling at $t=(\delta + \delta_c)T$ and it continues upto $t=T+ \mu T$. The armature current is given by equation (4.21). The solution of the equation yields,

$$i_a = \frac{-K'(I_{av})\omega_{av}}{R}(1-e^{-t'/T_a}) + I_{a2} \cdot e^{-t'/T_a} \tag{4.39}$$

where $t' = t-(\delta + \delta_c)T$.

Free wheeling continues upto $t= T+ \mu T$. The armature current at the end of free wheeling is

$$I_{a1}= - \frac{-K'(I_{av})\omega_{av}}{R}(1-e^{-(1-\delta'+\mu)T/T_a}) + I_{a2} \cdot e^{-(1-\delta'+\mu)T/T_a} \tag{4.40}$$

By elimination of variables from equations (4.33) and (4.40),

$$I_{a1}= \frac{-K'(I_{av})\omega_{av}}{R} + \frac{V}{R} \cdot \frac{1-e^{(\delta-\mu)T/T_a'}}{1-e^{(1-\delta_c)T/T_a - a(\delta-\mu)}} \tag{4.41}$$

$$I_{a2} = \frac{-K'(I_{av}).\omega_{av}}{R} + \frac{V}{R} \quad \frac{1-e^{-(\delta-\mu)T/T'_a}}{1-e^{-(1-\delta_c)T/T_a+a(\delta-\mu)}} \qquad (4.42)$$

where, $a = \left(\frac{T}{T_a} - \frac{T}{T'_a}\right)$.

The expression for μ is obtained in the same way as it has been shown in Section 2.2.1 of Chapter II as,

$$\mu = \frac{\frac{-K'(I_{av}).\omega_{av}}{V}(1-e^{(1-\delta_c)T/T_a-a\delta})+(1-e^{\delta T/T'_a})}{\frac{T.R}{L_s}(1-e^{(1-\delta_c)T/T_a-a\delta}) - \frac{K'(I_{av}).\omega_{av}}{V}.a.e^{(1-\delta_c)T/T_a-a\delta}} - \frac{T}{T'_a}.e^{\delta T/T'_a} \qquad (4.43)$$

The commutation interval ($\delta_c T$) is determined in the same way as it was done in Section 2.2.1 of Chapter II.

$$\delta_c = -\frac{B}{2A} \pm \frac{\sqrt{B^2-4AC}}{2A} \qquad (4.44)$$

The expressions for A,B and C are the same as shown in Section 2.2.1 except that E is replaced by $K'(I_{av}).\omega_{av}$.

Pure free wheeling interval may or may not exist depending upon the parameters L, L_s,C and L_m. If L_s and C are such that after the capacitor C has been charged to maximum voltage V_2, it may not get sufficient time to

discharge to the minimum value of V_1 volts. In that case, the commutation interval can be determined from equation (4.34) with $V_1=V$. without appreciable error. The expressions for A,B and C will be the as above except that the terms containing γ_δ will be absent.

The expressions for μ and δ_c as shown in equations (4.43) and (4.44) are interdependent. As a first step, δ_c is determined from equation (4.44) ignoring μ. Then μ is calculated using this value of δ_c and δ_c is again corrected corresponding to the value of μ.The average armature current is given by

$$I_{av} = \frac{1}{T}\left[\int_0^{\delta T} . i_a \, dt + I_{a2} . \delta_c T + \int_0^{(1-\delta-\delta_c')T} i_a \, dt\right] \qquad (4.45)$$

The value of I_{av} can also be determined by,

$$I_{av} = \frac{V(\delta-\mu)-K'(I_{av}).\omega_{av}.(1-\delta_c)}{R} + \frac{C(V+V_1)}{T} \qquad (4.46)$$

The expressions for torque and speed are the same as given by equations (4.18) and (4.26).

4.3.5 Performance and Experimental Verification

Experiments were carried out on two d.c. series motors (Machines III and IV) whose particulars are given in Appendix B.

The chopper used is a two thyristor chopper using load dependent commutation as shown in Figure 2.1. The source consisted of a d.c. generator having an armature circuit inductance of 25 mH (saturated). A large buffer condenser bank of 8000 μF was used at the source terminals to neutralize the effect of source inductance. Machine III is a generalised machine connected as a series motor. Both the stator and rotor of this machine are made of laminated low hysteresis steel sheets. Therefore, the eddy currents in the field core will be much less in this machine. Machine IV is a d.c. series motor with laminated armature, laminated pole cores and solid yoke construction. The eddy current effects in this case is considerable. The values of λ, σ and index n for the test machines as determined by step response are also shown in Appendix B. The variation of (L_a+L_f), the total incremental inductances of the above test machines, was determined using equation (4.30) as functions of steady state d.c. current I_a and it has been shown in Figure 4.7(c). The variation of $K(I_a) \approx K(I_{av})$ for these two machines are shown in Figure 4.8(a). Figures 4.8(b) and 4.8(c) show the calculated torque-speed characteristics of the two machines for fixed values of δ (neglecting the source inductance) using equations (4.26), (4.27) and (4.28) which take the

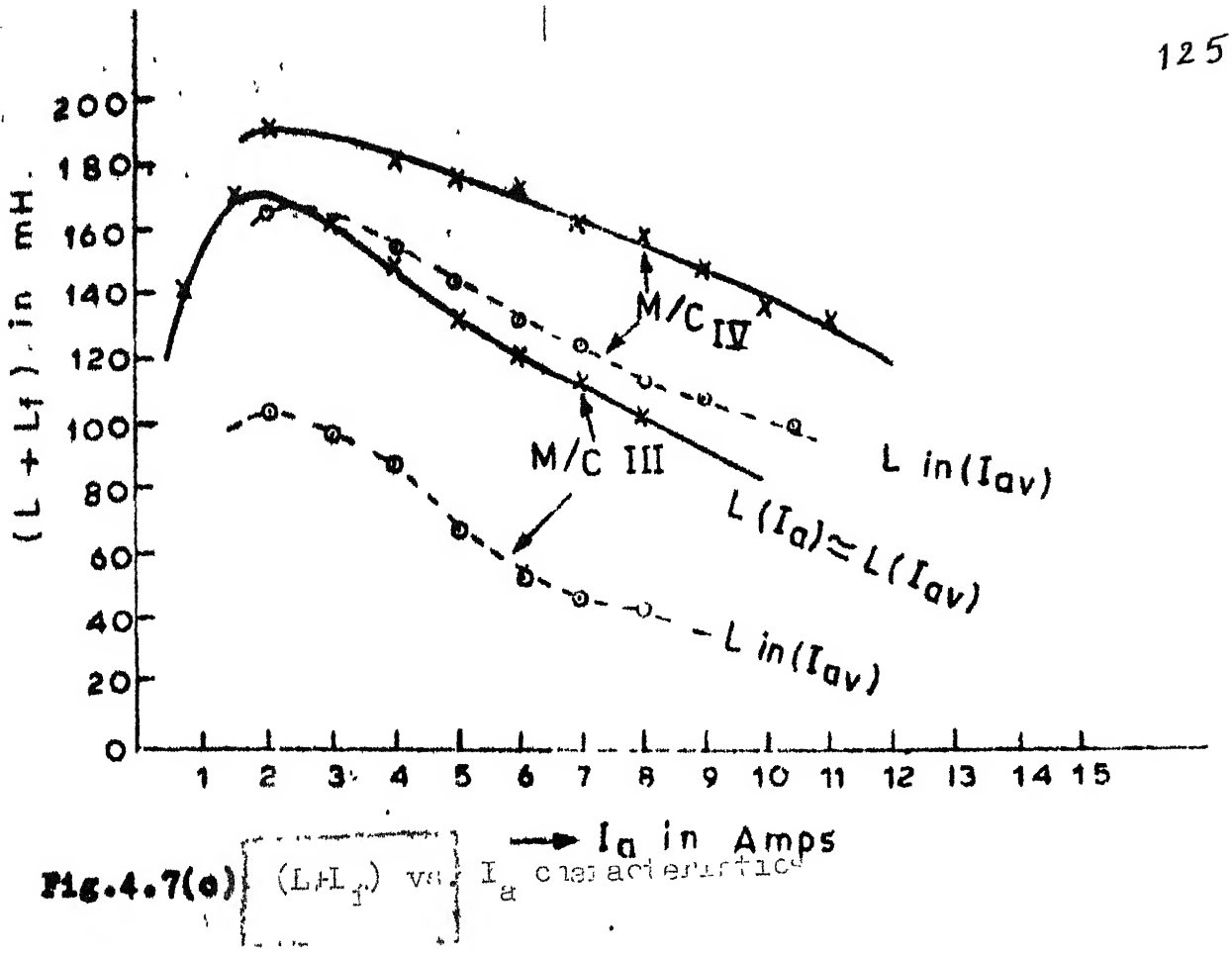

Fig.4.7(a) $(L+L_f)$ vs. I_a characteristics

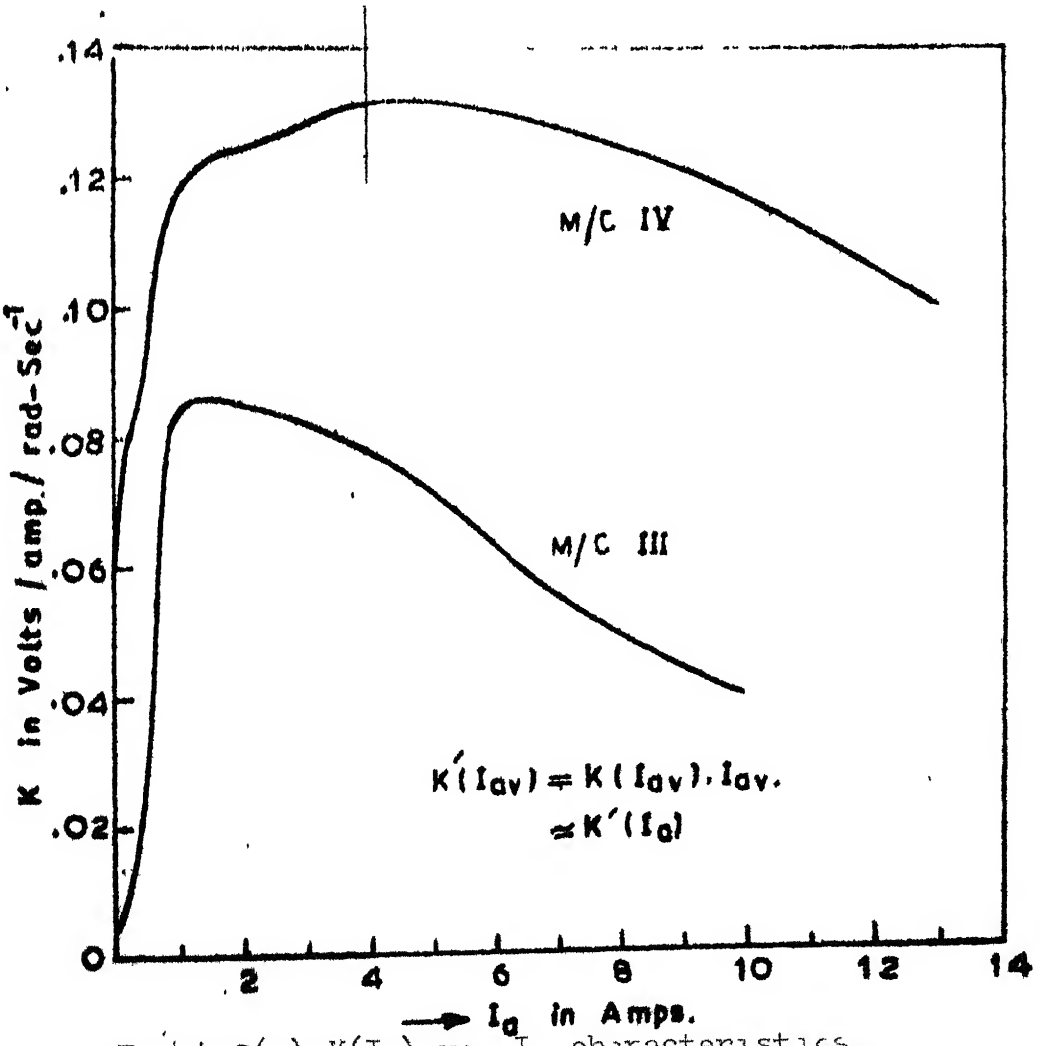

Fig.4.8(a) $K(I_a)$ vs. I_a characteristics

effect of commutation pulse into account. The experimental curves obtained after using a large buffer condenser bank (8000 μF) at the source terminals are also shown in Figures 4.8(b) and 4.8(c). The calculated curves corroborate very well with the experimental results for both the machines, except for higher values of torque for machine III. In machine III sparking at the commutator was noticed from 6 amperes onwards. This increased the effective value of armature circuit resistance. This explains the difference between the predicted and experimental characteristics for higher values of torque in the case of machine III. Torque - speed curves calculated neglecting eddy currents are also shown in Figure 4.8(b) and 4.8(c). It is observed that the effect of eddy currents on the torque-speed characteristics of chopper fed d.c. series motor is quite small and can be neglected without much loss of accuracy. Discontinuous conduction was completely absent. The normalised p.u. armature current ripple was calculated using equation (4.29). The Figures 4.9(a) and 4.9(b) show the calculated and measured values of p.u. normalised armature current ripple versus I_{av} for fixed values of δ for machines III and IV respectively. The experimental values of ripple were measured when a buffer condenser bank was connected at the

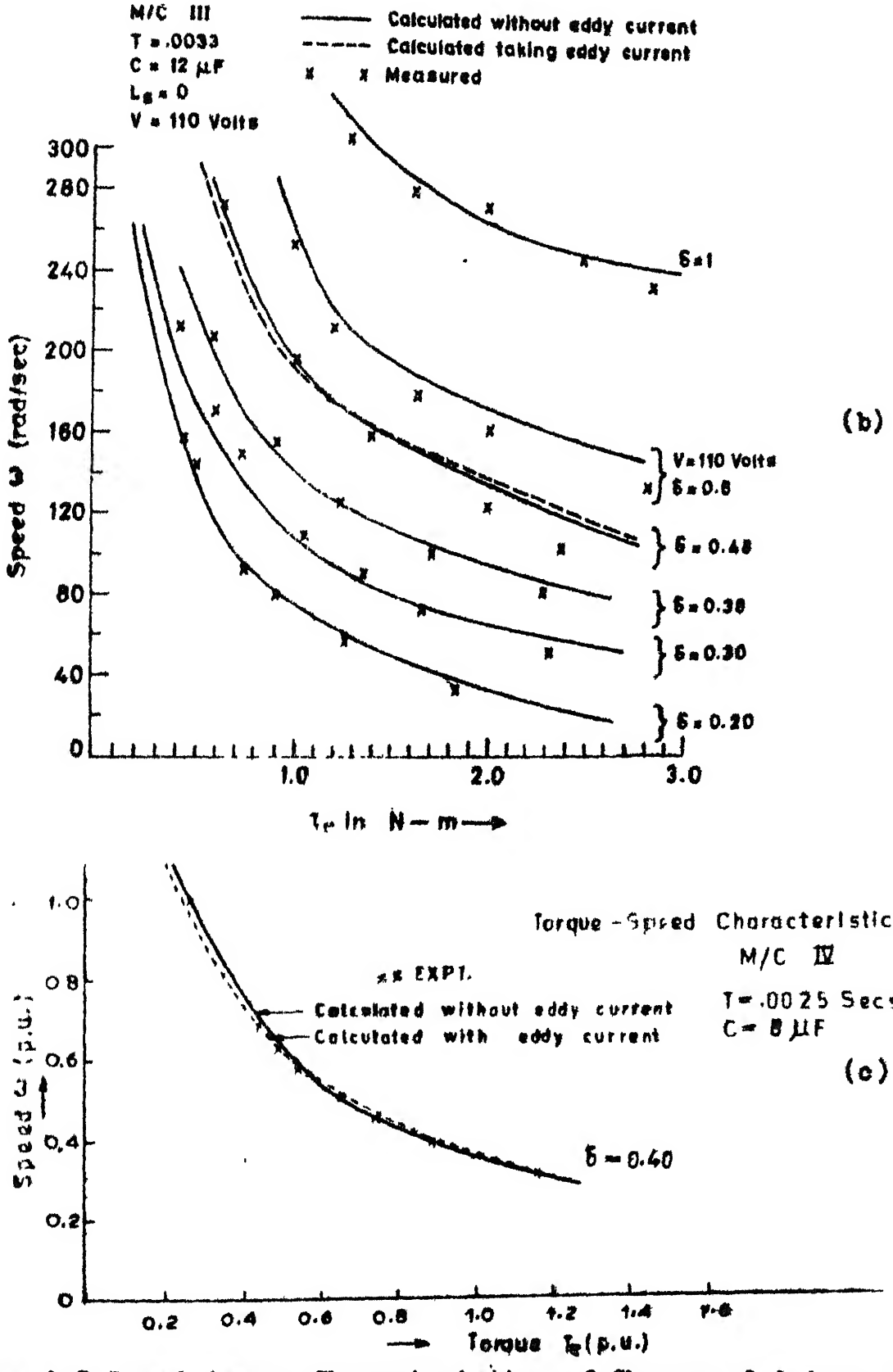

Fig.4.8 Speed torque Characteristics of Chopper fed d.c. series motors.

source terminals. Figure 4.9(a) shows the curves of calculated p.u. ripple for machine III using (i) unsaturated value of armature circuit inductance (ii) value of armature circuit inductance at rated d.c. current; (iii) the average value of incremental inductance as a function of I_{av} as determined from equation (4.30); (iv) the average value of incremental inductance as a function of I_{av} and also taking into account the eddy currents by taking $\alpha = 0.1$ and 0.2 respectively. In the first three cases, eddy currents were not taken into account. It is seen that approach (iv) gives better prediction of current ripple with satisfactory accuracy for $\alpha = 0.2$. Whereas the approaches (i) to (iii) give large amount of errors in the prediction of current ripple. The approaches (ii), (iii) and (iv) were used to calculate current ripple in case of machine IV. This machine has more eddy current effect because of solid iron yoke. Figure 4.9(b) re-establishes the fact that in this case also approach (iv) gives better results. Thus, though eddy currents have negligible effect on the steady state torque-speed characteristics, they considerably influence the ripple in the armature current. It is also seen that the induced eddy currents in the series field cores and other parts of the magnetic circuit of machine increases

Calculated ripple in p.u.

i) with armature ckt. inductance(unsaturated)
ii) with armature ckt. inductance(rated current)
iii) with incremental $L_{in}(I_{av})$
iv) with $L_{in}(I_{av})$ and eddy currents
x x Measured

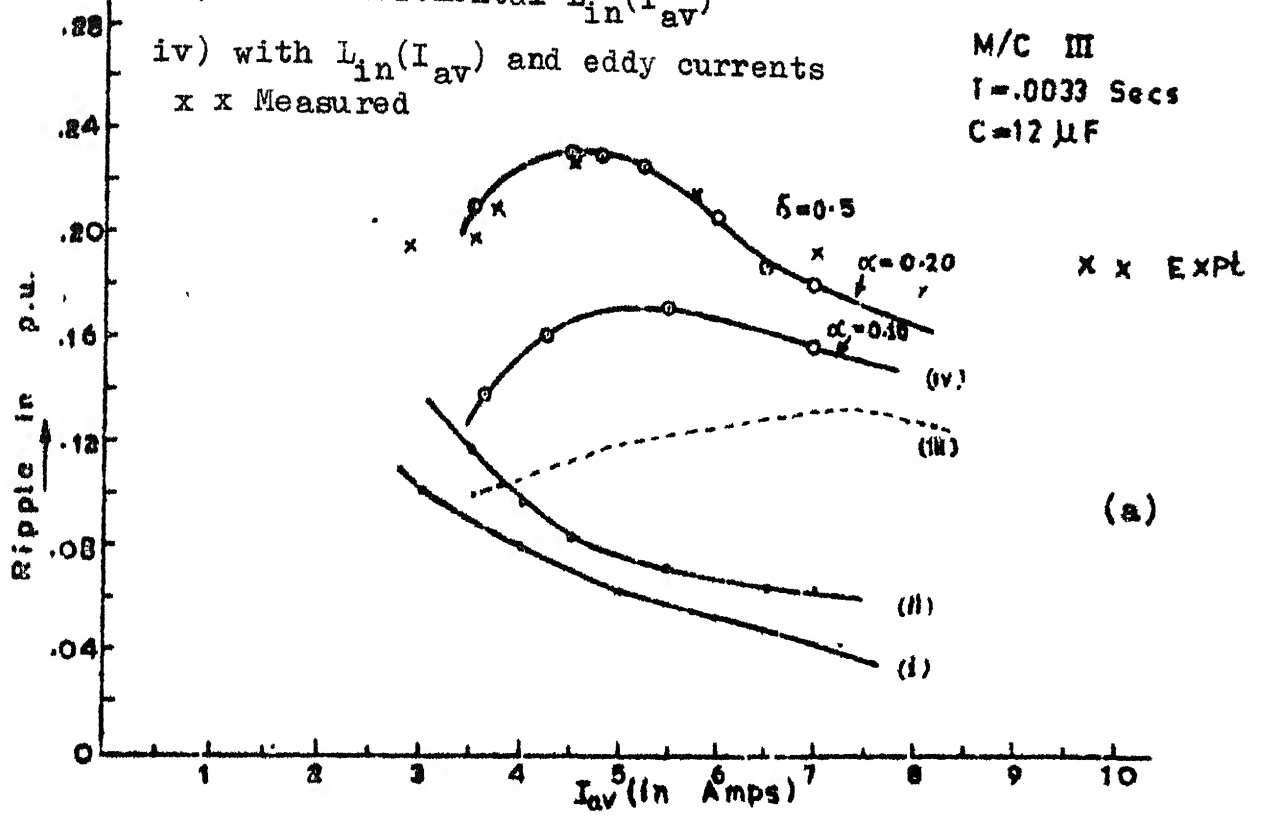

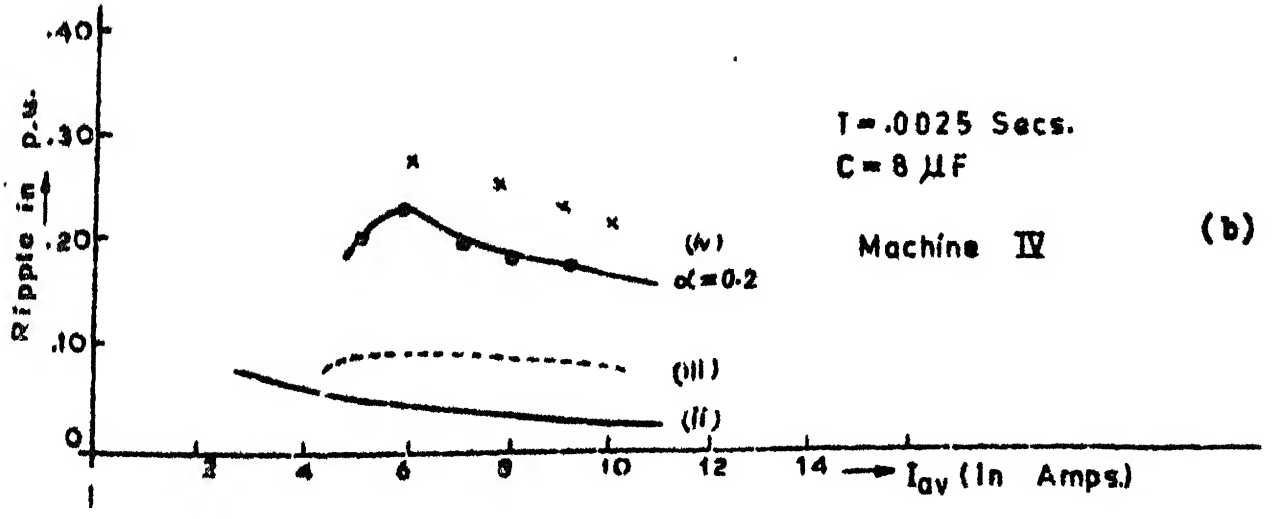

Fig 4.9 P.U. Normalised ripple vs. I_{av}.

the magnitude of current ripple. The machine having solid iron in the magnetic circuit will have more eddy currents induced. This will increase the magnitude of current ripple (Figure 4.9(b)).

Figure 4.10 shows a typical calculated torque speed characteristics of machine IV taking the effect of source inductance into account. The source had a saturated inductance of 25 mH. The characteristic was calculated using equations (4.43), (4.44), (4.45), (4.26),and (4.18). The experimental characteristic was determined for $\delta = 0.4$ after disconnecting the buffer condenser bank from the source terminals. For this chopper operating frequency of 400 Hz and C=8 μF, L_s= .025H, L_m = 0.001H, commutation difficulties were encountered for higher values of load current due to partial discharge of commutating capacitor during free wheeling mode. Calculated torque-speed characteristic for $\delta = 0.4$ neglecting the source inductance has also been shown in Figure 4.10 for comparison. It is found, that, if the source inductance is not taken into account, there is a large amount of error in the prediction of torque and speed. Figure 4.11 shows the calculated torque-speed characteristic for $\delta = 0.4$ and C=16μF taking source inductance into account. In this case, $\gamma_o = \frac{1}{\sqrt{L_s \cdot C}}$ being low, the

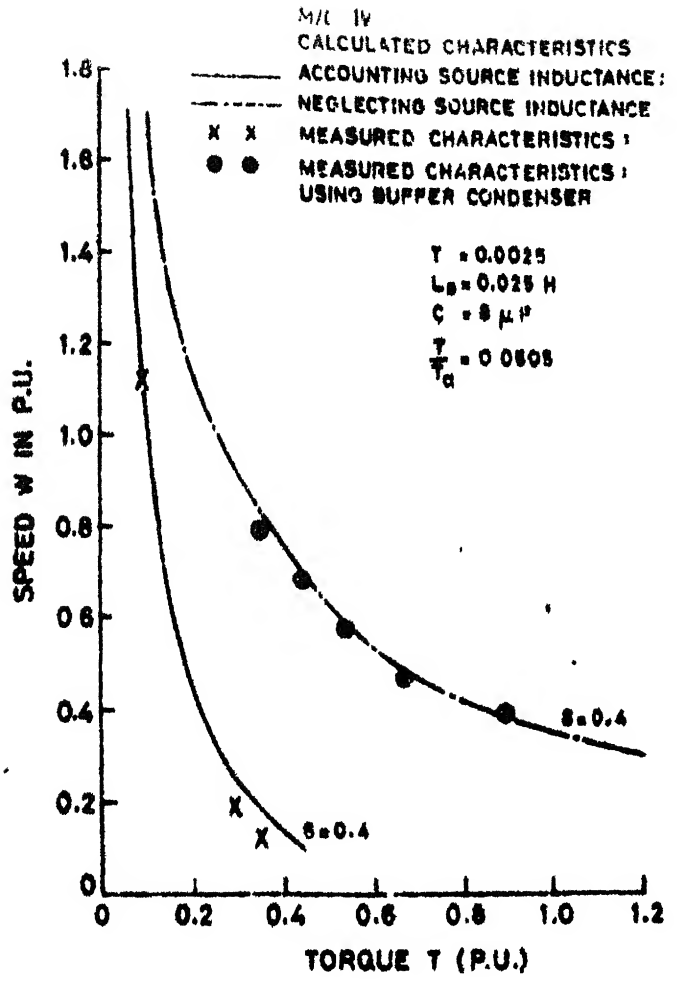

Fig. 4.10 Torque Speed Characteristics (L_s= .025H, C=8μF)

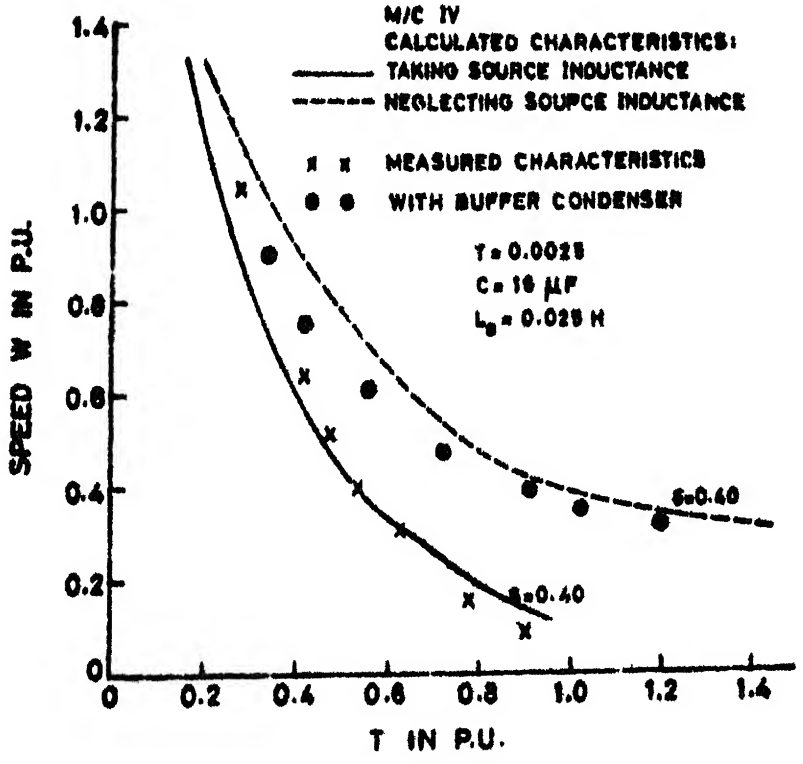

Fig. 4.11 Torque Speed Characteristics (L_s= .025H, C=16μF)

commutating capacitor does not get enough time to discharge from a voltage $V_2(>V)$ to a voltage $V_1(<V)$. In this case, the commutation interval ($\delta_c T$) was calculated from equation (4.34) with $V_1=V$. The torque was calculated using equations (4.45) and (4.18). The experimental characteristic was determined after disconnecting the buffer condenser bank from the source terminals. No commutation problem arose in this case. Calculated characteristic neglecting the source inductance has also been shown in Figure 4.11 for comparison. Figure 4.11 shows that the source inductance has considerable influence on the speed torque curves. The method presented here permits the prediction of speed torque curves with satisfactory accuracy. Measured points obtained with a buffer condenser at the source terminals have also been shown. The closeness of these curves with the characteristic calculated neglecting source inductance indicates that the buffer condenser neutralises the effect of source inductance.

4.4 CONCLUSIONS

The following important conclusions can be drawn from the above study.

1. The approach suggested for modelling of d.c. series motor fed by chopper, taking the effects of saturation of magnetic circuit, eddy currents and armature reaction,

permits the calculation of machine performance with satisfactory accuracy.

2. The effect of eddy currents on the torque-speed curves of chopper fed series motor is quite small. The eddy currents, however, have considerable effect on the magnitude of ripple in armature current.

3. The armature current ripple can be calculated with satisfactory accuracy, if the eddy current effects and the average incremental inductance are used as reported here.

4. Source inductance effectively reduces the 'on' time of the chopper and adversely affects the torque-speed characteristics of the motor by increasing the stiffness of the characteristics. If an oversized capacitor is not used for commutation especially for low frequency operation, it will produce serious commutational problems for the type of chopper used here. If a suitable buffer condenser bank is used at the source terminals, it will neutralize the effect of source inductance.

CHAPTER V

PERFORMANCE AND ANALYSIS OF CHOPPER FED D.C. SERIES MOTOR UNDER REGENERATIVE BRAKING

5.1 INTRODUCTION

Regenerative braking in traction drives is becoming very popular because of saving of energy of the order of 20 to 30 percent. D.C. choppers provide an economic and efficient way to implement regenerative braking because of the ability to regenerate at low speeds.

A few papers [14-16] have been published on regenerative braking of d.c. series motors, describing circuits and instability involving loss of current control resulting in high currents at large speeds. The methods of predicting regenerative braking performance and loss of regenerative braking at low speeds and detailed investigation of performance have been described in this chapter. The method of analysis is general in the sense that it takes into account the effect of saturation of the magnetic circuit, armature reaction, chopper commutation interval and the effect of source inductance. In deriving the performance equations, approximations suggested by Dubey and Shepherd [9] have been

used. The steady state dynamic behaviour of a series motor has been investigated with respect to braking torque, regenerative power fed back and efficiency of regeneration. The boundary of critical speeds below which regeneration fails has been derived. The effects of commutation capacitor, frequency of operation of chopper and filter inductance on the braking performance have been investigated.

It has been shown that for a given chopper operating frequency, the presence of source inductance and the use of an over sized commutating capacitor improves the stability of the machine characteristics and the control becomes better. Moreover, at higher chopper operating frequency, the commutating capacitor may get charged to a voltage greater than the source voltage ensuring reliable commutation. At low chopper operating frequency, the commutating capacitor in case of two thyristor load current commutated chopper may get partially discharged to a voltage less than the supply voltage during regeneration interval and it will adversely affect the commutation of the chopper. It has been shown that neglecting the source inductance in the analysis may lead to erroneous prediction of machine performance. The use of a suitable value of buffer condenser at the source terminals, neutralizes the effect

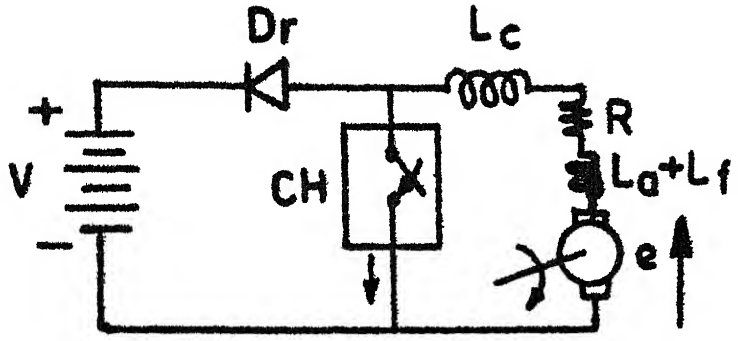

Chopper is 'on'

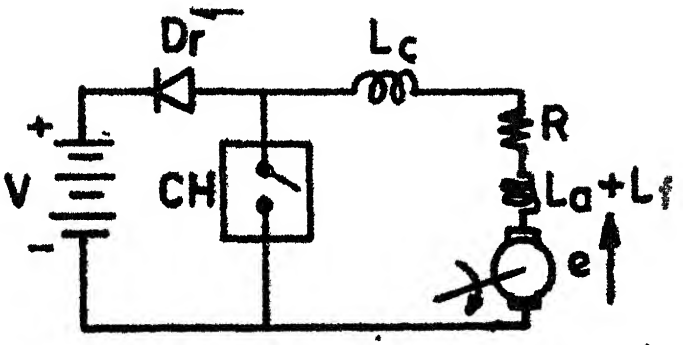

Chopper is 'off'

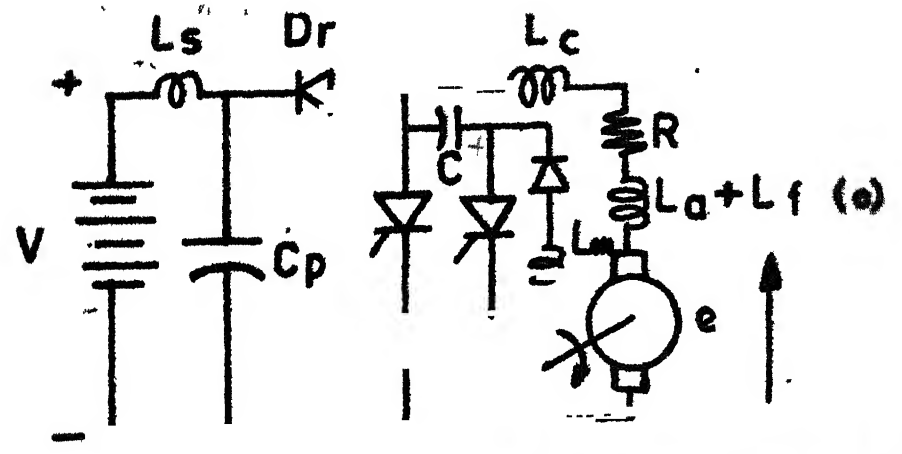

Fig.5.1 Regenerative braking of chopper controlled d.c. series motor.

of source inductance on the machine performance characteristics. The characteristics presented are useful in selecting a proper value of filter inductance for a fixed value of chopper operating frequency that will ensure stability of operation over a wide range and at the same time limit the armature current ripple within low specified limits. They are useful in selecting a suitable value of commutation capacitor.

Figures 5.1(a) and 5.1(b) show the idealised equivalent circuits of a chopper fed d.c. series motor under regenerative braking. In choppers using load dependent commutation, such as shown in Figure 5.1(c), the output voltage wave form is neither a square wave nor can it be approximated by a square wave without loss of accuracy. Figures 5.2(a) and 5.2(b) show the idealised voltage and current wave forms of such choppers.

5.2 PERFORMANCE EQUATIONS

The analysis is carried out based upon the assumptions mentioned in Sections 2.2 and 4.2. For a d.c. series motor, the induced back e.m.f. is given by

$$e = K(i_a).i_a.\omega \qquad (5.1)$$

In an actual machine, K will vary due to saturation of

magnetic circuit and armature reaction which depend on the armature current. In case of chopper controlled series motor, the average effect of saturation and armature reaction can be taken into account by considering K to be a function of average current, I_{av}. Thus, equation (5.1) can be replaced by

$$E_{av} = K(I_{av}).I_{av}.\omega = K'(I_{av}) \cdot \omega \qquad (5.2)$$

where, $K'(I_{av}) = K(I_{av}).I_{av}$.

$K'(I_{av})$ is obtained from the internal characteristic of the machine.

5.2.1 Analysis when fed by Square Wave Output Chopper

In this case, there are only two modes of operations, i.e.,duty interval and regenerative interval. The corresponding voltage and current wave forms are shown in Figure 5.2(a).

I. Duty Interval: $(0 \leq t \leq \delta T)$

$$E_{av} = R.i_a + L \cdot \frac{di_a}{dt} \qquad (5.3)$$

where, $R = (R_a + R_f + R_c)$,

$L = (L_a + L_f + L_c)$

Assuming initial value of i_a to be I_{a1}, this gives,

$$i_a = \frac{E_{av}}{R}(1-e^{-t/T_a}) + I_{a1} \cdot e^{-t/T_a} \qquad (5.4)$$

II. Regeneration Interval: ($\delta T \leq t \leq T$)

$$E_{av} = R \cdot i_a + L \frac{di_a}{dt} + V \qquad (5.5)$$

Taking initial value of $i_a = I_{a2}$,

$$i_a = \frac{E_{av}-V}{R}(1-e^{-t'/T_a}) + I_{a2} \cdot e^{-t'/T_a} \qquad (5.6)$$

where, $t' = t - \delta T$.

In steady state condition, the expressions for I_{a1} and I_{a2} are obtained with the help of equations (5.4) and (5.6) as,

$$I_{a1} = \frac{E_{av}}{R} - \frac{V}{R} \frac{1-e^{-(1-\delta)T/T_a}}{1-e^{-T/T_a}} \qquad (5.7)$$

$$I_{a2} = \frac{E_{av}}{R} - \frac{V}{R} \frac{1-e^{(1-\delta)T/T_a}}{1-e^{T/T_a}} \qquad (5.8)$$

$$\text{Normalised p.u. ripple} = \left[\frac{I_{a2} - I_{a1}}{(V/R)}\right] = \left[\frac{1-e^{-(1-\delta)T/T_a}}{1-e^{-T/T_a}} - \frac{1-e^{(1-\delta)T/T_a}}{1-e^{T/T_a}}\right] \qquad (5.9)$$

The average armature current I_{av} is given by

$$I_{av} = \frac{E_{av} - (1-\delta)V}{R} \qquad (5.10)$$

P_{em} = total electromagnetic power developed by the machine

$$= E_{av} \cdot I_{av} \qquad (5.11)$$

Let P_{rdy} be the dynamic power loss = $I_{rms}^2 \cdot R$.

P_{rg} = Regenerative power

$$= \frac{V}{T} \cdot \int_0^{(1-\delta)T} i_a \cdot dt$$

$$= \frac{V^2}{R} \left[\left(\frac{E_{av}}{V} - 1\right)(1-\delta) + \left(\frac{E_{av}}{V} - 1\right)\left(\frac{T_a}{T}\right) \cdot \left(e^{-(1-\delta)T/T_a} - 1\right) \right.$$

$$\left. - \left(\frac{E_{av}}{V} - \frac{1-e^{(1-\delta)T/T_a}}{1-e^{T/T_a}}\right) \cdot \left(\frac{T_a}{T}\right) \cdot \left(e^{-(1-\delta)T/T_a} - 1\right) \right] \qquad (5.12)$$

T_{br} = Electromagnetic braking torque

$$= K'(I_{av}) \cdot I_{av} \qquad (5.13)$$

η_{rg} = efficiency of regeneration

$$= \frac{P_{rg}}{E_{av} \cdot I_{av}} \qquad (5.14)$$

5.2.2 Analysis for Nonsquare Output Voltage Chopper using Load Dependent Commutation

In this case, there are three distinct modes of operation, namely, duty interval, commutation interval and regeneration interval.

I. Duty Interval: $(0 \leq t \leq \delta T)$

The differential equation describing this mode of operation is given by equation (5.3) and i_a is given by equation (5.4) with the same initial condition.

II. Commutation Interval: $(\delta T \leq t \leq (\delta + \delta_c)T)$

It is assumed that commutation takes place at constant value of load current $i_a = I_{a2}$, the commutation interval ($\delta_c T$) during which the commutating capacitor gets charged from a voltage of -V to +V is given by

$$\delta_c = \frac{2CV}{I_{a2} \cdot T} \qquad (5.15)$$

III. Regeneration Interval: $(\delta+\delta_c)T \leq t \leq T$

The equation describing this mode is given by equation (5.5) with the initial condition $i_a(t=(\delta+\delta_c)T) = I_{a2}$. The solution of i_a is given by equation (5.6) with $t' = t-(\delta + \delta_c)T$. The expressions for I_{a1} and I_{a2} are obtained from equations (5.4) and (5.6) taking equation (5.15) into account as

$$I_{a2} = \frac{E_{av}}{R} - \frac{V}{R} \cdot \frac{1-e^{(1-\delta')T/T_a}}{1-e^{(1-\delta_c)T/T_a}} \qquad (5.16)$$

$$I_{a1} = \frac{E_{av}}{R} - \frac{V}{R} \cdot \frac{1-e^{-(1-\delta')T/T_a}}{1-e^{-(1-\delta_c)T/T_a}} \qquad (5.17)$$

where, $\delta' = (\delta + \delta_c)$.

In the above equations, δ_c is unknown. It can be determined from equation (5.15) as follows.

$$\delta_c = \frac{2C.V}{T} \cdot \frac{(1-e^{(1-\delta_c)T/T_a})}{\frac{V}{R}\left\{\left(\frac{E_{av}}{V} - 1\right) - \frac{E_{av}}{V} \cdot e^{(1-\delta_c)T/T_a} + e^{(1-\delta')T/T_a}\right\}} \qquad (5.18)$$

Now expanding the terms containing $e^{-\delta_c \cdot T/T_a}$ in interms of its power series, yields a quadratic in δ_c after neglecting all terms containing 3rd and higher powers in δ_c, as

$$A.\,\delta_c^2 + B\,\delta_c + C = 0 \qquad (5.19)$$

where,

$$A = \left[\frac{T}{T_a} \cdot \frac{E_{av}}{V} \cdot e^{T/T_a} - \frac{T}{T_a} \cdot e^{(1-\delta)T/T_a} + \frac{C.R}{T_a} \cdot e^{T/T_a}\right]$$

$$B = \frac{E_{av}}{V}(1-e^{T/T_a}) - (1-e^{(1-\delta)T/T_a}) - \frac{2C.R}{T_a} \cdot e^{T/T_a}$$

$$C = -\frac{2C.R}{T}(1-e^{T/T_a})$$

$$\text{or,}\quad \delta_c = -\frac{B}{2A} \pm \frac{\sqrt{B^2-4AC}}{2A} \qquad (5.20)$$

Now for a given $\frac{E_{av}}{V}$, the positive realistic value of δ_c is obtained from equation (5.20).

The steady state average armature current I_{av} is given by

$$I_{av} = \left[\frac{E_{av}}{V}(1-\delta_c)-(1-\delta')\right]\frac{V}{R} + \frac{2.C.V}{T} \qquad (5.21)$$

The developed electromagnetic torque T_{br} is given by equation (5.13).

$$\text{The normalised p.u. ripple} = \frac{I_{a2}-I_{a1}}{\left(\frac{V}{R}\right)} = \left[\frac{1-e^{-(1-\delta')T/T_a}}{1-e^{-(1-\delta_c)T/T_a}} - \frac{1-e^{(1-\delta')T/T_a}}{1-e^{(1-\delta_c)T/T_a}}\right] \qquad (5.22)$$

The regenerative power is given by

$$P_{rg} = \frac{V}{T}\int_0^{(1-\delta')T} . i_a . dt$$

$$= \frac{V^2}{R}\left(\frac{E_{av}}{V}-1\right)(1-\delta') + \frac{V^2}{R}\left(\frac{E_{av}}{V}-1\right).\frac{T_a}{T}.\left(e^{-(1-\delta')T/T_a}-1\right)$$

$$- \frac{V^2}{R}\left(\frac{T_a}{T}\right).\left\{\frac{E_{av}}{V} - \frac{1-e^{(1-\delta')T/T_a}}{1-e^{(1-\delta_c)T/T_a}}\right\}.\left(e^{-(1-\delta')T/T_a}-1\right) \qquad (5.23)$$

where, $\delta' = (\delta + \delta_c)$.

The efficiency of regeneration η_{rg} is given by

$$\eta_{rg} = \frac{P_{rg}}{E_{av} \cdot I_{av}}$$

$$= \frac{(\omega_r - 1)(1-\delta) + \frac{T_a}{T}\left\{ e^{(1-\delta')T/T_a} + e^{\delta T/T_a} - e^{(1-\delta_c)T/T_a} - 1 \right\}}{\omega_r \left\{ (1-\delta_c) \cdot \omega_r - (1-\delta') + \frac{2CR}{T} \right\}} \qquad (5.24)$$

where, $\omega_r = \left(\frac{E_{av}}{V}\right)$

The critical speed of regeneration for a fixed value of δ may be defined as that speed for which P_{rg} just becomes zero. From equation (5.23), it is found that $P_{rg} = 0$ when $\delta' = 1$. Substituting $\delta' = 1$ in the expression of I_{av} in equation (5.21), one gets,

$$I_{av} = \frac{(1-\delta_c)\, E_{av}}{R} + p \qquad (5.25)$$

where $p = \frac{2C \cdot V}{T}$.

From equations (5.2) and (5.25),

ω_{cr} = critical speed of regeneration for a fixed value of δ

$$= \frac{(I_{av} - p) \cdot R}{(1-\delta_c) \cdot K' (I_{av})} \qquad (5.26)$$

To determine ω_{cr} for a given δ , the equation (5.18) is rewritten as,

$$\delta_c = \frac{2CR}{T}\left[\frac{1-e^{(1-\delta_c)T/T_a}}{\left(\frac{E_{av}}{V}\right)_{cr}\cdot\left(1-e^{(1-\delta_c)T/T_a}\right)}\right] = \frac{2CR}{T}\cdot\left(\frac{V}{E_{av}}\right)_{cr}$$

as $\delta' = \delta + \delta_c = 1$, under critical condition. Now for a given δ, δ_c is known under critical condition. Therefore,

$$\left(\frac{E_{av}}{V}\right)_{cr} = \frac{2C.R}{\delta_c.T} \qquad (5.27)$$

Then $\left(\frac{E}{V}\right)$ is calculated using equation (5.27). The average armature current I_{av} is determined from equation (5.25) and then ω_{cr} is obtained from equation (5.26). Thus, equations (5.26), (5.27) together with equation (5.13) give the boundary of regeneration on the speed-torque plane. Below this boundary on the speed-torque plane, the machine fails to regenerate.

5.2.3 Calculation of Current Ripple

The normalised current ripple for a load current commutated chopper is given by equation (5.22). In case of chopper with square wave output voltage, the expression for normalised current ripple is given by equation (5.9) and it is the same expression given by equation (5.22) with $\delta_c = 0$. For calculation of current ripple, incremental inductance should be used instead of d.c. inductance. Due to presence

of ripple in the d.c. current, it gives rise to mini-hysteresis loops. As a result, the effective inductance offered to the ripple is the incremental inductance which is much lower than the d.c. inductance. If the hysteresis effect is small, then the approximate incremental inductance can be determined by computing the slope $(\frac{\Delta\phi}{\Delta i})$ of the mean d.c. magnetising characteristics for different values of current as described in Section 4.3.3 of Chapter IV. The effective time constant T_a of the armature circuit should be calculated by taking the combined average incremental inductances.

5.2.4 Analysis in Presence of Source Inductance

All the possible modes of operation are described below.

I. Duty Interval: $(0 \leq t \leq \delta T)$

The differential equation describing this mode of operation is given by equation (5.3) and i_a is given by equation (5.4) with the same initial condition.

II. Commutation Interval: $(\delta T \leq t \leq (\delta + \delta_c) T)$

With the assumption of constant current during commutation, the commutation interval ($\delta_c T$) during which

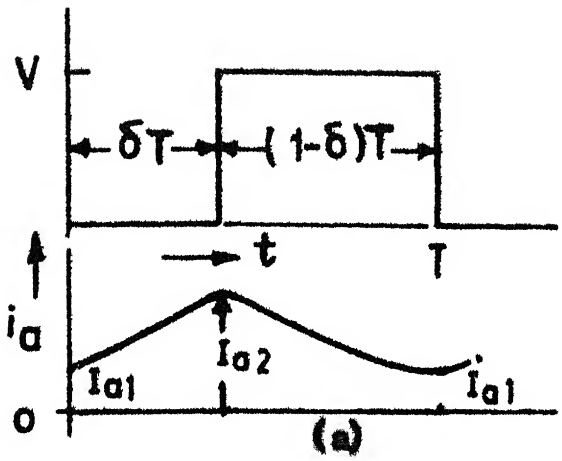

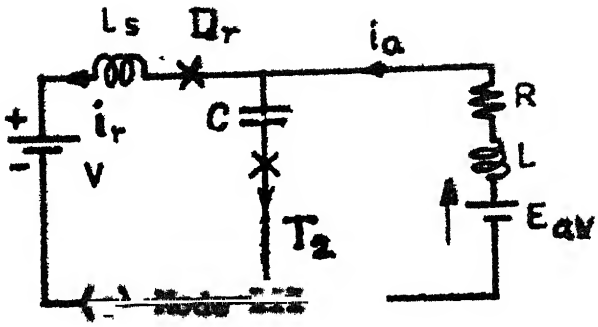

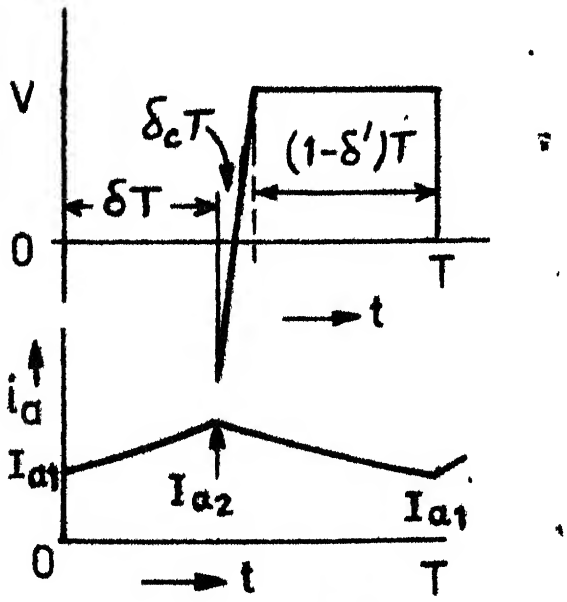

(b)

Fig.5.2 Idealised output voltage and current wave forms under regenerative braking.

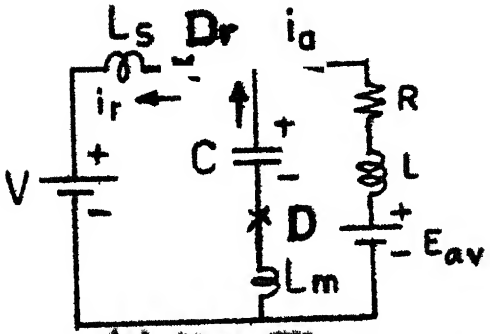

(b) Mode IV

Fig.5.3 Equivalent circuits.

the capacitor C gets charged from $-V_1$ to $+V$ volts is given by the equation

$$\delta_c = \frac{C(V+V_1)}{I_{a2}\cdot T}$$

III. Regeneration Interval I: $(\delta+\delta_c)T \leq t \leq (\delta+\delta_c+\delta_c')T$

This mode starts when the capacitor C has been charged to a voltage V with upper plate positive as shown in Figure 5.3(a). At this time, the diode D_r being forward biased, regeneration will start. But due to the presence of source inductance L_s, the entire armature current cannot be transferred immediately to the source and so the capacitor C will get charged to a voltage $V_2 > V$. The equivalent circuit is shown in Figure 5.3(a). The differential equations are,

$$L.\frac{di_a}{dt'} + R.i_a + L_s \cdot \frac{di_r}{dt'} + V = E_{av} \qquad (5.28)$$

$$\frac{1}{C}\int_0^{t'} i_c.dt' = L_s \cdot \frac{di_r}{dt'} \qquad (5.29)$$

with $i_a(t' = 0) = I_{a2}$

$$i_a - i_r = i_c \qquad (5.30)$$

where, t' is the time redefined from the beginning of this mode. Taking Laplace's transform of equation (5.28)

and (5.29) after neglecting the voltage drop across the resistance R, the capacitor current i_c is given by

$$i_c = \mathcal{L}^{-1}\left[\frac{E_{av}-V}{L(s^2+\gamma_1^2)} + \frac{I_{a2}\cdot s}{s^2+\gamma_1^2}\right]$$

or,

$$i_c = \frac{E_{av}-V}{L}\cdot\frac{1}{\gamma_1}\cdot\sin\gamma_1 t' + I_{a2}\cdot\cos\gamma_1 t' \qquad (5.31)$$

where,

$$\gamma_1 = \sqrt{\frac{L+L_s}{L.L_s.C}}$$

since, γ_1 is a large quantity, the first term in equation (5.31) can be ignored. Thus,

$$i_c = I_{a2}\cdot\cos\gamma_1 t' \qquad (5.32)$$

Now, substituting i_c from equation (5.32) into equation (5.28), the armature current i_a is given by

$$i_a = \frac{E_{av}-V}{R}(1-e^{-\alpha t'}) + I_{a2}\cdot e^{-\alpha t'} - \frac{L_s}{L+L_s}\cdot I_{a2}\left\{e^{-\alpha t'} - \cos\gamma_1 t' + \frac{\alpha}{\gamma_1}\sin\gamma_1 t'\right\}$$

Now, as γ_1 is a large term, $\frac{\alpha}{\gamma_1}\cdot\sin\gamma_1 t'$ can be neglected. Again, $\frac{L_s}{L+L_s}\cdot I_{a2}\cdot(e^{-\alpha t'} - \cos\gamma_1 t')$ is also small compared to the first two terms. Therefore,

$$i_a = \frac{E_{av}-V}{R}\left(1-e^{-\alpha t'}\right)+I_{a2}\cdot e^{-\alpha t'} \qquad (5.33)$$

This interval ends when $i_c=0$, which gives

$$\delta_c' = \frac{\pi}{2\gamma_1 T} \qquad (5.34)$$

The armature current at the end of this interval is

$$i_a(\delta_c' T)=I'_{a2} = \frac{E_{av}-V}{R}\left(1-e^{-\delta_c' T/T'_a}\right)+I_{a2}\cdot e^{-\delta_c' T/T_a'} \qquad (5.35)$$

If the armature circuit inductance is sufficiently large, then it can be assumed that $I'_{a2} \approx I_{a2}$. However, for some values of δ and depending upon the parameters L_s, L and C, this mode of operation may not be completed before the beginning of the next cycle. In that case, I'_{a2} is replaced by I_{a1} in equation (5.35). The maximum voltage V_2 to which the capacitor C may be charged is given by

$$V_2 = \frac{1}{C}\int_0^{\delta_c' T} i_c\cdot dt+V = V+\frac{I_{a2}}{C\gamma_1}\cdot\left[\sin\gamma_1\cdot\delta_c' T\right] = V+\frac{I_{a2}}{C\gamma_1} \qquad (5.36)$$

IV. Regenerative Interval II: $(\delta+\delta_c+\delta_c')T \leq t \leq \beta T$

This interval starts when the capacitor current i_c in the previous mode has already reached zero value and the capacitor C has been charged to a voltage $V_2 > V$. The

overcharged capacitor starts discharging partially against the supply and machine armature circuit via L_m and diode D. The equivalent circuit of this mode is shown in Figure 5.3(b). The differential equations describing this mode are

$$L.\frac{di_a}{dt'} + R.i_a + \frac{1}{C}\int_0^{\beta_1 T} i_c.dt' + L_m\frac{di_c}{dt'} = E_{av} - V_2 \qquad (5.37)$$

and

$$-L_m.\frac{di_c}{dt'} - \frac{1}{C}\int_0^{\beta_1 T} i_c.dt' + L_s\frac{d}{dt'}(i_a - i_c) = V_2 - V \qquad (5.38)$$

where t' is the redefined time from the beginning of this interval. The initial conditions are,

$$i_a(0) = I'_{a2},\ i_c(0) = 0.$$

The solution of i_c is obtained by solving equations (5.37) and (5.38) after neglecting voltage drop across R, as

$$i_c = -I_{max} \cdot \sin \gamma_1' t' \qquad (5.39)$$

where,

$$I_{max} = \frac{V_2(L+L_s) - V.L - L_s E_{av}}{\sqrt{L\,L_s + L\,L_m + L_s L_m}} \cdot \sqrt{\frac{C}{L+L_s}}$$

and

$$\gamma_1' = \sqrt{\frac{L+L_s}{C(LL_s + LL_m + L_s L_m}} \approx \gamma_1 \text{ as } L_m \text{ is very small}$$

compared to L.

The final voltage V_1 on the condenser is given by

$$V_1 = V_2 + \frac{I_{max}}{C\,\gamma_1} \cdot [\cos \gamma_1 \beta_1 T - 1] \qquad (5.40)$$

The minimum possible value of V_1 will occur if $\gamma_1 \beta_1 T = \pi$

i.e. $\beta_1 = \frac{\pi}{\gamma_1 T}$ (5.41)

The armature current during this interval is obtained by substituting i_c from equation (5.39) into equation (5.37) and solving for i_a which gives,

$$i_a = \frac{E_{av}-V}{R}(1-e^{-t'/T'_a}) + I'_{a2} \cdot e^{-t'/T'_a} \qquad (5.42)$$

$$i_a(\beta_1 T) = I''_{a2} = \frac{E_{av}-V}{R}(1-e^{-\beta_1 T/T'_a}) + I'_{a2} \cdot e^{-\beta_1 \cdot T/T'_a} \qquad (5.43)$$

If the armature circuit inductance is sufficiently high, then I'_{a2} can be replaced by I_{a2}.

V. Regenerative Interval III: $(\delta + \delta_c + \delta'_c + \beta)T \leq t \leq (1-\delta-\delta_c-\delta'_c-\beta)T$

This interval starts when i_c becomes zero in the previous mode. If i_c has not reached zero value before the beginning of the next cycle, then this mode will not exist. The differential equation describing this mode is given by equation (5.5) with initial condition $i_a(t'=0) = I''_{a2}$. The solution of i_a is

$$i_a = \frac{E_{av}-V}{R}\,(1-e^{-t'/T'_a}) + I''_{a2}\cdot e^{-t'/T'_a} \qquad (5.44)$$

where, t' is the time redefined from the beginning of this mode. The armature current at the end of this interval is

$$i_a(t=T)=I_{a1} = \frac{E_{av}-V}{R}\left\{1-e^{-(1-\delta'')T/T'_a}\right\} + I''_{a2}\cdot e^{-(1-\delta'')T/T'_a} \qquad (5.45)$$

where $\delta'' = (\delta + \delta_c + \delta'_c + \beta_1)$

Substituting the value of I''_{a2} from equation (5.43) and taking $I'_{a2} \simeq I_{a2}$, yields,

$$I_{a1} = \frac{E_{av}-V}{R}\left\{1-e^{-(1-\delta-\delta_c-\delta'_c)T/T'_a}\right\} + I_{a2}\cdot e^{-(1-\delta-\delta_c-\delta'_c)T/T'_a} \qquad (5.46)$$

I_{a2} is obtained for $t = \delta T$ in equation (5.4) as,

$$I_{a2} = \frac{E_{av}}{R}\,(1-e^{-\delta T/T_a}) + I_{a1}\cdot e^{-\delta T/T_a} \qquad (5.47)$$

By elimination of variables from equations (5.46) and (5.47),

$$I_{a1} = \frac{E_{av}}{R} - \frac{V}{R}\left[\frac{1-e^{-(1-\delta-\delta_c-\delta'_c)T/T'_a}}{1-e^{-(1-\delta_c-\delta'_c)T/T'_a - a\delta}}\right] \qquad (5.48)$$

and

$$I_{a2} = \frac{E_{av}}{R} - \frac{V}{R}\left[\frac{1-e^{(1-\delta-\delta_c-\delta'_c)T/T'_a}}{1-e^{(1-\delta_c-\delta'_c)T/T'_a + a\cdot\delta}}\right] \qquad (5.49)$$

where, $a = \left(\frac{T}{T_a} - \frac{T}{T'_a}\right)$.

The average armature current is given by

$$I_{av} = \frac{1}{T}\left[\int_{0}^{\delta T} i_a.dt + I_{a2}\,\delta_c T + \int_{\delta' T}^{\delta_c' T} i_a.dt + \int_{(\delta'+\delta_c)T}^{\beta_1 T} i_a.dt + \int_{(\delta'+\delta_c'+\beta_1)T}^{(1-\delta'-\delta_c'-\beta_1)T} i_a.dt\right] \quad (5.50)$$

The expression for regenerative power is given by

$$P_{rg} = \frac{V}{T}\left[\int_{\delta' T}^{\delta_c' T} (i_a - i_c)dt + \int_{(\delta'+\delta_c')T}^{\beta_1 T} (i_a - i_c)dt + \int_{(\delta'+\delta_c'+\beta_1)T}^{(1-\delta-\delta_c-\delta_c'-\beta_1)T} i_a.dt\right] \quad (5.51)$$

The electromagnetic developed torque is given by equation (5.13).

The values of δ_c and δ_c' in the above equations are unknown. They can be determined as follows. The value of V_2 is obtained from equation (5.36). Substituting the values of V_2, I_{max}, γ_1 etc. in equation (5.40), yields,

$$V_1 = V + \frac{I_{a2}}{C\gamma_1} + \frac{I_{max}}{C\gamma_1}.(\cos\gamma_1 \cdot \beta_1 T - 1)$$

Now taking $I_{max} \approx I_{a2}$

$$V_1 = V + \frac{I_{a2}}{C \gamma_1} \cdot \cos \gamma_1 \cdot \beta_1 T \qquad (5.52)$$

Substituting V_1 from equation (5.52) into equation $\delta_c = \frac{C(V+V_1)}{I_{a2}}$ gives

$$\delta_c = \frac{2C.V}{T.I_{a2}} + \frac{1}{\gamma_1 T} \cos \gamma_1 \beta_1 T$$

$$= \delta_{c1} + \frac{1}{\gamma_1 T} \cos \gamma_1 \beta_1 T \qquad (5.53)$$

where,

$$\delta_{c1} = \frac{2C.V}{I_{a2}.T}$$

The value of δ_c is determined as shown below.

Substituting I_{a2} from equation (5.49) into equation (5.53) and then expanding the terms $e^{-\delta_c T/T_a}$ in terms of their power series and neglecting all higher order terms in δ_c greater than two yields a quadratic in δ_c as

$$A' \delta_c^2 + B' \delta_c + C' = 0$$

or,

$$\delta_c = -\frac{B'}{2A'} \pm \frac{\sqrt{B'^2 - 4A'C'}}{2A'} \qquad (5.54)$$

where,

$$A' = \left(\frac{E_{av}}{V}\right)\left(\frac{T}{T'_a}\right)e^{(1-\delta'_c)T/T'_a + a\delta} - \left(\frac{T}{T'_a}\right)e^{(1-\delta-\delta'_c)T/T'_a}$$

$$+ \frac{CR}{T_a}\cdot\left(\frac{T}{T_a}\right)\cdot e^{(1-\delta'_c)T/T_a + a\delta} - \frac{1}{\gamma_1 T}\left(\frac{E_{av}}{V}\right)\cdot\left(\frac{T}{T'_a}\right)^2$$

$$\cdot e^{(1-\delta'_c)T/T'_a + a\delta}$$

$$B' = \frac{E_{av}}{V}\left(1-e^{(1-\delta'_c)T/T_a' + a\delta}\right)-\left(1-e^{(1-\delta-\delta'_c)T/T_a'}\right)$$

$$- \frac{2CR}{T_a'}\cdot e^{(1-\delta'_c)T/T_a' + a\delta} - \frac{1}{\gamma_1 T}\left\{\frac{E_{av}}{V}\left(\frac{T}{T_a'}\right)\right.$$

$$\left.\cdot e^{(1-\delta'_c)T/T'_a + a\delta} - \frac{T}{T_a'}\cdot e^{(1-\delta-\delta'_c)T/T_a}\right\}\cos\gamma_1\beta_1 T$$

$$C' = -\frac{2CR}{T}\left(1-e^{(1-\delta'_c)T/T'_a + a\delta}\right) - \frac{1}{\gamma_1 T}\left(\frac{E_{av}}{V}\right)$$

$$\cdot\left(1-e^{(1-\delta'_c)T/T'_a + a\delta}\right)\cdot\cos\gamma_1\beta_1 T + \frac{1}{\gamma_1 T}\cdot$$

$$\left(1-e^{(1-\delta-\delta'_c)T/T'_a}\right)\cdot\cos\gamma_1\beta_1 T$$

The positive realistic value of δ_c is obtained from equation (5.54).

For the test machine and the chopper used the parameters of which are given in Appendix B (Machine IV) δ_c' is quite high ($\delta_c' = \frac{\pi}{2\gamma_1 T}$) for chopper operating frequency of 400 Hz. As a result, except for very low values of δ , the next cycle begins before the end of regenerative interval I and thus the later two modes of operation are absent. In this case, the commutating capacitor does not get enough time to charge to maximum voltage V_2. The commutation interval ($\delta_c T$) in this case, can be determined from equation (5.15) without much loss of accuracy. The corresponding expression for I_{av} is obtained from equation (5.50) dropping the last two terms. The available δ_c' in this case is then obtained as $\delta_c'=(1-\delta-\delta_c)$. The corresponding expression for P_{rg} is obtained from equation (5.51) dropping the last two terms. The critical speed of regeneration is determined from equation (5.27). The expressions for I_{av} and P_{rg} for this case are given below.

$$I_{av} = \frac{E_{av}}{R} \cdot \delta + (\frac{T_a}{T}) \cdot \frac{E_{av}}{R} (e^{-\delta T/T_a} - 1) + \frac{E_{av}-V}{R} \cdot \delta_c' + (\frac{T_a'}{T}) \cdot \frac{E_{av}-V}{R} (e^{-\delta_c' T/T_a'} - 1) + I_{a2}\left\{\delta_c + \frac{T_a'}{T}(1-e^{-\delta_c' T/T_a'})\right\} \qquad (5.55)$$

$$P_{rg} = V\left[\frac{E_{av}-V}{R}\cdot\delta_c' + \frac{T'_a}{T}\left(\frac{E_{av}-V}{R}\right).\left(e^{-\delta_c' T/T'_a}-1\right)\right.$$

$$\left.+I_{a2}\left(\frac{T'_a}{T}\right).\left(1-e^{-\delta_c' T/T'_a}\right)\right] \qquad (5.56)$$

where, $\delta_c' = (1-\delta-\delta_c)$.

5.3 EFFECTS OF VARIOUS PARAMETERS ON STABILITY UNDER REGENERATIVE BRAKING

Stability problem arises in chopper controlled d.c. series motor under regenerative braking. The stability of braking characteristics can be explained as follows. If we consider a simple series generator feeding an external load, the operating point is where the resistance line cuts the magnetisation characteristics as shown in Figure 5.4(a) i.e.

$$\frac{I_a R}{V} = \frac{E}{V}$$

For a given load current, the machine will fail to self excite when the slope of the load line is the same as that of the magnetisation curve. Now, under regenerative braking condition using a square wave chopper, the equation describing the steady state operation is given by

$$\frac{E_{av}}{V} = \frac{R.I_{av}}{V} + (1-\delta)$$

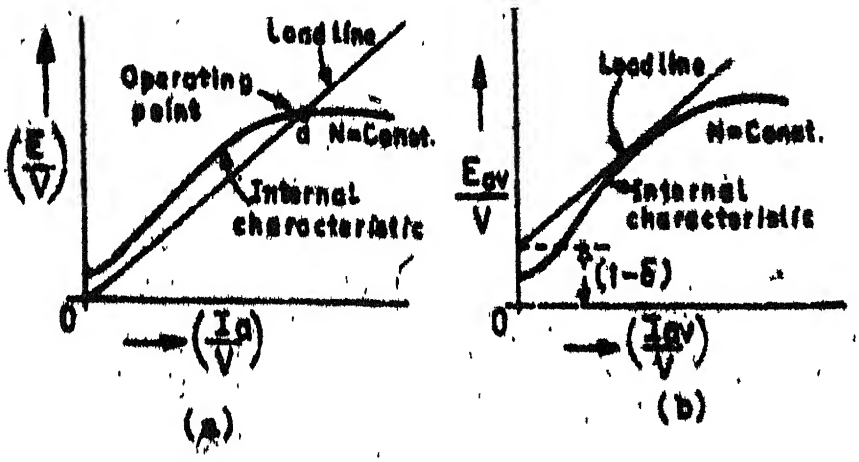

Fig. 5.4 Building up of chopper controlled series generator.

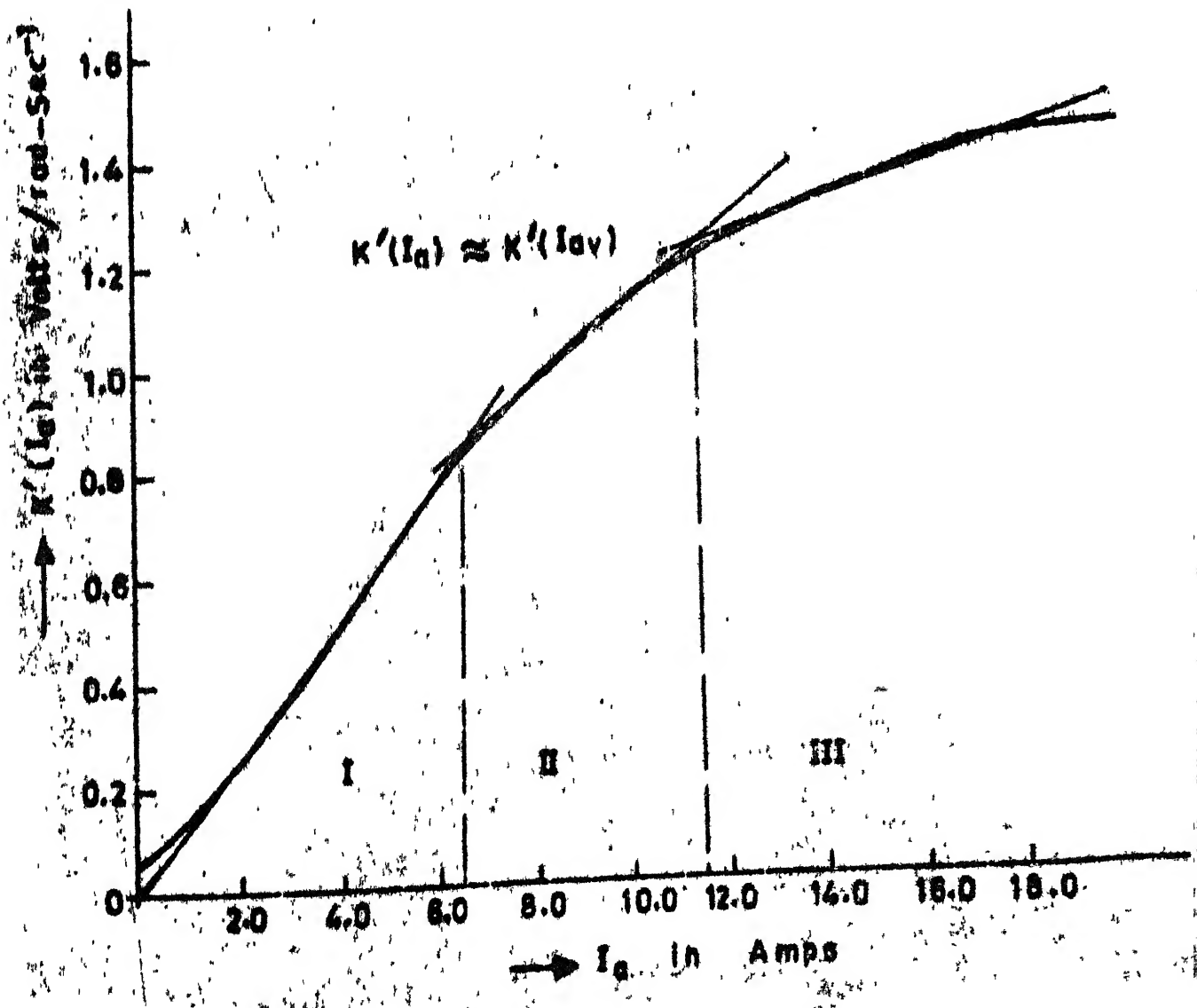

Fig. 5.5 K'(I_a) vs. Armature current I_a.

In this case, the load line shifts from the origin by $(1-\delta)$ as shown in Figure 5.4(b). So, for lower values of δ, the machine may fail to self excite even at a much higher speed. The small amount of torque that is produced under this situation is the dynamic braking torque owing to residual magnetism.

Now when regenerative braking is carried out with a load current commutated chopper, the equation is given by

$$\frac{E_{av}}{V}(1-\delta_c) = \frac{R.I_{av}}{V} + (1-\delta) - (\frac{2C.R}{T} + \delta_c)$$

In this case, the load line shifts down and therefore it improves the stability. Higher is the value of C, both δ_c and $\frac{2C.R}{T}$ will increase and hence the stability will improve. This is on the assumption that $\frac{E_{av}}{V} < 1$.

When there is some source inductance, the commutation process may continue upto the end of regenerative interval I as shown in Section 5.2.4. If a capacitor value larger than that required for safe commutation is used capacitor does not discharge to a value lower than the supply voltage. This oversized capacitor increases the commutation interval $\delta_c T$ and also $\delta_c' T$ and hence will improve the stability of braking characteristics. If a suitable buffer condenser is

used across the source terminals, then the effect of source inductance is neutralized and stability of the characteristics will be determined corresponding to the case when no source inductance is present.

5.4 PERFORMANCE CALCULATION AND EXPERIMENTAL VERIFICATION

The experiments were carried out on a d.c. series motor under regenerative braking, details of which are given in Appendix B, using a two thyristor load current commutated chopper (as shown in Figure 5.1(c)). The values of $K'(I_a) \simeq K'(I_{av})$ has been shown in Figure 4.8(a) of Chapter IV. For the given test machine, $K'(I_a)$ can be approximated by three straight lines as shown in Figure 5.5. Figure 5.6(a) and 5.6(b) show the calculated speed-torque characteristic of the motor with square wave output voltage and nonsquare output voltage chopper using load dependent commutation respectively without taking source inductance into account. The nature of the calculated characteristics are some what similar for higher values of torque for fixed values of δ but they differ considerably at low values of braking torque. The variation in characteristics are due to commutation pulse. In Figure 5.6(b), it is observed that for $\delta < 0.45$, the torque speed characteristics exhibit steep negative slopes

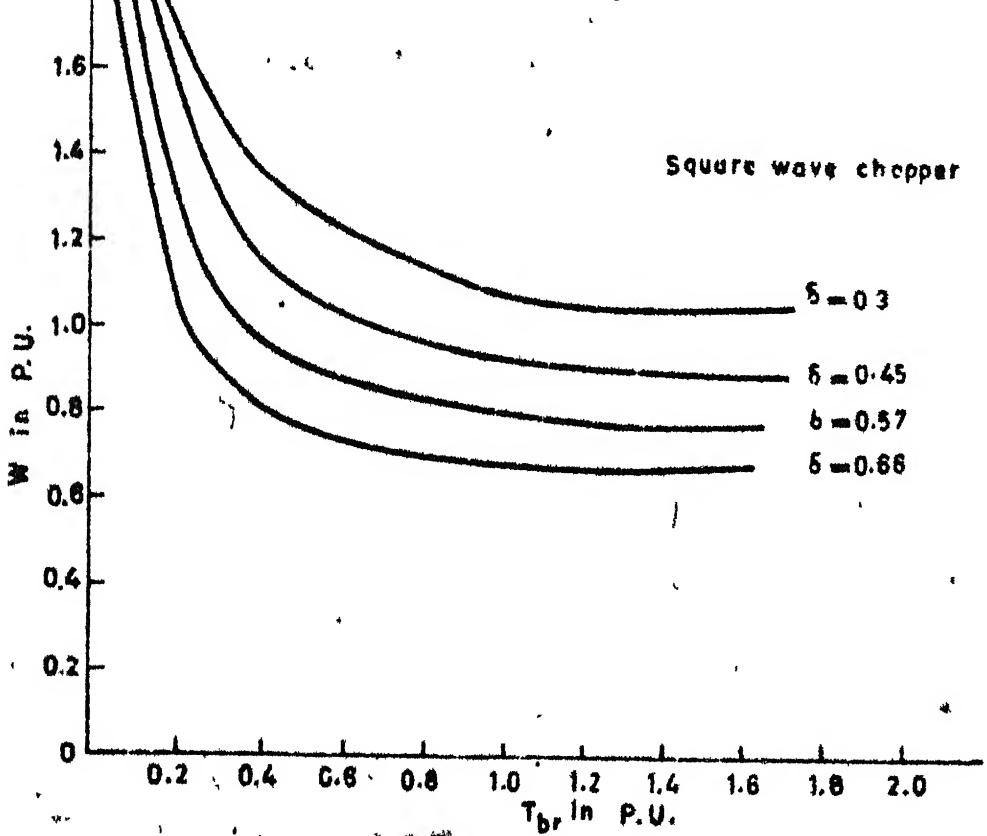

(a)

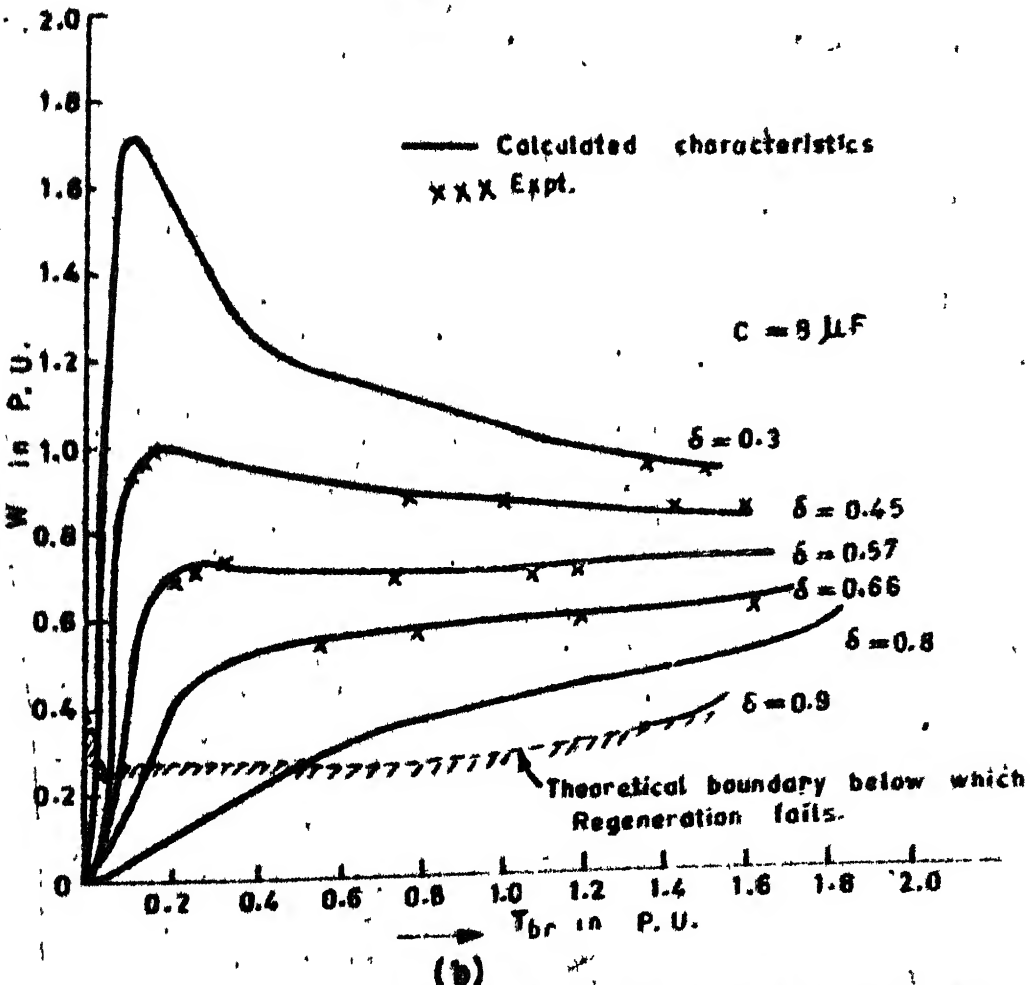

(b)

Fig. 5.6 Speed vs. braking torque characteristics.

under light braking conditions. The experimental characteristics were determined after using a buffer condenser bank (8000μF) at the source terminals. Under light braking condition, the actual characteristics were unstable for $\delta < 0.45$. Only two operating points have been shown for $\delta = 0.3$ as machine operation was unstable for lower values of torque. As the torque was reduced the machine operation shifted to low torque and high speed with negligible regenerative power. For $\delta > 0.57$, the characteristics exhibit positive slopes under all braking conditions for the given values of filter inductance and commutating capacitor and the operation is found to be stable and control is smooth. Discontinuous conduction was not observed.

The theoretical boundary below which regeneration fails has been shown in Figure 5.6(b) by dotted lines. The figures 5.7(a) and 5.7(b) give strategy for changing δ with variation of speed ω to produce constant braking torques for a square wave output chopper and for a load current commutated chopper respectively without taking source inductance into account. The effect of commutation capacitor on the torque speed characteristics has been demonstrated in Figure 5.8, where it is observed that

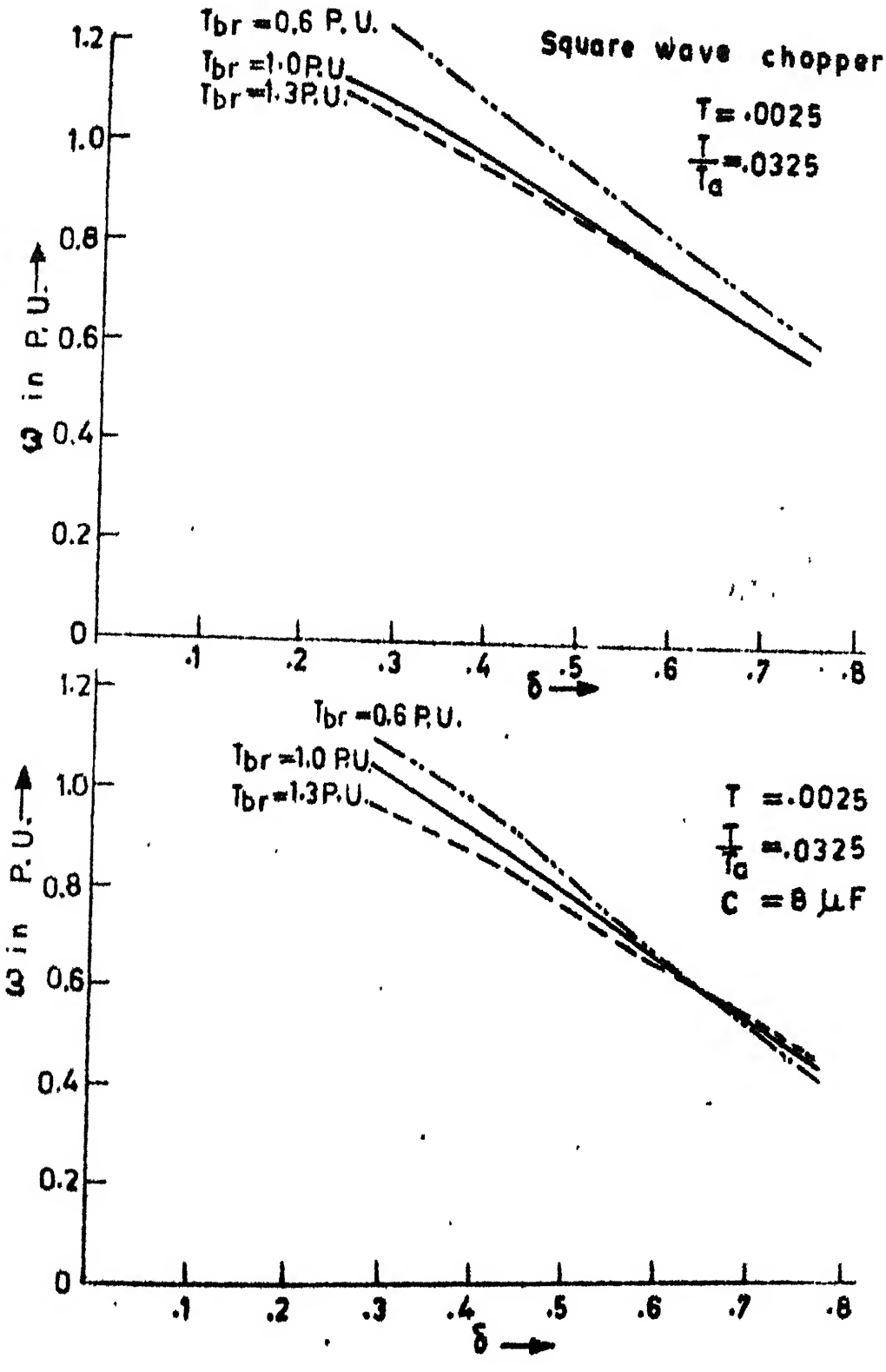

Fig.5.7 Speed vs. duty ratio for constant braking torque.

an increased value of commutating capacitor has considerable stabilizing effect on the steady state performance of the machine. It is also seen that for higher values of torque, the commutating capacitor does not influence the characteristics significantly.

Figures 5.9(a) and 5.9(b) show the calculated speed versus regenerative power characteristics for a square wave and for a load current commutated chopper respectively for fixed values of δ without taking source inductance into account. The experimental values were determined by using buffer condenser at the source terminals. For higher values of braking torque, the nature of the characteristics are some what similar but for low values of torque, the characteristics differ. By increasing the value of commutating capacitor, it is observed that for a fixed value of δ, the regeneration takes place at lower values of speed. Under heavy braking condition there is not much change in the regenerative power due to increased value of capacitor and the characteristics converge asymptotically. Experimental results have also been plotted in Figure 5.8 and in Figure 5.9(b) and show a good agreement between measured and predicted values. Fig. 5.9(c) shows calculated curves for P_{rg} versus ω for fixed values of δ with different

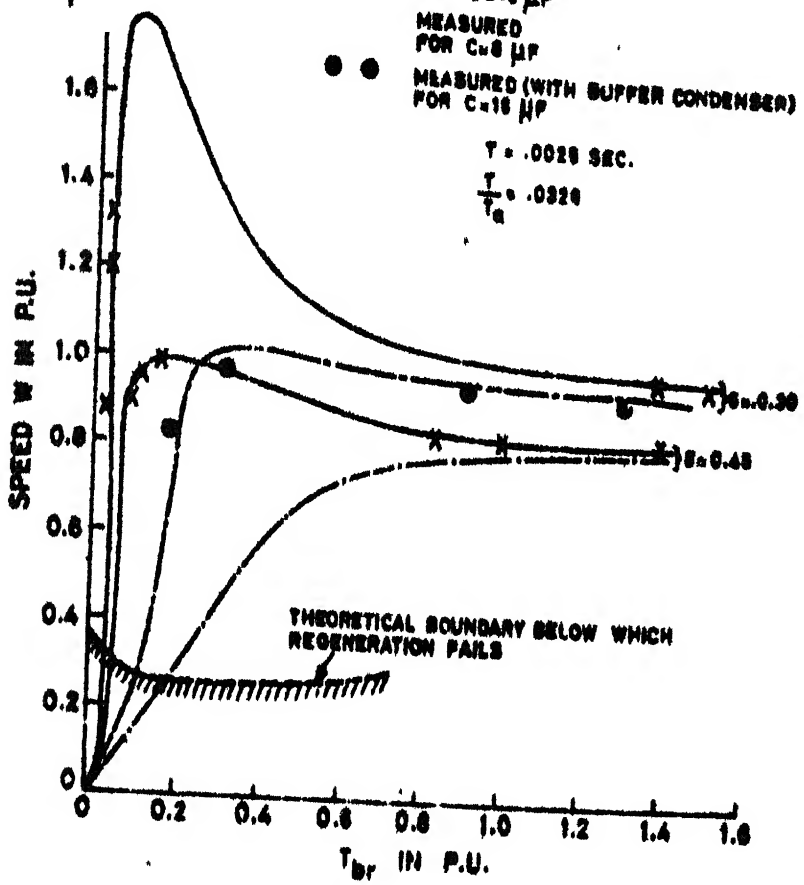

Fig. 5.8 Speed vs. braking torque characteristics (for C = 8 μF, and C= 16 μF).

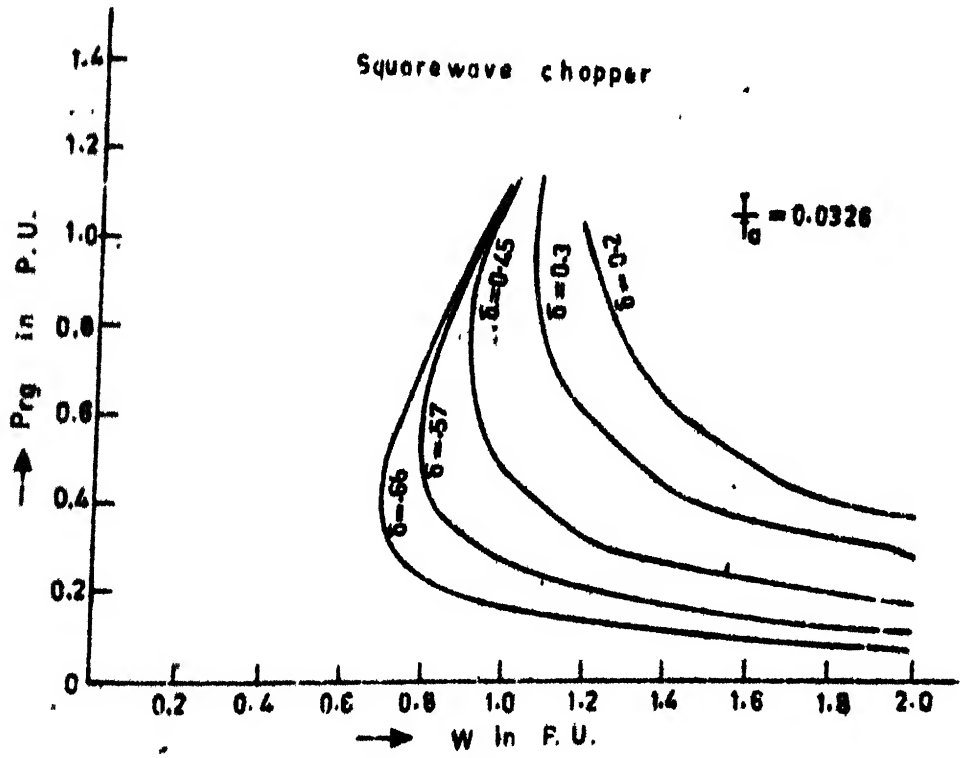

Fig. 5.9(a) P_{rg} vs. speed characteristics (square wave chopper).

values of $(\frac{T}{T_a})$ ratio. If $(\frac{T}{T_a})$ is increased, it is found that the regenerative power remains almost same for the same speed at fixed value of δ for higher values of braking torque. If the ratio $(\frac{T}{T_a})$ is decreased which can be done either by increasing the chopping frequency or by adding extra filter inductances in the armature circuit, the stability of braking characteristics improves as seen in Figure 5.8 for the same value of commutating capacitor ($C = 8\mu F$) and fixed value of $\delta = 0.3$. The use of an increased value of commutating capacitor ($C = 16\mu F$) also have similar effects on the braking characteristics for the same value of $(\frac{T}{T_a})$ ratio and δ. It is found from Figure 5.9(c) by decreasing $\frac{T}{T_a}$ by a large amount, does not increase the regenerative power for higher values of torque. But regenerative braking can be carried out stably at much lower value of speed for low values of δ in this case.

Figure 5.10 shows the calculated curves (neglecting source inductance) for armature current ripple in p.u. for (i) constant $\frac{T}{T_a}$ corresponding to combined d.c. inductance of armature circuit at rated current (ii) $\frac{T}{T_a}$ corresponding to variable incremental inductance $L_{in}(I_{av})$ of the combined armature circuit. The experimental values of ripple in p.u. measured after putting buffer condenser at the

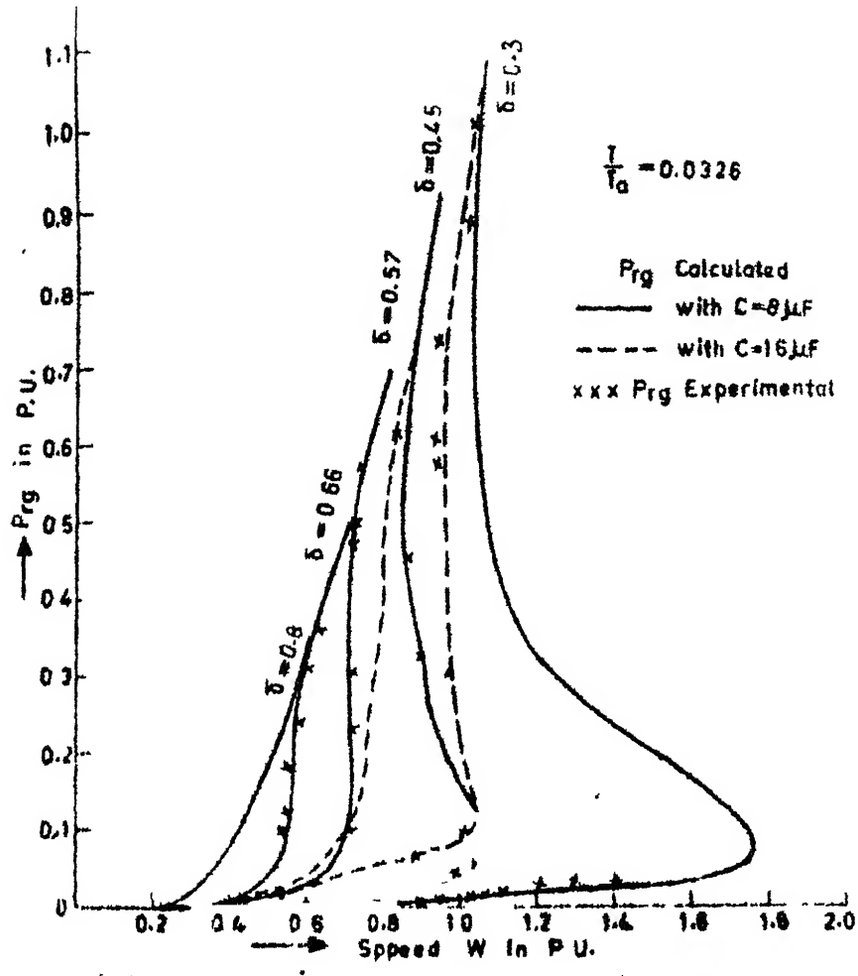

Fig.5.9(b) P_{rg} vs. Speed Characteristics (for C=8 f and C=16 F)

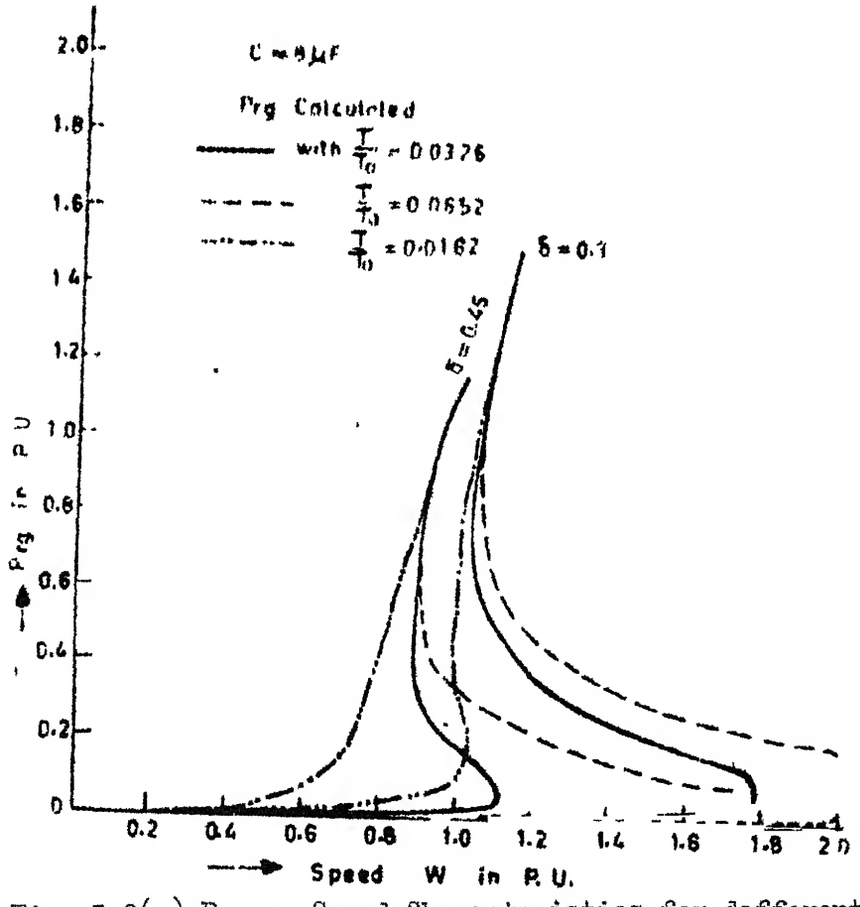

Fig. 5.9(c) P_{rg} vs. Speed Characteristics for different T/T_a

source terminals have also been shown in Figure 5.10. It is observed that a large error occurs in the prediction of ripple using constant value of d.c. inductance at rated current. The use of incremental inductance $L_{in}\ (I_{av})$ results in a better prediction of ripple. However, in both cases, the influence of eddy current fluxes in the motor field cores were not taken into account for prediction of ripple.

Figure 5.11(a) shows the calculated curves of efficiency of regeneration η_{rg} versus speed ω for the load current commutated chopper controlled d.c. series machine using equation (5.24). For a fixed value of δ, the efficiency η_{rg} is maximum near about the rated current operation. Figure 5.11(b) shows the typical curves of η_{rg} versus ω for a square wave chopper for fixed values of $\delta = 0.45$ and $\delta = 0.57$ respectively for different $\frac{T}{T_a}$ ratio. It is found that if $\frac{T}{T_a}$ ratio is increased, the efficiency of regeneration falls marginally at higher values of braking torque.

To determine experimentally the influence of source inductance, the buffer condenser bank across the source was disconnected. The source consisted of a 3KW, 220V d.c. separately excited generator having an armature inductance

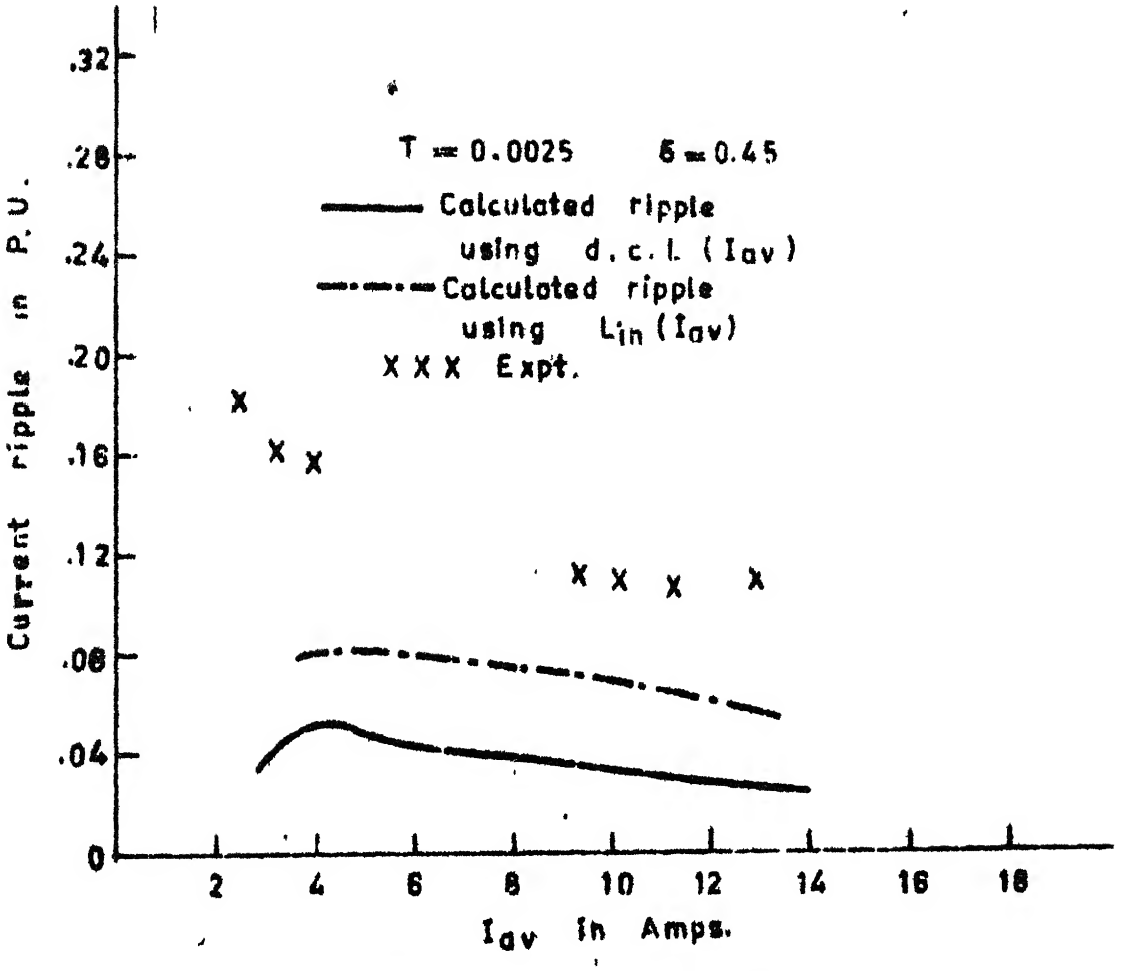

Fig. 5.10 Normalised p.u. ripple vs. I_{av}.

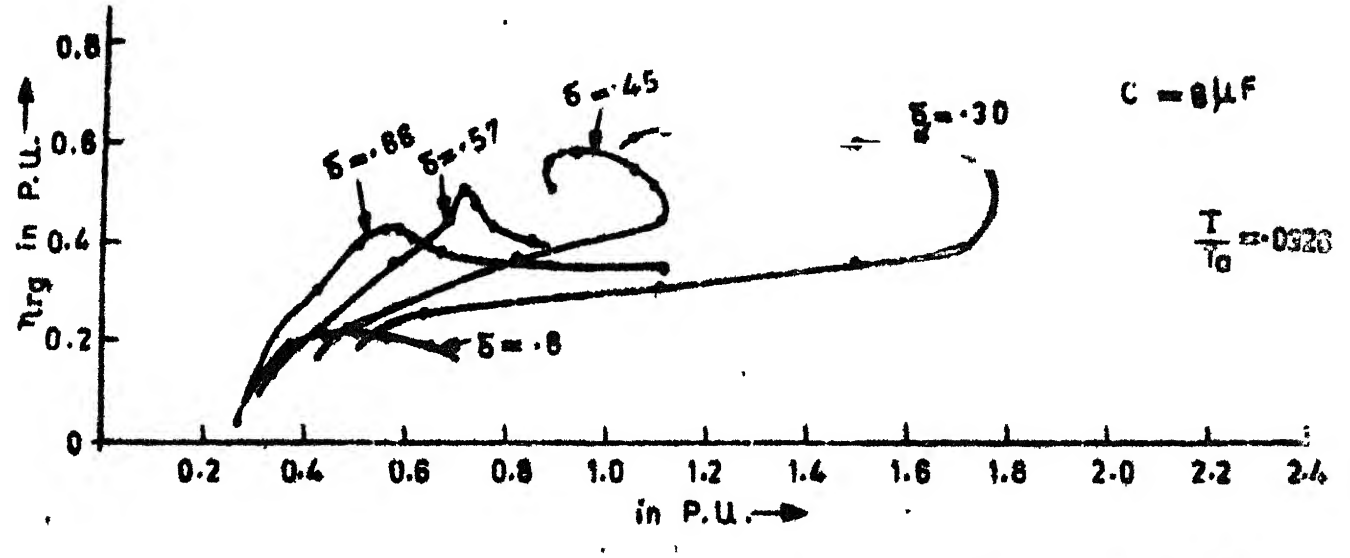

Fig. 5.11(a) Efficiency of regeneration (η_{rg}) vs. speed.

of 40 mH (D.C.). The self inductance of the choke used was 300 mH. For this chopper operating frequency of 400 Hz, the circuit parameters L, L_s, C and L_m are such that the commutating capacitor current i_c does not get enough time to come to zero value during regeneration interval I before the beginning of the next cycle. As a result, the next two modes of operations are completely absent. Discontinuous conduction is found to be absent. Figure 5.12 shows the predicted and measured speed-torque characteristics of the test motor for two values of δ, i.e., 0.32 and 0.49. Speed-torque characteristic calculated for $\delta = 0.32$ neglecting source inductance, has also been shown in Figure 5.12. It is found that considerable amount of error is introduced if source inductance is neglected. Moreover, the nature of the characteristics predicted neglecting source inductance are somewhat different. For the same value of commutating capacitor, while the actual characteristics predict stable operation, those obtained neglecting source inductance show negative slopes for lower values of torque indicating instability. Figure 5.13 shows the corresponding regenerative power versus speed for two values of δ. The calculated values agree well with the experimental. On experimenting for different values of δ, it was found that for $\delta \geq 0.57$,

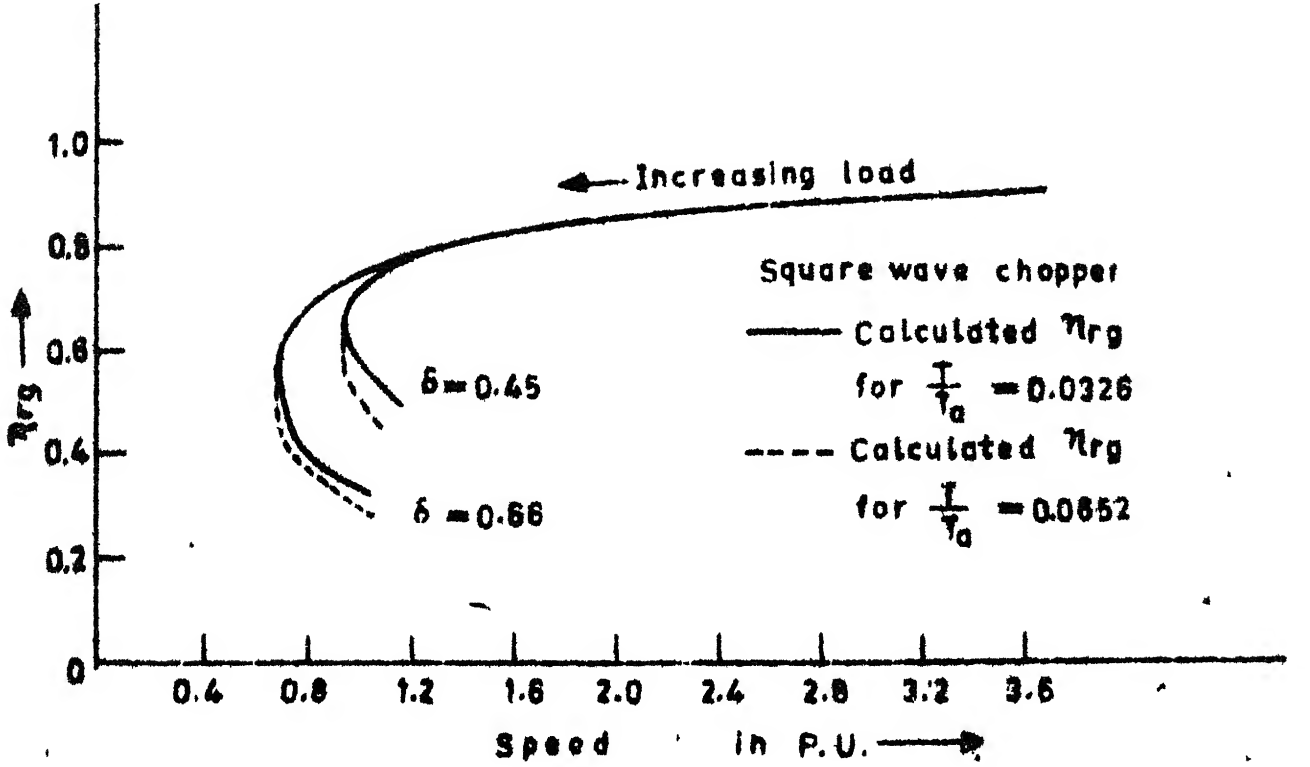

Fig. 5.11(b) Efficiency of regeneration (η_{rg}) vs. speed for different T/T_a.

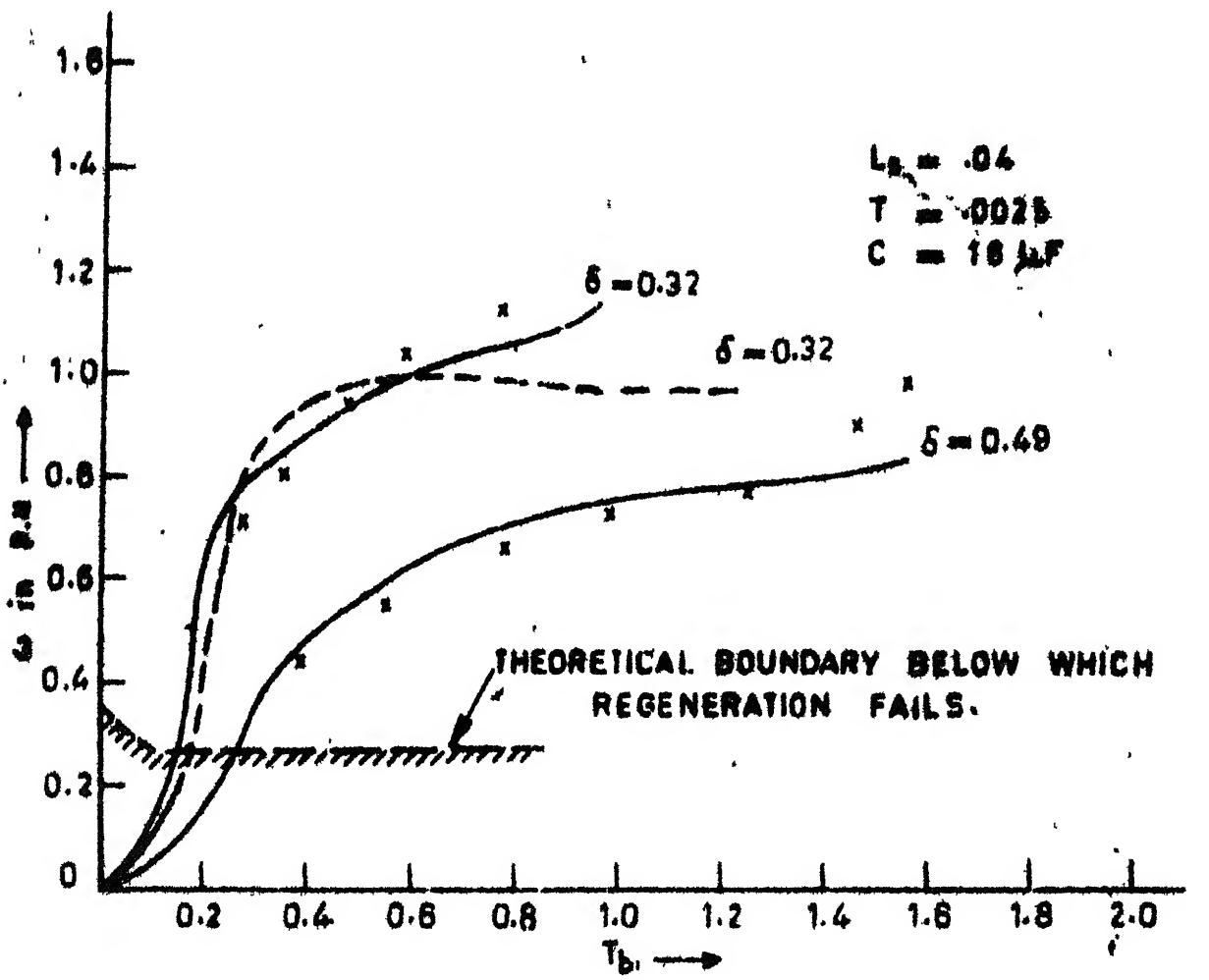

Fig. 5.12 Speed vs. braking torque characteristics in presence of source inductance.

regeneration did not take place. The difference in the nature of the characteristics of Figures 5.6(b) and 5.12 is quite noticeable. While characteristics with source inductance in Figure 5.12 show stable operation in complete range of speed torque, it is not so when buffer condenser is put across the source terminals.

5.5 CONCLUSIONS

The following conclusions can be drawn from the above study.

1. Armature reaction, magnetic saturation, effects of various modes of operation of chopper and the effect of source inductance should be taken into account for reliable prediction of braking torque and regenerative power.

2. The method of analysis presented in this chapter is general and can be used for performance calculation of d.c. series motor under regenerative braking mode using choppers with and without square wave output voltage. It takes into account the effects of all the factors mentioned above. Further more, it permits the prediction of braking performance with satisfactory accuracy.

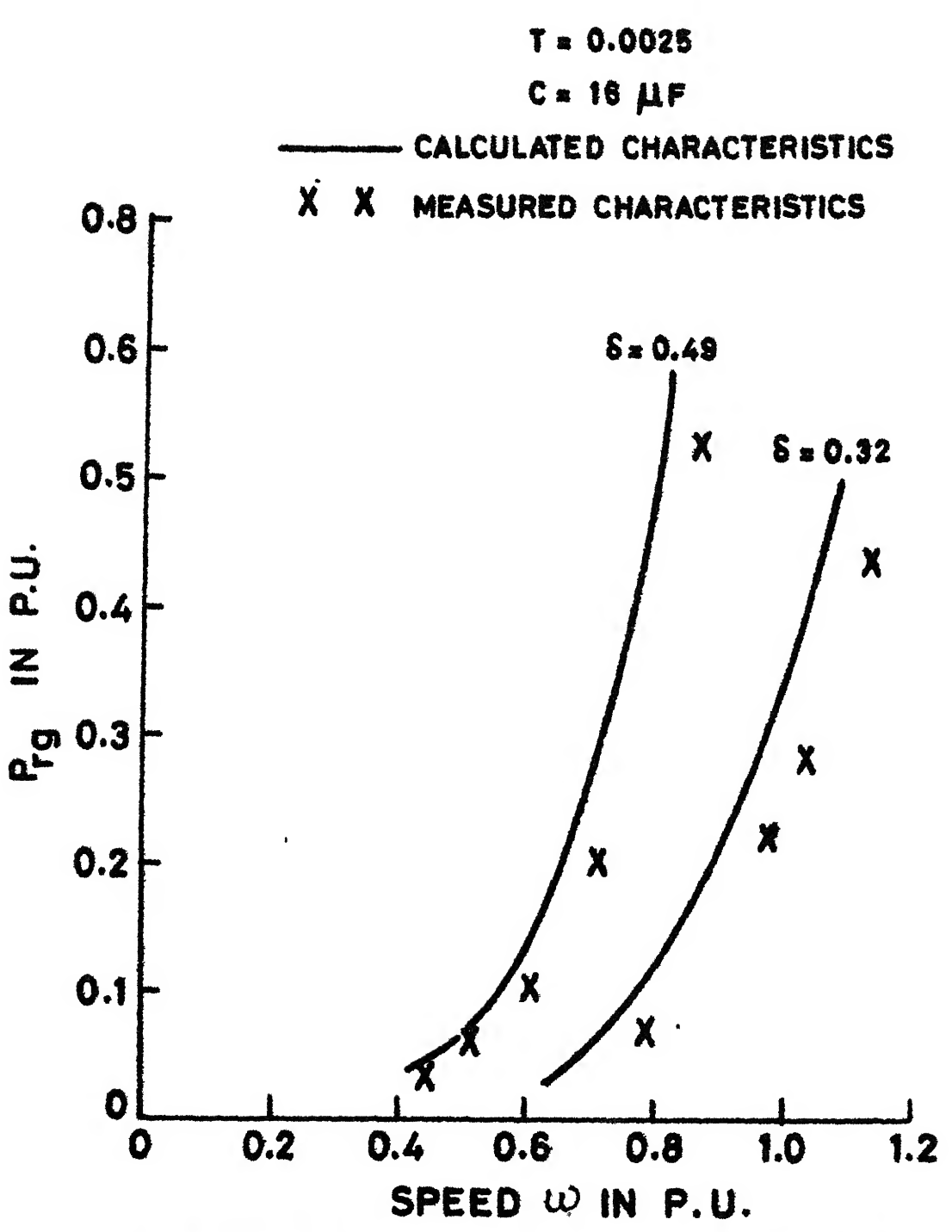

Fig.5.13 P_{rg} vs. speed in presence of source inductance.

3. The net electromagnetic braking torque increases with speed in the stable operating region for fixed value of δ.

4. The choice of an oversized commutating capacitor along with a suitable filter inductance at the motor armature circuit improves the stability of operation under regenerative braking even at low values of δ.

5. The source inductance improves the stability of machine braking characteristics and thus control is better. However, for the same machine speed and δ, the regenerative power is reduced in the presence of source inductance. An oversized commutating capacitor is recommended to avoid commutation failure in case of load current commutated chopper especially when the source contains appreciable amount of inductance. The use of a suitable buffer condenser neutralizes the effect of source inductance.

CHAPTER VI

EFFECT OF SOURCE INDUCTANCE ON THE DESIGN OF CHOPPER COMMUTATION CIRCUITS

6.1 INTRODUCTION

The function of chopper commutation circuits is to extinguish a specified peak value of load current and then to maintain a reverse voltage across the thyristor, which has been extinguished, for a period greater than its turn off time. Typical d.c. choppers use two thyristors, two or more diodes. Some choppers use three thyristors and several diodes. Commutating capacitors along with a few inductances are used to provide forced commutation in chopper circuits. William McMurray [23] has given a comparative study of several chopper circuits working on the principle of forced commutation. In this chapter, the influence of source inductance on the commutating capabilities of some standard chopper commutation circuits has been presented.

In the analysis presented here, load current is assumed constant during commutation interval.

6.2 CASE I: TWO THYRISTOR CHOPPER USING LOAD CURRENT DEPENDENT COMMUTATION

The circuit diagram of a typical two thyristor load current commutated chopper is shown in Figure 2.1. Due to

source inductance, the commutating capacitor C gets charged to a voltage V_2 (greater than V), given by equation (2.9). during free wheeling interval and then if sufficient time is available, the overcharged capacitor will discharge partially through L_m, D, L_s, supply mains and D_F. The minimum value of the voltage on the capacitor (for low frequency choppers) is given by equation (2.11). This voltage is available for commutation of the main thyristor. The circuit turn off time t_c is given by the following equation

$$t_c = \frac{V_1 . C}{I_{a2}} = \frac{V . C}{I_{a2}} - \sqrt{L_s . C} \qquad (6.1)$$

Typical idealised wave forms of v_c and i_c during commutation are shown in Figure 6.1. Since the maximum voltage on the capacitor is higher with source inductance, the voltage ratings of capacitor, thyristors and diode increase accordingly. When there is no source inductance, then $V_1 = V$ and the time for which the main thyristor will remain reverse biased is given by

$$t_{co} = \frac{V . C}{I_{a2}} \qquad (6.2)$$

From equations (6.1) and (6.2) we get,

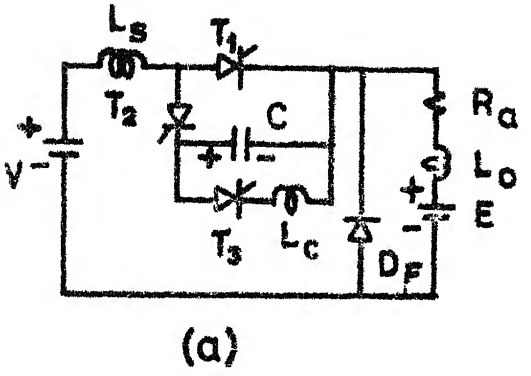

(a)

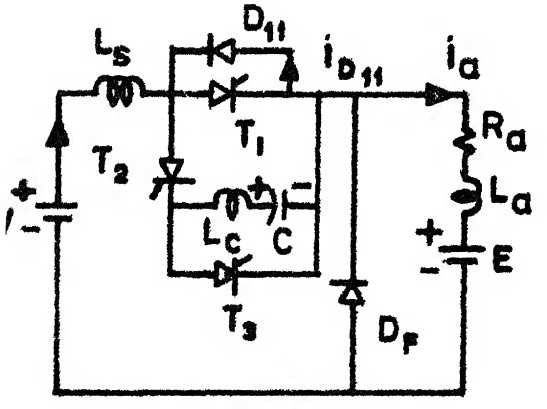

(b)

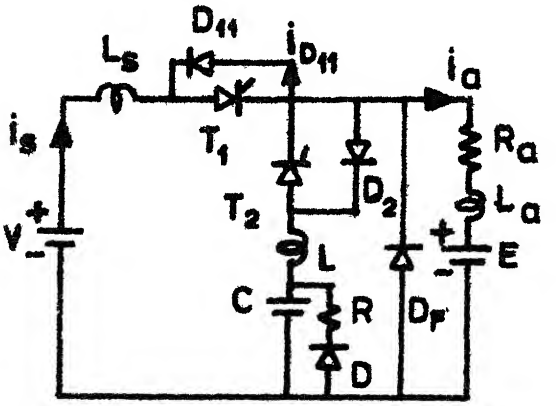

(c)

Fig. 6.3 Chopper circuits

CASE I

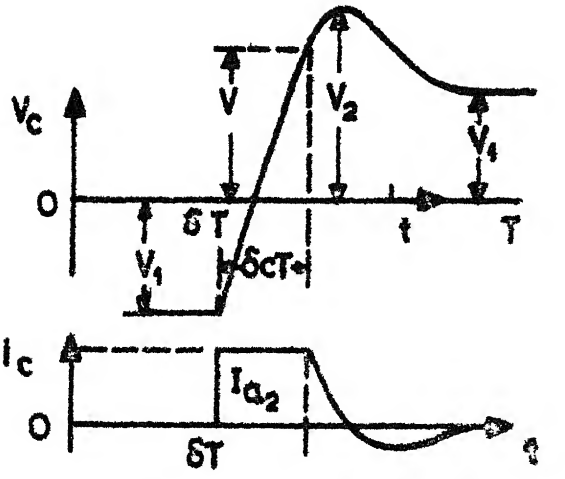

Fig.6.1 Wave forms of V_c and i_c

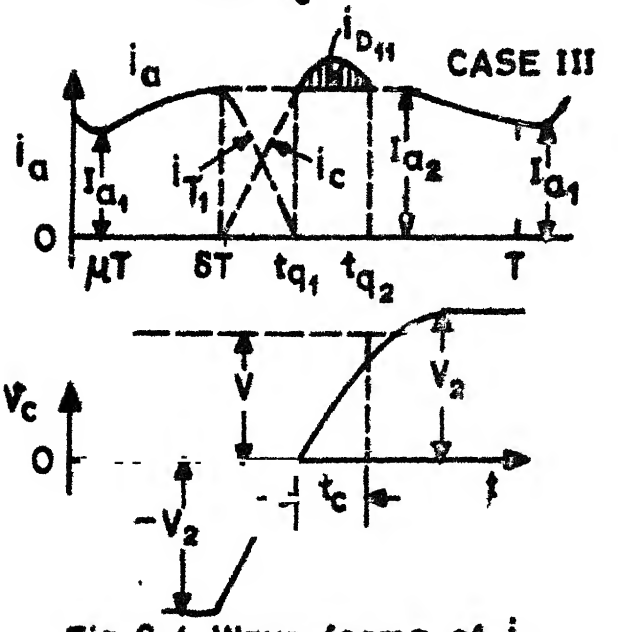

Fig 6.4 Wave forms of i_a and V_c

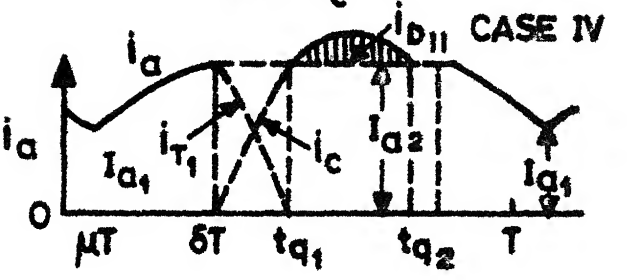

Fig.6.6 Load and capacitor current wave forms

$$\frac{t_c}{t_{co}} \triangleq \text{Normalised commutation time}$$

$$= 1 - \frac{\sqrt{L_s.C}}{\frac{V.C}{I_{a2}}}$$

or,

$$\frac{t_c}{t_{co}} = 1 - \frac{X_c}{X_o} \qquad (6.3)$$

where,

$$X_c = \sqrt{\frac{L_s}{C}} \text{ , and } X_o = \frac{V}{I_{a2}}$$

Proceeding as above, it can be shown that the maximum normalised voltage v_n on the capacitor is given by the following equation.

$$(\frac{V_2}{V}) = v_n = 1 + \frac{X_c}{X_o} \qquad (6.4)$$

Figure 6.2 shows the variation of $\frac{t_c}{t_{co}}$ versus X_o with X_c as parameter. It is seen that at a given value of X_o, the available circuit turn off time reduces with the increase of X_c, i.e. the source inductance reduces the turn off time of the main thyristor. Thus the value of commutation capacitor should be chosen taking source inductance into account for reliable commutation.

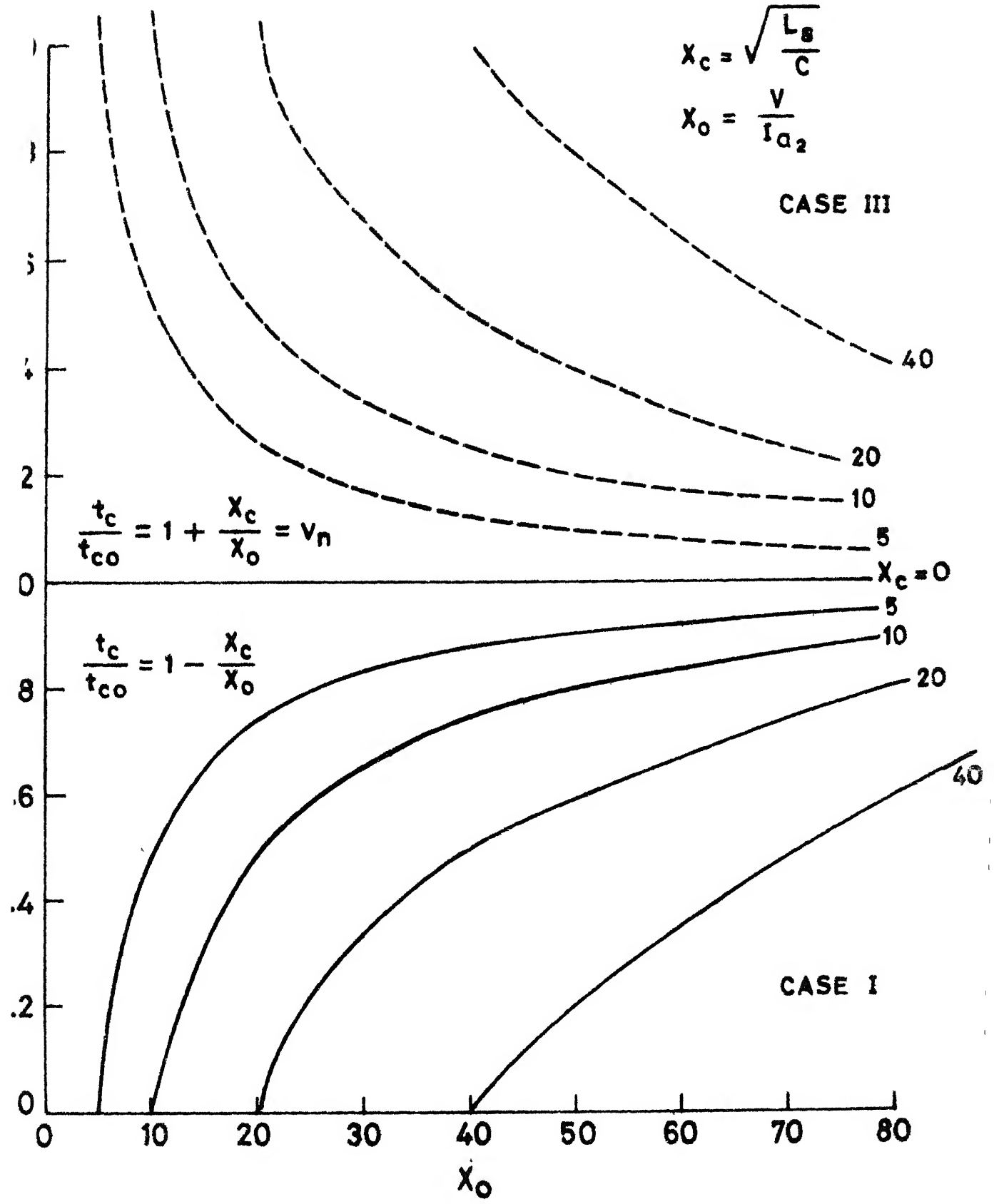

Fig. 6.2 Normalised turn off time vs. X_o

The variation of v_n with X_o with X_c as a parameter is also shown in Figure 6.2 by the dotted lines. These curves can be employed for obtaining the voltage ratings of commutation capacitor, thyristors and diodes.

6.3 CASE II: THREE THYRISTOR CHOPPER WITH LOAD CURRENT DEPENDENT COMMUTATION

If diode D in Figure 2.1 is replaced by a thyristor or a three thyristor chopper as shown in Figure 6.3(a) is used, then after the capacitor is overcharged to a voltage V_2 due to source inductance, it will not have a path to discharge. In that case the voltage available with the capacitor for commutation will be V_2 and the normalised circuit turn off time will be given by the following equation.

$$\left(\frac{t_c}{t_{co}}\right) = 1 + \frac{X_c}{X_o} \qquad (6.5)$$

In this case the circuit turn off time increases linearly with $\sqrt{\frac{L_s}{C}}$ for a given X_o. Variation of $\left(\frac{t_c}{t_{co}}\right)$ with X_o with X_c as parameter is shown in Figure 6.2 by dotted lines (case II). Here the source inductance increases the circuit turn off time. The increase in the voltage rating of the thyristors, diodes and capacitor is the same as in Case I.

Here, reliable commutation can be achieved with a lower value of capacitor compared to case I. However, thyristors, diode and capacitor of higher voltage ratings will be required. If the same value of capacitor is used as for case I, while the voltage ratings will be same, commutation will be more reliable due to higher value of circuit turn off time.

6.4 CASE III: THREE THYRISTOR CHOPPER WITH A DIODE IN ANTIPARALLEL TO THE MAIN THYRISTOR

The circuit diagram of such a chopper is shown in Figure 6.3(b). In this case, an additional path has been provided for recharging of capacitor C through D_{11}, T_2, and L_c during commutation of the main thyristor T_1. To commutate the main thyristor T_1 which is carrying a load current of I_{a2}, T_2 is triggered. The condenser C which is charged to a voltage of $-V_2$ generates a sinusoidal current pulse i_c. When i_c becomes equal to I_{a2} thyristor T_1 turns off. A current equal to $(i_c - I_{a2})$ now flows through the diode D_{11} and thyristor T_1 is reverse biased by drop across D_{11}. The capacitor voltage and current waveforms are shown in Figure 6.4. Current through diode D_{11} flows for $t = t_{q1}$ to $t = t_{q2}$. The capacitor current i_c is given by,

$$i_c = \frac{V_2}{\sqrt{L_s/C}} \cdot \sin(\omega_c' t) \qquad (6.6)$$

where,

$$V_2 = V + \sqrt{\frac{L_s+L_c}{C}}\ I_{a2}$$

and,

$$\gamma_o = \frac{1}{\sqrt{L_s.C}}$$

Now,

$$t_{q1} = \frac{1}{\gamma_o'} \sin^{-1}\left\{ I_{a2}\cdot \sqrt{\frac{L_c}{C}} \right\}$$

and

$$t_{q2} = \frac{1}{\gamma_o'}\left[\pi - \sin^{-1}\left\{ \frac{I_{a2}\sqrt{\frac{L_c}{C}}}{V_2} \right\}\right]$$

The circuit turn off time, $t_c = (t_{q2} - t_{q1})$

$$= \frac{1}{\gamma_o'}\left[\pi - 2\sin^{-1}\left\{ \frac{I_{a2}\sqrt{\frac{L_c}{C}}}{V_2} \right\}\right]$$

(6.7)

It can be shown that

$$V_2 = V + \sqrt{\frac{L_s+L_c}{C}}\ .\ I_{a2} \qquad (6.8)$$

Substituting for V_2 in equation (6.7), yields

$$t_c = \frac{1}{\gamma_o'}\left[\pi - 2\sin^{-1}\left\{ \frac{I_{a2}\sqrt{\frac{L_c}{C}}}{V + \left(\sqrt{\frac{L_s+L_c}{C}}\right) I_{a2}} \right\}\right] \qquad (6.9)$$

When there is no source inductance, the capacitor charges to a voltage V_2' given by

$$V_2' = V + \sqrt{\frac{L_c}{C}} \cdot I_{a2} \qquad (6.10)$$

The turn off time available in the absence of source inductance is given by

$$t_{co} = \frac{1}{\omega_o}\left[\pi - 2\sin^{-1}\left\{\frac{I_{a2}\cdot\sqrt{\frac{L_c}{C}}}{V + \sqrt{\frac{L_c}{C}}\cdot I_{a2}}\right\}\right] \qquad (6.11)$$

$$\frac{t_c}{t_{co}} = \text{normalised turn off time}$$

$$= \frac{\pi - 2\sin^{-1}\left\{\frac{1}{\frac{V}{I_{a2}}\cdot\sqrt{\frac{C}{L_c}} + \sqrt{\frac{L_s+L_c}{L_c}}}\right\}}{\pi - 2\sin^{-1}\left\{\frac{1}{\frac{V}{I_{a2}}\cdot\sqrt{\frac{C}{L_c}}+1}\right\}}$$

$$= \frac{\pi - 2\sin^{-1}\left\{\frac{1}{X + \sqrt{1+y}}\right\}}{\pi - 2\sin^{-1}\left\{\frac{1}{X+1}\right\}} \qquad (6.12)$$

where,

$$X = \frac{V}{I_{a2}} \Big/ \sqrt{\frac{L_c}{C}} \quad \text{and} \quad y = \frac{L_s}{L_c}$$

It can be shown that the normalised maximum voltage v_n to which the capacitor gets charged in the presence of a source inductance is given by the following equation

$$\frac{V_2}{V_2'} = v_n = \frac{X + \sqrt{1+y}}{X + 1} \qquad (6.13)$$

Normalised curves of $(\frac{t_c}{t_{co}})$ and v_n versus X have been plotted in Figures 6.5(a) and 6.5(b) respectively with y as a parameter. It is found from these curves that the source inductance slightly improves the commutation capability of the chopper. However this is achieved at the expence of significant increase in voltage ratings of thyristors, diodes and capacitors as in the previous cases. The increase in voltage rating due to presence of source inductance can be computed from the curves of Figure 6.5(b).

6.5 CASE IV: TWO THYRISTOR CHOPPER USING LOAD INDEPENDENT COMMUTATION

The circuit diagram of such a chopper described by J. Gothiere and H. Hologne [24] is shown in Figure 6.3(c). The sequence of operation of this chopper is briefly given below. With the triggering of the main thyristor T_1, the current from the source starts flowing. The load current is still free wheeling through the free wheeling diode D_F. A part of the source current flows through D_2, L and C charging the capacitor C to a voltage almost equal to 2V.

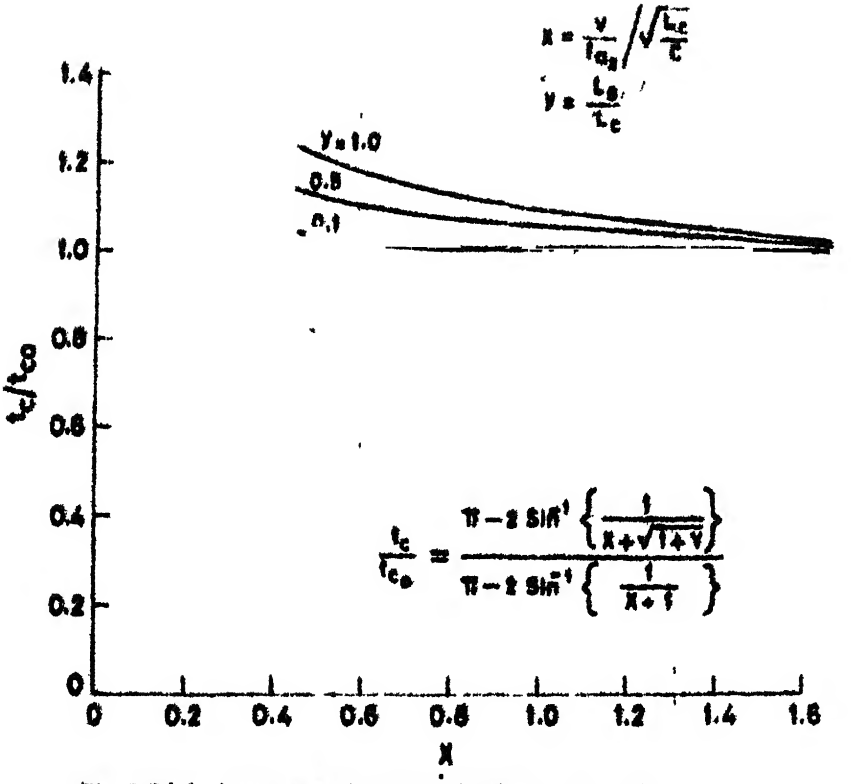

Fig. 6.5(a) Normalised turn off time vs. X

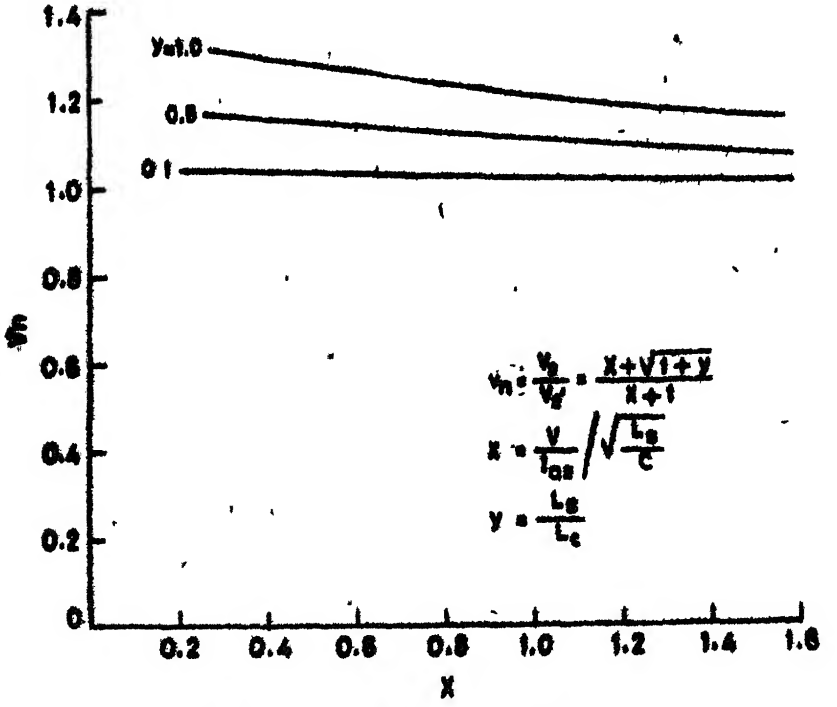

Fig. 6.5(b) Normalised voltage vs. X

The free wheeling action stops when the source current i_s equals I_{a1} of the load current. The load current then continues to increase exponentially. At the end of the duty interval, T_2 is triggered and the capacitor discharges through the load and also through the source via diode D_{11}. A typical current wave form of this chopper has been shown in Figure 6.6. When i_c reaches I_{a2}, the main thyristor is blocked and the capacitor current in excess of the load current, flows through D_{11} and the supply. The main thyristor T_1 remains reverse biased until i_c falls back to I_{a2}. The differential equation governing i_c during commutation interval is given by

$$L \frac{di_c}{dt} + \frac{1}{C} \int_0^{t'} i_c \, dt - L_s \cdot \frac{d}{dt} (I_{a2} - i_c) = 2V - V$$

with $i_c(o) = 0$.

The solution of the above equation is given by,

$$i_c = \frac{V}{\sqrt{\frac{(L+L_s)}{C}}} \cdot \sin(\omega_o' t) \qquad (6.14)$$

where,

$$\omega_o' = \frac{1}{\sqrt{(L+L_s)C}}$$

Let at $t = t_{q1}$, $i_c = I_{a2}$.

$$\therefore t_{q1} = \frac{1}{\gamma_o'} \cdot \sin^{-1}\left\{\frac{I_{a2} \cdot \sqrt{\frac{L+L_s}{C}}}{V}\right\}$$

Again, at $t = t_{q2}$, $i_c = I_{a2}$

$$\therefore t_{q2} = \frac{1}{\gamma_o'}\left[\pi - \sin^{-1}\left\{\frac{I_{a2}\sqrt{\frac{L+L_s}{C}}}{V}\right\}\right]$$

The circuit turn off time for the main thyristor T_1 is given by

$$t_c = t_{q2} - t_{q1} = \frac{1}{\gamma_o'}\left[\pi - 2\sin^{-1}\left\{\frac{I_{a2}\sqrt{\frac{L+L_s}{C}}}{V}\right\}\right]$$

When there is no source inductance, the turn off time is given by

$$t_{co} = \frac{1}{\gamma_o}\left[\pi - 2\sin^{-1}\left\{\frac{I_{a2}\cdot\sqrt{\frac{L}{C}}}{V}\right\}\right]$$

where,

$$\gamma_o = \frac{1}{\sqrt{L.C}}$$

$$\therefore \frac{t_c}{t_{co}} = \text{normalised turn off time}$$

$$= \sqrt{1+\frac{L_s}{L}} \cdot \left[\frac{\pi - 2\sin^{-1}\left\{\frac{I_{a2}\cdot\sqrt{\frac{L+L_s}{C}}}{V}\right\}}{\pi - 2\sin^{-1}\left\{\frac{I_{a2}\cdot\sqrt{\frac{L}{C}}}{V}\right\}}\right]$$

$$= \sqrt{1 + \frac{L_s}{L}} \left[\frac{\pi - 2 \sin^{-1} \left\{ \frac{X_{co}}{X_o} \cdot \sqrt{1 + \frac{L_s}{L}} \right\}}{\pi - 2 \sin^{-1} \left\{ \frac{X_{co}}{X_o} \right\}} \right]$$

where,

$$X_{co} = \sqrt{\frac{L}{C}} \quad \text{and} \quad X_o = \frac{V}{I_{a2}} \ ,$$

Figure 6.7 shows typical plots of normalised 'turn off' time $(\frac{t_c}{t_{co}})$ versus $(\frac{X_{co}}{X_o})$ with $\frac{L_s}{L}$ as parameter. It is found that for lower values of $\frac{X_{co}}{X_o}$ ratio, the normalised turn off time increases with $\frac{L_s}{L}$ and hence with the source inductance. For higher values of $\frac{X_{co}}{X_o}$, the normalised turn off time decreases rapidly with the increase of $(\frac{L_s}{L})$. Thus for this type of chopper, the source inductance improves commutation for lower values of $(\frac{X_{co}}{X_o})$ but it deteriorates for higher values of $(\frac{X_{co}}{X_o})$ as seen from the curves in Figure 6.7. Since the chopper is used from small to large values of load current, the net effect of source inductance is to reduce the circuit turn off time by a large amount. In order to get a required value of circuit turn off time, a large value of C will be required. This will make the resonant frequency small making it necessary to operate the chopper of frequencies much lower than the

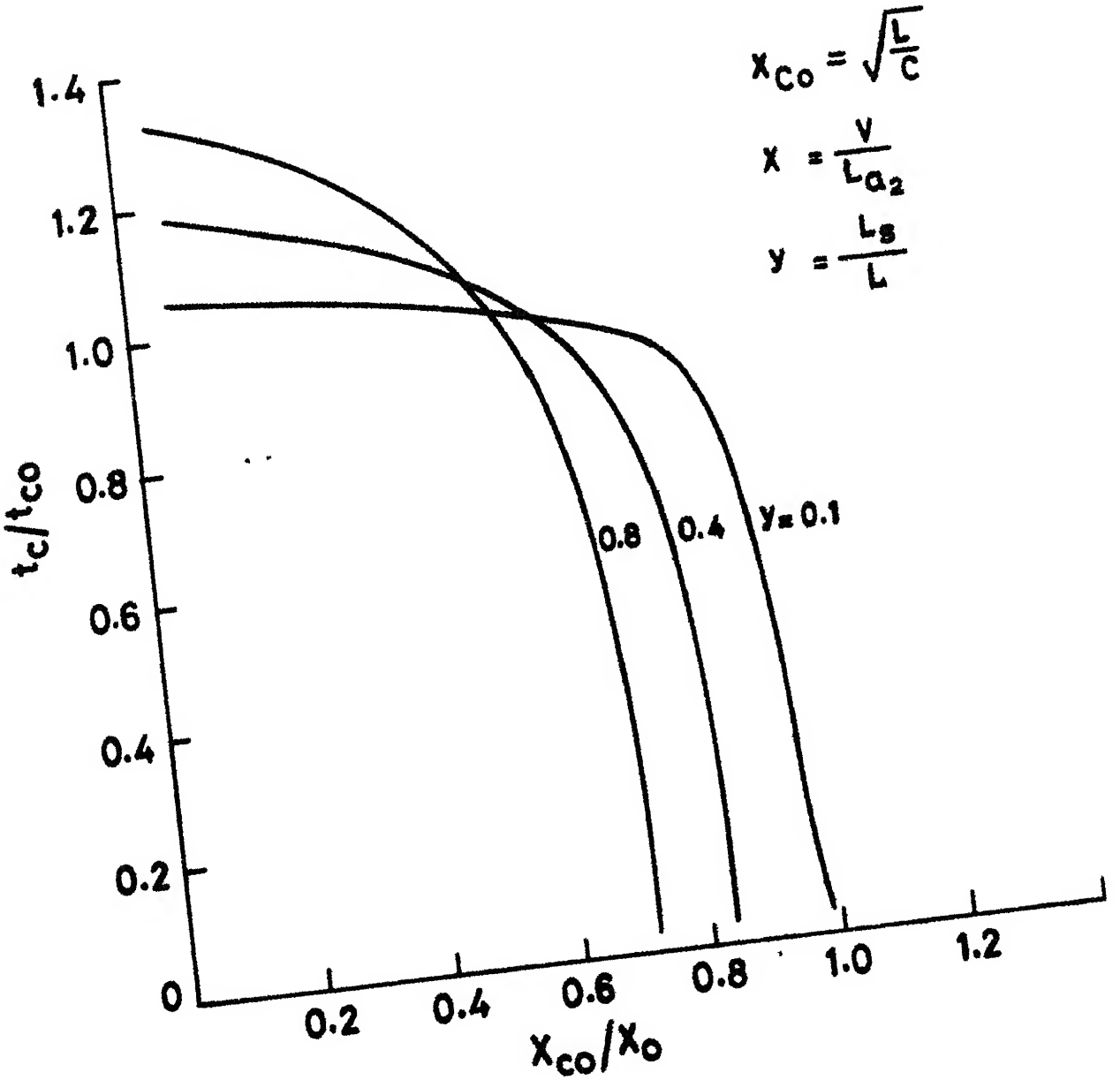

Fig. 6.7 Normalised turn off time vs (X_{Co}/X_o)

normal. To overcome this problem it is customary to put a filter capacitor at the input terminals of the chopper. If source does not have the ability to absorb power when reverse current flows, this ability will also be made available by filter capacitor.

Source inductance does not have any effect on the voltage ratings of thyristors, diodes and capacitor.

6.6 CONCLUSIONS

1. For a two thyristor chopper using load dependent commutation (case I) where a discharge path is available for the capacitor during free wheeling, the source inductance reduces the circuit turn off time and thus adversely affects the commutation of the chopper. It increases the voltage ratings of the thyristors, diodes and capacitor. A higher value of capacitor has to be used to ensure commutation.

2. In case of three thyristor choppers using load independent commutation where no discharge path is available for the condenser (case II), the source inductance increases the circuit turn off time and thus it helps commutation. In this case, a lower value of capacitor ensures reliable commutation. But this is at the expense of higher voltage ratings of the components.

3. For a three thyristor chopper using an antiparallel diode across the main thyristor (case III, Figure 6.3(b)) the source inductance slightly improves the commutation of the chopper. However this is at the expense of substantial increase in the voltage ratings of the components.

4. In the case of chopper using resonant pulse commutation (case IV Figure 6.3(c)), source inductance adversely affect commutation by reducing the circuit turn off time. In such circuits, a capacitor should always be used at the input terminals of the chopper. The voltage ratings of the components remain unaffected.

CHAPTER VII

IMPORTANT CONCLUSIONS

From the work reported in the previous chapters the following important conclusions are drawn.

7.1 CHOPPER CONTROLLED D.C. SEPARATELY EXCITED MOTOR

7.1.1 Motoring Operation

1. Discontinuous conduction does take place in case of chopper controlled d.c. separately excited motor unless an external inductor is used in the armature circuit or the chopper is operated at a high frequency. Discontinuous conduction makes speed regulation poor.
2. In presence of source inductance commutation capacitor of chopper with load current dependent commutation initially charges to a voltage higher than the source voltage. In absence of a discharge path, chopper commutation will improve. If discharge path is available, commutation will be poor. In both the cases the voltage ratings of capacitor, thyristors and diodes will increase.
3. In chopper circuits where commutation capacitor can discharge through the source and the load, discontinuous conduction has adverse effect on commutation.

4. Speed-torque curves become more drooping in presence of source inductance.

5. Effect of source inductance on motor speed-torque curves and chopper commutation can be reduced or neutralised by the use of a buffer condenser at the input terminals of the chopper.

6. The analytical method presented takes into account the effect of source inductance, chopper commutation interval and armature reaction of the motor and permits the prediction of the performance of chopper controlled d.c. motor with satisfactory accuracy.

7.1.2 Regenerative Braking Operation

7. The analytical method presented in Chapter III is general in the sense that it takes into account the effect of source inductance, chopper commutation interval and the effect of armature reaction of the machine in the analysis. It can be used for choppers with or without square wave output voltage. The predicted performance agrees well with experimental results.

8. The boundaries separating the regions of continuous and discontinuous conduction on the normalised torque speed plane for the square wave case can be employed to select a suitable $\frac{T}{T_a}$ ratio to optimize the regenerative power, the efficiency of regeneration, eliminate or reduce the region of discontinuous conduction and to reduce the armature current ripple below a low specified limit. These boundaries can also be used to obtain a conservative estimate of a suitable $\frac{T}{T_a}$ ratio in the case of a chopper with load current dependent commutation.

9. The source inductance reduces the regenerative power for the same value of duty ratio δ and speed. It also reduces the upper control range of δ.

10. In the presence of source inductance, the commutating capacitor initially charges to a voltage greater than the source voltage. Subsequently it discharges and if enough time is available it will discharge to a voltage less than the source voltage. Thus, a higher value of commutating capacitor is to be chosen to ensure reliable commutation. The voltage ratings of thyristors, diodes and capacitor increase due to source inductance.

7.2 CHOPPER CONTROLLED D.C. SERIES MOTOR

7.2.1 Motoring Operation

11. The method of analysis presented is general and it is applicable to choppers with or without square wave output voltage. It takes into account the saturation of the magnetic circuit, armature reaction of the machine, the eddy current effect and the effect of source inductance. It has been found that the eddy currents induced in the field cores do not influence the machine torque-speed characteristics significantly. But they influence the armature current ripple appreciably. Moreover, it is demonstrated that incremental inductances are to be used alongwith eddy currents for reliable prediction of current ripple.

12. As in the case of separately excited motor, speed-torque characteristics of the series motor also become more drooping due to source inductance.

13. In choppers involving discharge path for commutation capacitor through the source, commutation gets adversely affected in presence of source inductance. Commutation will however improve if no discharge path is available. In both the cases voltage ratings of thyristors, capacitor and diode increase.

14. Effect of source inductance on motor performance and commutation can be reduced or neutralised by the use of a buffer condenser at the input terminals of the chopper.

7.2.2 Regenerative Braking

15. The method of analysis takes into account the effects of armature reaction, magnetic saturation, influence of source inductance and the effect of commutation pulse. It permits the calculation of performance with satisfactory accuracy.

16. The electromagnetic braking torque increases with speed for a fixed value of δ under stable operating conditions. An increased value of commutating capacitor and a suitable filter inductance in series with the armature, improves the stability of braking characteristics.

17. The source inductance reduces the regenerative power for the same value of machine speed and duty ratio of the chopper. It improves the stability of the braking characteristics. A suitable value of buffer condenser neutralizes the effect of source inductance.

7.3 EFFECTS OF SOURCE INDUCTANCE ON DESIGN OF CHOPPER COMMUTATION CIRCUITS

Apart from the conclusions (2),(3),(5),(10),(13), (14), the following additional conclusions can be drawn.

18. For a three thyristor chopper using an antiparallel diode across the main thyristor (case III, Figure 6.3(b)), the source inductance slightly improves the commutation of chopper. However, the voltage ratings of the components are increased.

19. In case of chopper using resonant pulse commutation (case IV Figure 6.3(c)), source inductance adversely affects commutation by reducing circuit turn off time by a large amount. In such circuits a capacitor should always be used at the input terminals of the chopper. Voltage ratings of the components remain unaffected.

REFERENCES

[1] H. Irie, T. Fuji and T. Ishizaki, 'Thyristor chopper for separately excited d.c. motor control', Elect. Engineering in Japan (USA), vol. 88, No. 4, 1968, pp. 1-9.

[2] K. Nitta, H. Okitsu, T. Suzuki, Y. Kinonchi, 'A separately excited d.c. motor driven by discontimuous current' Elect. Engineering in Japan (USA) vol. 89 No. 11 1969, pp. 19-26.

[3] T.H. Barton, 'The steady state transfer function of a chopper drive' IEEE IAS Annual meeting, pp. 716-721, 1979.

[4] R. Parimelalagon & V.Rajagopalan, 'Steady state Investigation of a chopper fed d.c. motor with separate excitation; IEEE Trans. IGA vol. 7, pp. 101-108, 1971.

[5] Alexandrovitz and Z. Zabar, 'Analogue computer simulation of thyristorised static switch as applied to d.c. motor speed control' IEEE Trans. on IECI, Feb. 1970, pp. 10-13.

[6] P.D. Damle and G.K. Dubey, 'A digital computer program for chopper fed d.c. motors' IEEE Trans. on IECI, 1975, pp. 408

[7] G. Kimura and M. Shioya, 'Regenerative Braking of separately excited d.c. motor via chopper control' Elect. Engineering in Japan (USA) vol. 97, No. 4, 1977, pp.49-55.

[8] P.W. Franklin, 'Theory of d.c. Motor Controlled by Power Pulses' IEEE Trans. on Power Apparatus and Systems, vol. PAS-91, 1972, pp. 249-255.

[9] G.K. Dubey and W. Shepherd, 'Analysis of d.c. series motor controlled by Power Pulses', Proc. IEE, vol. 122 No. 22, Dec. 1975, pp. 1397-98.

[10] B. Millitt and M.H. Rashid, 'Analysis of d.c. chopper circuits by computer based piece wise linear technique', Proc. IEE, vol. 121 No. 3, March 1974, pp. 173-178.

[11] P.D. Damle and G.K. Dubey, 'Analysis of chopper fed d.c. series motor', IEEE Trans. on IECI, vol. 23 No. 1 1976, pp. 92-97.

[12] G.K. Dubey, 'Analytical methods of performance calculation of chopper controlled d.c. series motor', Journal of I.E. (India) Elect. Engg. Div., vol. 58, 1977, pp. 69-74.

[13] T. Fujimaki, K. Ohniwa and O. Miyashita, 'Simulation of chopper controlled d.c. series motor', IFAC Proc. Symposium on Power Electronics and Industrial Drives, Dusseldorf, 1977, pp. 609-618.

[14] R. Wagner, 'Possibilities of regenerative braking in a d.c. traction vehicle', Siemens Review, Jan. 1973, pp. 34-44.

[15] W. Farrer and P.D. McLouglin, 'Some design aspects of Thyristor Choppers for use in Rail Traction', IEE 2nd Internal Conference on Electrical Variable Speed Drives, Sept. 1979, pp. 116-121.

[16] P. Loderer, 'Gemischte Nutz-und Winderstands bremsung bei Gleichstromtriebfar Zeugen' Electriche Bahnen, vol. 44H.8, 1973, pp. 170-174.

[17] C.V. Jones, 'Unified theory of Electric Machines', Butterworths, London.

[18] H. Satpathi, G.K. Dubey and L.P. Singh, 'A general method of analysis of chopper fed D.C. Separately Excited Motor' Accepted for presentation at IEEE PES Winter Meeting, Jan. 31-Feb. ,1982.

[19] H. Satpathi, G.K. Dubey and L.P. Singh, 'Performance and Analysis of Chopper Fed D.C. Separately Excited Motor under Regenerative Braking', Electric Machines and Electromechanics, vol. 5, No. 4, 1980, pp. 293-308.

[20] D.B. Ranade and G.K. Dubey, 'A chopper for control of D.C. Traction Motor', Electric Machines and Electromechanics, vol. 4, 1979, pp. 299-319.

[21] B. Mellitt, M.H. Rashid, 'Voltage Time Interval Method for Measuring Machine Inductance', Proc. IEE, vol. 121, No. 9, Sept. 1974, pp. 1016.

[22] N. Keshavamurthy, P.K. Raja Gopalan, 'Effects of Eddy currents, on the rise and decay of flux in solid magnetic cores', Proc. IEE, vol. 109, pt. C, 1962, pp. 63-75.

[23] W. Mcmurray, 'Thyristor Commutation in D.C. Choppers - A Comparative Study', IEEE Trans. on Industry Applications, vol. IA-14, No. 6, Nov./Dec. 1978, pp. 547-558.

[24] J. Gothiere and H. Hologne, 'Thyristor Choppers for Electric Traction', ACES Review, No. 2, 1970, pp. 45-67.

[25] V.K. Verma, C.R. Baird and V.K. Aatre, 'Pulsewidth modulated speed control of D.C. Motors', Journal of The Franklin Institute, Feb. 1974, pp. 89-101.

[26] B.W. Williams, 'Complete state space digital computer Simulation of Chopper Fed D.C. Motors', IEEE Trans. on IECI, 1978, p. 255.

[27] K. Matsin, Y. Watanalee and S. Sato, 'A new thyristor chopper with Power Regenerative Function', Mem. Chube Institute of Technology (Japan), vol. 12A, Dec.,1976, pp. 43-53.

[28] H. Kahlen, 'D.C. Choppers for Driving and Braking Operation of D.C. Series Machines', Electrotech. Z.(ETZ) A (Germany), vol. 95(9), pp. 441-5, Sept. 1974.

[29] H. Locker, 'The D.C. Chopper used on Trolley Buses with full Electronic Control', Brown Boveri Review, vol. 67, No. 10, 1970, pp. 419-428.

[30] P. Knapp, 'Solid State Regulating Units for Motoring and Braking D.C. Traction Vehicles', Brown Boveri Review, vol. 57, 1970, p. 282.

[31] N. Matsui, Y. Adachi, 'Chopper Control of D.C. Separately Excited Motor and Improvement of its Characteristics', Bull. Nagoya Institute of Technology, No. 22, 1970, pp. 227-235.

[32] S.N. Bhadra et al., 'The Effect of Commutating Capacitor on the Regenerative Braking of a Thyristor Chopper Controlled D.C. Series Motor', Proc. All India Conference on D.C. Technology, Bangalore, Feb. 6-8,1978, pp. 534-544.

[33] K. Nitta, H. Okitsu, T. Suzuki and Y. Kinouchi, 'Characteristics of d.c. series motor operating with Thyristor Chopper Source', Trans. Soc. of Instrumentation and Control Engineering (Japan), vol. 8(4) Aug. 1972, pp. 422-430.

[34] M.H. Liveridge and B.M. Bird, 'The Separately Excited Motor in Battery Electric Traction', IEE Publication, 93 p. 260 (1972).

[35] J.P. Ellington, H. Mellion, 'The determination of control system characteristics from a transient response', IEE Monogram, M. pt. C, 1958, pp. 370-373.

36 H. Satpathi, G.K. Dubey and L.P. Singh, 'Generalised Method of Analysis of Chopper Fed D.C. Separately Excited Motor under Regenerative Braking', Accepted for publication in Electric Machine and Electromechanics.

[37] H. Satpathi, G.K. Dubey and L.P. Singh, 'Performance and Analysis of Chopper Fed D.C. Series Motor with Armature Reaction, Magnetic Saturation and Eddy Current Effect', under consideration for publication in IEEE Trans on Power Apparatus and Systems.

APPENDICES

(A) Particulars of the D.C. Separately Excited Motor:
220V, D.C., $\frac{1}{2}$ H.P., 1500 r.p.m.

The parameters determined by static test are

L_a = armature inductance (at rated current) = .088H

R_a = armature resistance = 4.13 ohms (hot)

L_m = Inductance of chopper charging circuit = .0005H

L_c = Inductance of filter inductance connected in armature circuit during regenerative braking
= 300 mH

Particulars of the Generator:
200V, D.C., 3 KW, separately excited, 1500 r.p.m.

L_s = Inductance of source = .040H (unsaturated D.C. value)

(B) Machine Particulars:

Machine I : 220V, D.C. separately excited, $\frac{1}{4}$ H.P. 1400 r.p.m. Laminated pole, Laminated armature and solid iron yoke.

Machine II : 220V, D.C. separately excited, 10 H.P., 1000 r.p.m. solid iron yoke, solid iron pole and laminated armature.

Machine III : (Generalised Machine)

Rotor : 230V, 8 Amp. (AC/DC)

Stator : 230V/115V, 3.6A/7.2A (A.C/D.C.) (series connection/parallel connection)

Laminated Stator and Laminated rotor.

Machine IV : 220V, D.C. series excited, 11.5 Amps, 1500 r.p.m.

Laminated pole, solid iron yoke and laminated armature.

Table B-1

	σ	λ	n	I_o	K_2
Machine I	1.2	22.0	1.0	0.12A	0.139
Machine II	1.2	94	0.7	0.9	3.33
Machine III	1.0	3.9	1.0	4.16	4.95
Machine IV	1.0	34.5	1.0	11.0	45.497

Least Square Formulation for determination of constants A_1, A_2, and A_3:

The dynamic values of i_m are determined from the transient recording of armature induced voltage under no load condition due to a step voltage input to the field windings. It is assumed that the effective magnetisation current can be represented by

$$i_m = I_o\,(1-A_1.e^{-\lambda_1 t} - A_2.e^{-\lambda_2 t} - A_3.e^{-\lambda_3 t})$$

where, I_o is the final steady state current due to a step input voltage to the field. Then, the time constants $1/\lambda_1$, $1/\lambda_2$, $1/\lambda_3$ are determined from semilog plots of $\epsilon = (I_o - i_m)/(I_o))$ versus time t as mentioned in Section 4.2.5. Then some relation of the output data x_k and the kth interval can be represented by

$$x_k = A_1.e^{-\lambda_1 t} + A_2.e^{-\lambda_2 t} + A_3.e^{-\lambda_3 t} \qquad (A.1)$$

Had equation (A1) represented the dynamics of the system correctly, and three sets of data would have been sufficient to determine A_1, A_2 and A_3. But because of inherent errors in the data as well as the inaccurate formulation of (A1) one has to take quite a number of data at regular intervals

utilizing a 'Least Square Error' criteria to get good estimation of the constants A_1, A_2, and A_3.

Let x_0, x_1, x_2 etc. represent the dynamic values of data at subsequent regular intervals, then

$$\begin{aligned} x_0 &= A_1 + A_2 + A_3 && \text{for } t = 0 \\ x_1 &= A_1 \cdot Z_1 + A_2 Z_2 + A_3 Z_3 && \text{for } t = T_1 \\ x_2 &= A_1 Z_1^2 + A_2 \cdot Z_2^2 + A_3 \cdot Z_3^2 && \text{for } t = 2T_1 \qquad \text{(A2)} \\ &\vdots \\ x_{n-1} &= A_1 \cdot Z_1^{n-1} + A_2 \cdot Z_2^{n-1} + A_3 \cdot Z_3^{n-1} && \text{for } t = (n-1)T_1 \end{aligned}$$

where, $Z_1 = e^{-\lambda_1 T_1}$, $Z_2 = e^{-\lambda_2 T_1}$, $Z_3 = e^{-\lambda_3 T_1}$ and $Z_1^{n-1} = (e^{-\lambda_1 T_1})^{n-1}$ and $Z_2^{n-1} = (e^{-\lambda_2 T_1})^{n-1}$ etc.

The equations (A2) can be written in matrix form as

$$\begin{bmatrix} X \end{bmatrix} = \begin{bmatrix} 1 & 1 & 1 \\ Z_1 & Z_2 & Z_3 \\ Z_1^{n-1} & Z_2^{n-1} & Z_3^{n-1} \end{bmatrix} \cdot \begin{bmatrix} A_1 \\ A_2 \\ A_3 \end{bmatrix} = \begin{bmatrix} D \end{bmatrix} \cdot \begin{bmatrix} A \end{bmatrix} \qquad \text{(A3)}$$

As $[D]$ is not a square matrix, $[A]$ cannot be determined by taking $[D]^{-1} \cdot [X]$. So, both sides of (A3) are premultiplied by $[D]^{T}$ so that $[D^{T}.D]$ is a square matrix and then the inversion is carried out to determine A_1, A_2 and A_3.

A70620

Date Slip A70620

This book is to be returned on the date last stamped.

.....	.....
.....	.....
.....	.....
.....	.....
.....	.....
.....	.....
.....	.....
.....	.....
.....	.....
.....	.....
.....	.....

CD 6.72.9

EE-1981-D-SAT-ANA